Reindeer habitat selection and movement changes with cumulative impacts from mining and wind power development

Bernardo Brandão Niebuhr[1,2], Erik Cronvall[3], Léonie Duris[2], Moudud Alam[4], Manuela Panzacchi[1], Bram van Moorter[1], Per Sandström[3], Anna Skarin[2]

[1] Norwegian Institute for Nature Research (NINA), Oslo, Norway

[2] Swedish University of Agricultural Sciences (SLU), Department of Animal Nutrition and Management, Uppsala, Sweden

[3] Swedish University of Agricultural Sciences (SLU), Department of Forest Resource Management, Umeå, Sweden

[4] Dalarna University, Falun, Sweden

Corresponding author: Bernardo Brandão Niebuhr
bernardo.brandao@nina.no
Norwegian Institute for Nature Research (NINA), Sognsveien 68, NO-0855 Oslo, Norway

Glossary

ZOI: zone of influence
HSA: habitat selection analysis
iSSA: integrated step selection analysis
RHC: Sámi reindeer herding community
GPS: global positioning system
SOS, EOS: start (end) of season
IRG: instantaneous rate of green-up
TPI: topographic position index
AIC: Akaike information criterion

Abstract

Industrial expansion often occurs in landscapes already affected by multiple disturbances, leading to cumulative impacts on biodiversity and local communities. With the societal pressure for an rapid 'green transition', land-use changes intensifies, yet most impact assessments remain local and project-based, disregarding cumulative impacts. We conceptualized and disentangled key dimensions of cumulative impacts and integrated them within habitat selection, calving site selection, and movement analyses in a case study of reindeer and Sámi reindeer husbandry in Scandinavia. Using GPS data collected before, during, and after the construction of four wind power plants, we quantified the effects of mining, wind power development, and other infrastructure across snow-free seasons and behavioural processes. We found strong avoidance of mines and wind power plants, with zones of influence extending up to 5-10 km at landscape scale and up to 5 km at patch scale. Impacts were strongest during calving but also present in summer and autumn. Wind power plants affected movement by acting as semi-permeable barriers, with reindeer avoiding crossing them and moving faster and more directionally near turbines during construction. At patch scale, cumulative impacts of several wind power plants were evident during calving. Our results highlight the need for regional and integrative land-use planning that accounts for cumulative impacts from multiple existing and planned developments. The framework we present here provides a general approach to quantify zones of influence and cumulative impacts of multiple features and infrastructure types across landscapes and ecological processes.

Keywords: cumulative effects, cumulative impact assessment, wind energy development, mining, habitat loss, habitat fragmentation, *Rangifer tarandus*, reindeer husbandry

Graphical abstract

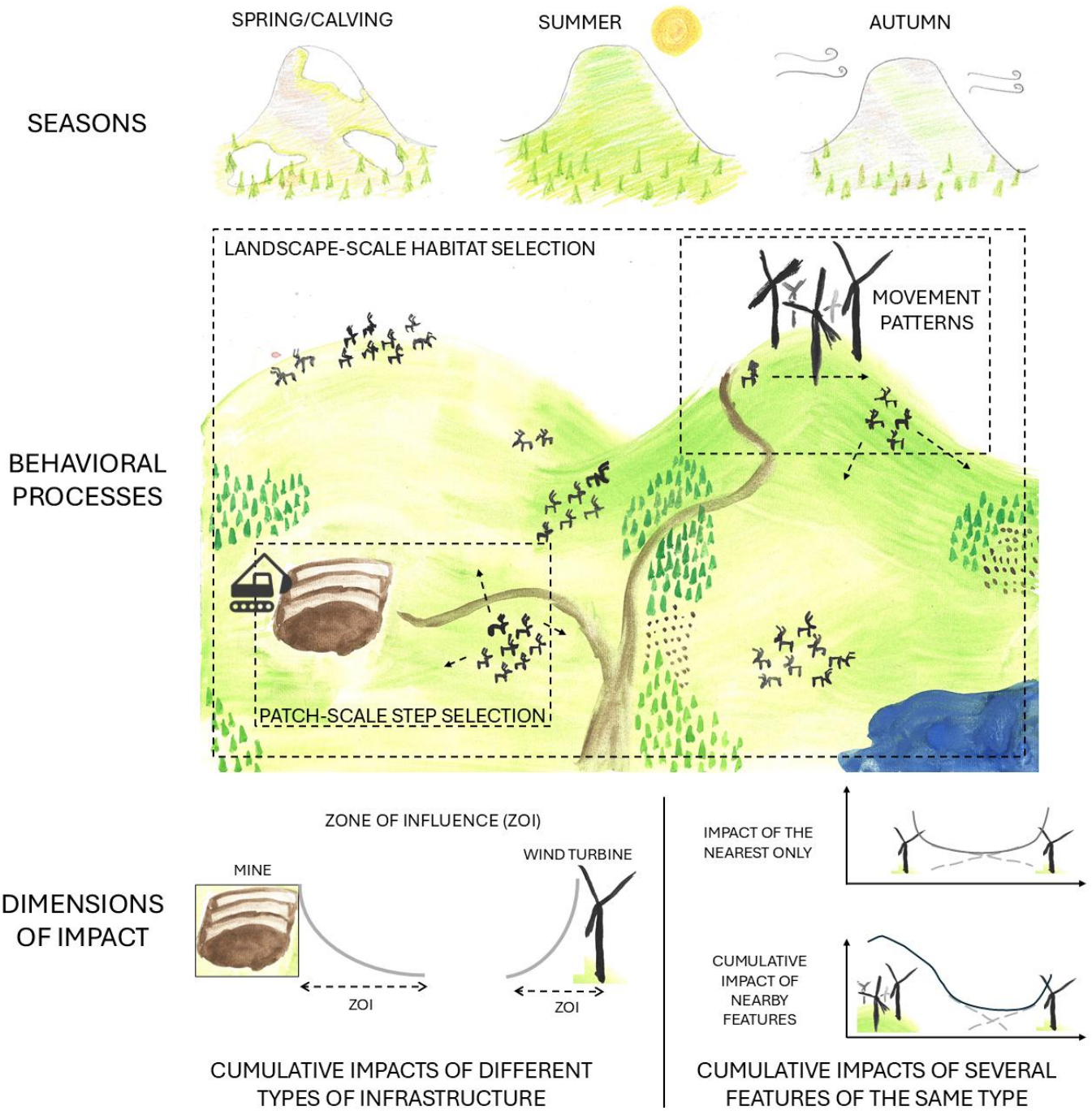

1. Introduction

The distribution, behaviour, and movement of animals is driven by trade-offs between how the resources, risks, and environmental conditions are perceived and change across landscapes (Matthiopoulos et al., 2023). Overall, animals search for resources while trying to avoid or decrease what they perceive as risks (Rio-Maior et al., 2019; Sih, 1980). Industrial activity and infrastructure decrease availability or remove resources from landscapes, increasing risks and disturbing animals. Furthermore, they create barriers and hinder movements towards resources (Benítez-López et al., 2010; Cowan et al., 2025). With societal pressure to promote a "green transition" in energy production, encroachment of anthropogenic infrastructure into natural areas has accelerated, with hydro, solar, and wind energy facilities rapidly expanding (Katzner et al., 2025) and mining activities intensifying to supply materials for renewable energy infrastructure (Sonter et al., 2020). When multiple land-use changes and development projects occur together, their impacts may accumulate across space and time, being stronger and lasting longer than single changes or projects (Gillingham et al., 2016). Nevertheless, impacts of multiple disturbances, often named cumulative impacts, remain poorly quantified in impact assessments and land-use planning processes. Even though more integrative land management tools such as strategic and regional planning exist (Gillingham et al., 2016; Halpern et al., 2008), most commonly impact assessments of new projects are done locally, for single projects in isolation, and do not include the assessment of cumulative impacts (Hodgson et al., 2019; Noble et al., 2017).

Habitat selection analyses evaluate how much animals use certain sets of environmental conditions, resources, and risks in relation to their availability in the landscape, making it possible to quantify and predict which areas correspond to suitable habitat, and which factors are selected or avoided, thus increasing or reducing habitat suitability (Fieberg et al., 2021; Hirzel and Le Lay, 2008; Matthiopoulos et al., 2023). As such, habitat selection models provide a quantitative framework to link animal decision-making to spatial variation in resources and risks and are a powerful tool for impact assessment and land-use planning. However, despite their widespread use, these approaches have only recently begun to formally incorporate the effects of multiple, co-occurring disturbances (e.g. Niebuhr et al., 2023b; Plante et al., 2018), and therefore remain limited in their ability to quantify cumulative impacts across landscapes. Cumulative impacts are complex and require understanding of multiple dimensions of impacts: how strong are impacts, how far the impact of single features reaches, and how the impacts accumulate when there are multiple disturbances close to each other (Fig. 1).

Impacts of single land use practices and infrastructure usually extend beyond the boundaries of the area they occupy (Niebuhr et al., 2022; Polfus et al., 2011). For this reason, assessments need to measure how strong impacts are and how far these impacts reach, identifying their *zone of influence* (ZOI) (Fig. 1). Zones of influence arise when animals change their behaviour, e.g when they avoid or are impeded to access habitats around disturbances (Katzner et al., 2025). The ZOI is species-, time-, and process-dependent (Martin, 2018; Pease, 2024), i.e. it can be different for distinct species, seasons, or behavioural processes under consideration, and can vary from a few meters to tens of kilometers for different types of infrastructure and contexts (Johnson et al., 2005; Moreira et al., 2015; Pease, 2024). The ZOI shows how large an area is affected by a disturbance and how impacts accumulate spatially for a species (Fig. 1A,B).

Moreover, *several features of the same type* might lead to cumulative impacts (Fig. 1A). For instance, many tourist cabins or renewable energy facilities might affect larger areas and lead to stronger effects than single features (Engen et al., 2023; Niebuhr et al., 2023b). Most studies assessing the effects of infrastructure only consider the (distance to the) nearest infrastructure and ignore the possibility of cumulative impacts (e.g. Torres et al., 2016). However, metrics based on the proportion or density of features in space might inherently capture the cumulative impact of multiple features. Building on this, Niebuhr et al. (2023b) proposed a method to assess ZOIs and evaluate cumulative impacts of several features of the same type, but this method has yet to be applied to real situations. On top of that, the

presence of different kinds of infrastructure and disturbance in landscapes (e.g. houses, roads, railways, mining) can also lead to *cumulative impacts of different types of infrastructure* (Fig. 1C).

Sámi reindeer husbandry is part of the livelihood and culture of the Indigenous Sámi people in northern Europe and involves a strong connection between reindeer, reindeer herders, and landscapes (Holand et al., 2022). Sámi reindeer herders follow the reindeer during their migrations and herd them during some specific occasions, but for most of the year reindeer move through habitats and forage for resources freely (Skarin et al., 2022a). Semi-domesticated reindeer has been shown to avoid human activity and infrastructure whenever the landscape conditions and context allow them (Skarin and Åhman, 2014). Reindeer husbandry has historically been affected by other land uses such as mining, forestry, and roads (Horstkotte et al., 2022). In the last decades, conflicts have increased because of the rapid expansion of renewable energy, particularly wind power development (Cambou et al., 2021; Eftestøl et al., 2023; Skarin et al., 2022b). In this context, assessing the impacts of individual projects and disturbances alone is insufficient to understand how reindeer behaviour and reindeer husbandry respond to industrial development. Instead, we need frameworks to assess compounding cumulative impacts of existing and planned industrial projects (Barrio et al., 2025).

[Figure 1 here]

The aim of our study was to estimate the dimensions of the cumulative impacts of industrial infrastructure on reindeer behaviour and movement using Malå Sámi reindeer herding community (RHC) in Sweden as our case. We used GPS locations from female reindeer collected before, during, and after the construction of four wind power plants to estimate the cumulative impact of an existing mine, wind power development, and other infrastructure on reindeer landscape- and patch-scale habitat selection and movement, across seasons. Within our analysis we estimated the ZOIs of the mine and the wind power plants and evaluated if these infrastructures affected reindeer calving site selection, both in space and in relation to pasture quality.

We expected reindeer to avoid the wind turbines, the mine, and other infrastructure types as a consequence of higher human presence and activity, such as major roads and settlements (Gundersen et al., 2022; Skarin and Åhman, 2014), and expected wind power plants and the roads to hinder reindeer movement and act as barriers in the landscape (Panzacchi et al., 2016, 2013; Skarin et al., 2015). We expected stronger effects during spring/calving, when reindeer are more sensitive (Skarin et al., 2022a), but also avoidance during other seasons. During summer, however, reindeer were expected to be less sensitive to infrastructure due to other stressors such as heat and insect harassment (Johnson et al., 2021; Skarin et al., 2004; Valente et al., 2020). We expected calving site selection to be strongly affected by the mine, and that females would choose calving sites away from the disturbances at the expanse of high-quality pasture.

2. Materials and Methods

2.1 Study area

The study was conducted in Malå RHC, Sweden, situated in the boreal forest areas all year (Fig. 2). Our assessment was the result of collaboration with reindeer herders in the RHC, who have provided GPS data and knowledge of the landscape and reindeer behaviour. In our study area, Boliden AB established the Kristineberg mine during the 1940s. This is an underground mine extracting copper, zinc, silver, and gold. Processed ore is transported by truck through Malå RHC to the Baltic coast for final processing. Industrial forestry was introduced during the 1950s. In 2010-2011 four wind power plants (Jokkmokksliden, Storliden, Ytterberg, Åmliden, Fig. 2) were established in the study area, with in total 70 wind turbines with a full height of 145-150 m. The area is intersected by 496 km of public roads, 2068 km of private roads, 184 km of power lines, and 261 km of trails which cut the pasture resources used by reindeer between spring and autumn (Table A3).

[Figure 2 here]

Based on herding activities, reindeer habitat requirement, and seasonal shifts, we divided our analyses into spring, summer, and autumn seasons (Skarin et al., 2022a). Spring, mainly denoted as the period when the calves were borne (and called hereafter calving season), was defined to start after the spring migration from the winter grazing area, in the beginning of May, and last until the end of June, when reindeer are gathered for calf marking. Summer season was defined as mid-July (after calf marking) to 15 of September, and autumn season from 16 September to end of November, when animals typically were migrated by the herders out of our study area towards the eastern winter areas, not overlapping with the wind power plants. The exact start and end dates of each season varied across years and were defined based on information from the reindeer herders (Table A1). The first half of the summer was usually marked by high insect activity known to disturb the reindeer and alter their behaviour (Skarin et al., 2010). The area available for reindeer from 30 April until 1 October was defined by the RHC borders and the Lapland border fence in the east (Fig. 2). However, the fence was leaking and reindeer moved east of the fence already by August.

2.2 Reindeer GPS data

Our analyses were based on locations of GPS-collared (Followit AB and Telespor AS) adult female reindeer recorded at two-hours intervals between 2008 and 2018, except for the years 2012-2014 (Table 1). Part of the data has already been analyzed for the calving season around two wind power plants in earlier work (Skarin et al., 2018, 2015). We expanded the analysis to include the Kristineberg mine and two additional wind power plants, putting it into a cumulative impact analytical framework (Fig. 2). All animal trajectories were manually checked and filtered based on herders' information, and locations within corrals were removed. We used the Bjørneraas et al. (2010) procedure to remove spikes and outliers. We also excluded data from individuals covering less than 14 consecutive days within a season. Data wrangling and preparation were done within R environment (R Core Team, 2024), with the support of RenGIS (Sametinget, 2022) for visualization and interpretation. The final dataset comprised 228, 200 and 177 reindeer-year tracked during calving, summer and autumn, respectively, with a total of ca. 300 thousand GPS positions (Tables 1 and C1).

Table 1. Development phases of the wind power plants and number of reindeer (total number of GPS positions in parenthesis) tracked in each year within calving, summer and autumn season in Malå reindeer herding community, Sweden.

Year	Development phase	Spring/Calving	Summer	Autumn
2008	Before construction	47 (18,388)	42 (27,018)	39 (24,993)
2009	Before construction	34 (15,395)	33 (17,880)	39 (15,223)
2010	Construction	45 (21,085)	43 (22,417)	28 (10,863)
2011	Construction	18 (8,117)	12 (5,491)	9 (4,328)
2015	Operation	40 (24,289)	38 (22,932)	37 (20,717)
2016	Operation	32 (13,334)	19 (8,535)	12 (3,277)
2017	Operation	5 (2,665)	7 (4,639)	11 (5,085)
2018	Operation	7 (3,396)	6 (3,392)	2 (1,230)

2.3 Calving site identification

We identified calving events and sites using a residence time analysis (Barraquand and Benhamou, 2008; Bracis et al., 2018) during calving season. It estimates the most probable time and location of reindeer parturition quantifying the time spent by females in a 200 m radius neighbourhood along the trajectory (Panzacchi et al., 2013; Skarin et al., 2018). We considered the occasion of the first peak (i.e. long time spent within 200 m) in the times series of residence time values as the most probable site for the parturition event (Panzacchi et al., 2013) (Fig. D1). The mean GPS location within that radius was estimated as the calving site. The analyses were made using the *recurse* and *adehabitatLT* packages in

R (Bracis et al., 2018; Calenge et al., 2023). From the 228 reindeer-years tracked during calving, we identified 187 calving sites across all years.

2.4 Environmental variables

We analyzed reindeer habitat selection and movement considering infrastructure and environmental variables known to influence reindeer behaviour (Panzacchi et al., 2015; Skarin et al., 2022a, 2018). We considered landscape and phenology variables including land use and land cover, elevation, slope, aspect, topographic position index (TPI), and date of start and end of season (SOS and EOS, respectively), in addition to the instantaneous rate of green up (IRG) for the calving site selection analysis. We used the Swedish National Land Cover Database, version NMD2018 (Naturvårdsverket, 2020) which comprises 25 classes and reclassified them into five main land cover classes: deciduous forest, coniferous forest, open areas, mires, and anthropogenic areas (Table A2). Forestry impacts were not assessed directly but forestry clear cuts from the Swedish Forestry Agency were grouped together with other open areas class and comprised 82% of that class. TPI is a measure of variation in the relief of a neighbourhood, computed by comparing the elevation of a site with the average elevation on the neighbourhood, for a given neighbourhood size (Weiss, 2001). The TPI was computed using three different neighbourhood sizes (150 m, 250 m, and 510 m) and the best TPI scale was defined through model selection (see below). TPI was classified into six classes (valley, lower slope, flat, middle slope, upper slope, ridge) following the slope-position classification proposed by Weiss (2001). SOS, EOS, and IRG are phenological variables based fitting a logistic curve to normalized difference vegetation data, obtained from remote sensing. The SOS and EOS represent the time of peak greening and browning of the vegetation in spring and autumn, respectively, and were computed for each pixel in the landscape using the package *phenofit* in R (Kong et al., 2022). The IRG, a measure of "springness", is related to forage quality (Bischof et al., 2012) and was calculated at each calving site location from May 1st to June 29th using the *smooth.spline* function from the *stats* package in R (R Core Team, 2024). The phonological metrics we based on MODIS satellite images downloaded from Google Earth Engine (MOD13Q1.061 Terra Vegetation Indices 16-Day Global 250 m).

We accounted for the cumulative impact of anthropogenic activities considering wind power turbines and mining, public and private roads, trails, houses, and power lines. Infrastructure data were obtained from the Swedish Mapping, Cadastral and Land Registration Authority (Lantmäteriet; Table A2).

To represent the spatial influence of wind power and mining, we computed ZOI variables decaying exponentially from the disturbance source and decreasing to nearly zero at varying distances (100, 250, 500, 1000, 2500, 5000, and 10000 m). These distances are referred to as the radius of the ZOI, i.e. the distance at which the effect ceases to be present (Niebuhr et al., 2023b). For wind turbines, we computed both the density of wind turbines in a given radius, which accounts for the cumulative impacts of several turbines, and the distance from the nearest turbine, which disregards all but the closest feature (Fig. B1). For mining, we only considered the ZOI of the nearest mine, since there was only one mine in the study area. Zone of influence variables were computed using the *oneimpact* package in R (Niebuhr et al., 2023b, 2023a).

2.5 Statistical cumulative impact analyses

We assessed variation in reindeer habitat selection and movement using a before–after (BA) design across the three wind power development phases: pre-construction, construction, and operation. We performed habitat selection analyses (Fieberg et al., 2021) including wind turbine disturbance (density or distance), development phase, and land cover type, together with additive effects of mining, other human infrastructure, and the landscape and phenology variables as predictors (Texts B1, C1). The assessment of the effect of the construction and operation of the wind power plants was included through interactions between the wind turbine disturbance variables, the development phase, and the land cover types. Our analyses included evaluation of the three dimensions of cumulative impacts described above (Fig. 1): ZOIs, cumulative impacts of features of same type, and cumulative impacts

of different types of features. Even though these impacts are conceptually presented separately here, they were estimated simultaneously for each season and behavioural process.

To estimate ZOIs and evaluate cumulative impacts of wind turbines, we applied the *cumulative zone of influence* proposed by Niebuhr et al. (2023b). The ZOIs were precomputed at multiple radii representing alternative spatial extents of impact and included in models either as wind turbine density or distance to the nearest wind turbine. By comparing models containing different ZOI radii and variable types through multi-model inference, we inferred the effect size, the spatial extent of wind turbine ZOI, and whether impacts accumulated across several wind power plants (Fig. B1). The cumulative influence of other anthropogenic infrastructure was evaluated using additive terms describing the ZOI of the mine and log-distance to the nearest road, trail, house, or power line (Texts B1, C1).

We fitted habitat selection models using all combinations of wind turbine ZOI radii and variable types (density vs. nearest), mining ZOI radii, and alternative spatial scales for TPI, together with additive effects of other predictors. Models were compared using the Akaike Information Criterion (AIC), and the most parsimonious model was selected as the model with the lowest AIC (Burnham and Anderson, 2002). The selected models allowed us to estimate the strength of infrastructure effects, identify the ZOI for wind turbines and the mine, and determine whether impacts accumulated across several wind power plants or across different infrastructure types. To avoid spurious inference due to collinearity, we evaluated predictor correlations using the variance inflation factor (VIF) and removed variables that presented VIF > 5 (James et al., 2021).

We analyzed reindeer responses at two hierarchical scales, corresponding to different behavioural processes: (i) landscape-scale habitat selection within the seasonal area available to reindeer (2^{nd} order selection, *sensu* Johnson (1980)), and (ii) foraging patch-scale selection and movement patterns using integrated step-selection analyses (Avgar et al., 2016). During the calving season we also analysed the selection of calving sites relative to the available calving habitat, at landscape-scale.

2.5.1 Landscape-scale habitat selection analysis

At landscape scale, we modelled habitat selection using habitat selection analyses (HSA) through binomial regression following Fieberg et al. (2021). We compared the environmental variables at each used GPS location to those at 10 positions spread randomly within the area available for each season. We ran models using the model structure as described above (Appendix B).

We used the same approach to evaluate the selection for calving sites, comparing the environmental conditions of each identified calving sites to those of 10 random sites drawn across the calving area. However, we reduced the number of environment variables, as we had a limited sample size (n = 187). Moreover, only 8 females over 59 (13%) selected calving sites less than 5km from the wind turbine locations before their construction. This results in limited observation to use in a before-after assessment and an evaluation on the changed behavior in relation to the wind power. Thus, we decided not to assess the cumulative impact of multiple wind turbines and their ZOI on the calving site selection (Appendix D).

2.5.2 Patch-scale integrated step selection analysis

At the foraging patch scale, we applied integrated step selection analyses (iSSA; Avgar et al., 2016), designed to simultaneously quantify the effects of the predictors on habitat selection and movement, while controlling for each other's mutual influence. Models were fitted using conditional logistic regression through the *amt* package in R (Signer et al., 2019) and followed the setup and interpretation proposed by Fieberg et al. (2021). In iSSA, the unit of analysis is the displacement made by reindeer between subsequent positions (referred to as 'step') in a use-availability design. For each used step, we sampled 10 random steps starting at the same position, using each step as a stratum. Step length and turning angle for the random steps were drawn from a Gamma distribution and a von Mises

distribution, respectively, fitted to the observed data for each individual. Random steps ending outside the limits of the availability area in each season were excluded and redrawn. For each step, we extracted the environmental variables at the end point of steps to assess habitat selection, and at the starting point of steps to assess effects on movement. We also computed whether steps crossed public roads and a buffer of 500 m around the wind turbines as binary variables (1 = cross, 0 = no cross) to evaluate if these infrastructure represented barriers for reindeer.

Similarly to the HSA, the models considered the effects of wind power, mining, other infrastructure, and landscape and phenological variables (Appendix C). For public roads and wind power plants, we included terms to assess both the avoidance of these infrastructures and their barrier potential. To assess the effects of wind turbines on reindeer movement, we added as main effects step length, log step length, and the cosine of the turning angle (movement parameters; Avgar et al., 2016), and the interaction of these movement parameters with land cover and with the wind farm ZOI variables (Appendix C, Text C1).

To interpret the results of both landscape- and patch-scale analyses, HSA and iSSA, we first examined the structure and coefficients of the best-ranked models for each season to identify the variables influencing reindeer responses. We visualized functional responses plotting the relative selection strength (RSS; Avgar et al., 2017) for wind turbines, mining, and land cover. To better understand the cumulative impacts at landscape-scale, we generated spatial predictions of habitat suitability before, during, and after wind power construction, and quantified proportional changes in suitability relative to the pre-construction phase. These predictions represent relative habitat selection and are interpreted as proxies for spatial patterns of use. The prediction maps illustrate the spatial extent of predicted cumulative impacts of multiple wind power plants and other infrastructure types and help visualize the ZOI of the mine and the wind power plants. To visualize the impacts of wind power plants on the movement parameters in the iSSA, we plotted the predicted movement rates and turning angles for movements close (distance = 0) and far (distance = 1 and 5 km) from the wind turbines, in each development phase.

2.5.3 Calving events in relation to green-up

We selected individuals whose movement trajectory at some occasion were recorded within 2 km of the wind turbines during the calving season (n = 54) from the others (n = 133), to assess the effect of wind power on calving site selection in relation to pasture quality. We conducted a series of basic analyses using the Kruskal-Wallis test, after checking for homoscedasticy and normality. Firstly, we tested the differences in calving dates across the different wind power development phases for individuals that roamed close to the wind turbines during calving season. Secondly, we tested the synchrony between calving date and forage quality, comparing the absolute time from calving to the maximum IRG across phases for the same individuals.

3 Results

Overall, we found compelling evidence of cumulative impacts on reindeer habitat selection, in all seasons, caused by the mine, the wind power plants, and other infrastructure such as public and private roads (Table 2, Appendix B and C). The impacts were stronger on landscape-scale habitat selection, with large ZOIs of 5 to 10 km for the combination of mining and wind power (Table 2, Text B2). There was evidence of cumulative impacts of several wind power plants at landscape-scale habitat selection during summer season and at patch-scale habitat selection during calving season. In all other seasons and processes, the reindeer responses were better explained by the impact of the nearest wind turbine. Selection of reindeer for calving sites was affected by the mine, with a 10km ZOI radius (Table 2, Appendix D). Roads were barriers to reindeer movement during all seasons. Reindeer avoided crossing wind power plants during their construction phase in calving season and avoided crossing them during the operation phase in summer (Table 2, Text C2). During calving season, the

movement patterns were also impacted during the construction phase, leading to a ZOI of 5 km (Table 2, Appendix C).

Table 2. Summary of the impacts of mining and wind power on reindeer habitat selection and movement across seasons, scales, and processes. Seasons and infrastructure type are presented as rows and the processes and scales as columns. We show if there was a negative (-; avoidance/barrier) or positive (+; selection) impact of the mine and the wind turbines*, the estimated zone of influence (ZOI), and whether the impact of wind turbines accumulated (cumulative, indicating density effects, and nearest, indicating effect of the nearest wind turbine). Columns on "habitat" and "step selection", respectively, correspond to impacts representing avoidance in case they are negative, or selection when they are positive. "Barrier" corresponds to if the probability of reindeer crossing the wind power plants was significantly reduced, and "movement patterns" to the changes in movement rates and tortuosity of reindeer movement when close to the wind turbines.

Season		Infrastructure	Development phase	Landscape-scale habitat selection	Patch-scale step selection	Barrier	Movement patterns
SPRING/CALVING	Calving season	Wind turbines	Construction	**Nearest ZOI 5 km (-)**	**Cumulative ZOI 5 km (-)**	**Yes (-)**	**Cumulative ZOI 5 km (-)**
			Operation	**Nearest ZOI 5 km (-)**	**Cumulative ZOI 5 km (-)**	**No**	No effect
		Mine		**ZOI 10 km (-)**	No effect	Not evaluated	Not evaluated
	Calving sites	Wind turbines	Construction	Not evaluated	Not evaluated	Not evaluated	Not evaluated
			Operation	Not evaluated	Not evaluated	Not evaluated	Not evaluated
		Mine		**ZOI 10 km (-)**	Not evaluated	Not evaluated	Not evaluated
SUMMER	Summer season	Wind turbines	Construction	**Cumulative ZOI 10 km (+)**	**Nearest ZOI 5 km (+)**	**No**	No effect
			Operation	**Cumulative ZOI 10 km (+)**	**Nearest ZOI 5 km (+)**	**Yes (-)**	No effect
		Mine		**ZOI 10 km (-)**	**ZOI 5 km (-)**	Not evaluated	Not evaluated
AUTUMN	Autumn season	Wind turbines	Construction	**Nearest ZOI 10 km (-)**	No effect	**No**	No effect
			Operation	**Nearest ZOI 10 km (-)**	No effect	**No**	No effect
		Mine		**ZOI 10 km (-)**	No effect	Not evaluated	Not evaluated

3.1 Landscape-scale habitat selection

At landscape scale, there was a consistent avoidance of the mine in all seasons, with a ZOI radius of 10 km (Table 2, Fig. 3, Tables B4-B7). This is illustrated by the large white region around the mine in Kristineberg in the habitat suitability maps in Fig. 3, showing low habitat suitability. Moreover, reindeer selected calving sites were affected by the mine, also with 10-km ZOI (Table D2).

Comparing the difference in habitat suitability during the construction and operation phases with pre-construction habitat suitability, we observed strong avoidance of the wind power plants during calving and autumn season, with ZOIs of 5 km and 10 km, respectively (Table 2, Fig. 3). The impact was stronger during calving, both in the construction and the operation phase of the wind turbines (Fig. B3-B4, Fig. B9-B10). During these seasons, there was no evidence of cumulative impacts of the several wind power plants, instead the nearest turbine explained best the habitat selection patterns. In contrast, in summer the mountains where the wind turbines are located were highly selected before they were constructed. The selection was even stronger for areas close to wind turbines during the operation phase (Fig. 3, Fig. B6-B7) within a 10 km ZOI. Public roads were avoided in all seasons, and private roads and trails were avoided during calving and summer. Power lines were only avoided during calving (Table B4).

[Figure 3 here]

3.2 Patch-scale habitat selection

At patch scale, the wind turbines were avoided during calving, with a 5 km ZOI, and there were cumulative impacts of multiple wind turbines (Table C6). Comparing the impact of a single, isolated wind turbine with the impact of a wind power plant, the impact of a single turbine was small. In contrast, the impact of a wind power plant with 10 wind turbines was considerably larger, leading to avoidance of the wind power plant in coniferous forests and open areas (Fig. 4). The cumulative impact was most pronounced during the construction period (Fig. C1).

[Figure 4 here]

In summer, the mine was avoided but the high elevation areas close to the wind turbines were selected, similarly to what we found in the landscape-scale HSA, but with shorter ZOI radii and weaker effect sizes (Tables 2 and C7, Fig. C5). During autumn, we did not find effects of the mine and the wind turbines on patch-scale habitat selection (Table C8). Public and private roads were avoided in all seasons in the iSSA, but power lines and houses were not (Table C5).

3.3 Movement patterns

Reindeer avoided crossing wind power plants in calving during construction (and marginally during operation; $p = 0.07$; Table C5-C6), and also avoided crossing them in summer during the operation phase. Reinder avoided crossing public roads in all seasons (Table 2, Text C2). Movement parameters were affected by the cumulative impact of several wind turbines, but only in calving during the construction phase (Fig. 5, Table C9). During this period, animals presented higher movement rates (longer step lengths; Fig. 5A) and moved more linearly (turn angles more concentrated around zero; Fig. 5B) when moving close to the wind power plants then when far from them. This means that grazing was disturbed when reindeer were close to the wind turbines. We did not test for the impacts the mine or of other infrastructure on movement parameters. We did see a shift in movement patterns away from Jokkmokks- and Storliden wind power plants to the north along the RHC boundary as the reindeer moved from their calving lands east of the wind power plant towards their summer lands further west (Fig. 2)

[Figure 5 here]

3.4 Calving events in relation to green-up

The results of the Kruskal-Wallis tests showed that there were no differences in calving date among wind development phases for the individuals that roamed close to the wind turbines during calving in our study ($p > 0.05$). However, we observed a larger variation in date of calving during the operation phase compared to the other phases (Fig. D2). Moreover, there were no significant differences in the absolute difference between calving date and date of maximum IRG across phases among individuals who had been close to the wind turbines ($p = 0.1$) (Fig. D3).

4 Discussion

Understanding and managing cumulative impacts is a key challenge in environmental impact assessment and land-use management and planning. Even though cumulative impacts are widely acknowledged, most impact assessments remain focused on single projects and local effects, overlooking how multiple disturbances interact across landscapes (Foley et al., 2017; Gillingham et al., 2016). At the same time, anthropogenic impacts need to be understood from the perspective of the organisms and systems affected (Moreau et al., 2012; Skarin and Åhman, 2014), as they emerge through behavioural responses to changes in resources, risks, and environmental conditions. In this study, we address this knowledge gap by quantifying three key dimensions of cumulative impacts within a unified analytical framework: effect size, zone of influence, and accumulation across features of the same as well as different land use types. By applying this approach to a social-ecological system affected by both historical land-use conflicts and new infrastructure, we demonstrate how cumulative impacts can be explicitly measured and compared between seasons. We do this through analyses on different hierarchical levels, that relate to distinct behavioural processes: landscape-level habitat selection, linked to how animals select for their seasonal ranges within the landscape; landscape-level calving site selection, identifying where animals select to have their calving within the calving range; and patch-scale habitat selection and movement, which account for fine-scale animal movement while foraging for resources within the seasonal ranges. Including different seasons and behavioural processes, we aimed at acquiring a general understanding of cumulative impacts of human infrastructure on reindeer habitat.

4.1 Cumulative impacts of mining and wind power on reindeer habitat selection and movement

In all analyses, we found strong evidence that mining, wind power development, and other infrastructure affected reindeer habitat selection at large spatial scales, with impacts often accumulating. This avoidance was particularly pronounced at the landscape-scale, where ZOIs extended up to 5-10 km, including selection of calving sites. Such large-scale avoidance is expected at higher hierarchical levels, especially when animals have sufficient space to avoid disturbances (Skarin and Åhman, 2014). Our findings align with previous studies on *Rangifer* and other terrestrial species, which have documented similar responses to mining (Boulanger et al., 2021; Eftestøl et al., 2019; Plante et al., 2018), wind power (Eftestøl et al., 2023; Helldin et al., 2012; Klich et al., 2020; Skarin and Alam, 2017), and other infrastructure (Boulanger et al., 2024; Panzacchi et al., 2015; Prokopenko et al., 2017). Besides creating avoidance, wind power also affected reindeer movement patterns and hindered their movement. Together, these results confirm our expectations and show that impacts of infrastructure accumulate and span multiple behavioural processes, affecting the ability of reindeer to access high quality pastures and to have ‘grazing peace’, as referred to by Sámi reindeer herders (Inga, 2007).

We found that the size of the ZOI and how impacts accumulated was context-dependent, as it varied in space, across seasons and wind development phases, and with the scale and process observed. Evidence for cumulative impacts of several nearby features, evaluated using the method proposed by Niebuhr et al. (2023b) to distinguish between single and multi-feature effects, was found in specific cases – during calving at patch scale and during summer at landscape scale – but in many situations reindeer responses were better explained by the distance to the nearest wind turbine. Likewise, the extent of the ZOI of wind power plants, mine, and other disturbance also changed across time and space, as has been observed for other ecosystems and species (Martin, 2018; Pease, 2024). From an impact assessment perspective, our findings support that the magnitude and extent of impacts must be evaluated within a regional and temporal perspective, considering the whole landscape context with their previously existing and new anthropogenic pressures, and how species move within it along the year (Vistnes and Nellemann, 2008).

We observed the strongest impacts in spring during the spring/calving season. During this period, reindeer avoided the wind turbines at both landscape and patch scale, and the mine at landscape scale, including selection of calving site. They changed movement patterns near wind turbines especially during construction phase, when the industrial activities were most intense. Reindeer avoided crossing the wind power plants during construction, and marginally during operation, indicating a stronger barrier effect of construction activities. This agrees with the previous studies, which detected a 76% decrease in number of reindeer crossings through the construction sites of Jokkmokksliden and Storliden wind power plants (Skarin et al., 2015), and that this movement partly resumed during operation phase (Skarin et al. 2018). Additionally, increased movement rates (measured as increased step length) and more directional movement close to wind power plants during construction suggest that reindeer spent less time grazing when exposed to the wind turbine construction sites. These findings align with previous research showing a high sensitivity to disturbance during calving (Johnson et al., 2005; Moreau et al., 2012; Pinard et al., 2012; Wolfe et al., 2000) and underscore the importance of considering seasonal vulnerability in impact assessments (Johnson et al., 2021; Skarin and Åhman, 2014). Our re-analysis of a larger area considering the four main wind power plants also showed clear presence of cumulative impacts of multiple wind turbines at patch scale during calving season, which suggests that clustering of infrastructure can amplify impacts during a critical life-history stage for both adult reindeer and their calves (Vistnes and Nellemann, 2008).

Our results for calving season confirm and amplify those of previous studies with reindeer movement in Malå RHC, which showed the wind power plants of Jokkmokksliden and Storliden, together with the power lines and roads built with them, are avoided during both construction and operation (Skarin et al., 2018, 2015; Skarin and Alam, 2017). Skarin et al. (2018) also observed the avoidance of wind turbines was higher when they were visible for reindeer, and decreased when out-of-sight, for instance behind hills or on forested areas. This viewshed effect could not be tested through our analysis but should be further developed and applied within a cumulative impact framework. Likewise, the effects of the sound from wind turbines needs to be further explored as a mechanism for creating avoidance and barriers, particularly as part of cumulative impacts. We developed exploratory analyses based on weather-calibrated models of sound propagation from the wind turbines for the Malå RHC (Skarin et al., 2021), but modelled sound produced measures that were correlated with the distance to wind turbines, and was not evaluated further in our study.

Despite these strong habitat selection responses, and consequent the impacts during autumn seasons, when reindeer breed, we could not directly evaluate the effect of the wind turbines on the timing of parturition. A larger sample size could improve the power to detect such effects and allow further evaluation of potential ZOIs and cumulative impacts on timing of calving. However, the increased variation in timing of parturition in relation to green-up in 2018, independently of the proximity to wind power plants, may be related to climate-driven shifts in vegetation phenology and environmental conditions (Couriot et al., 2023; Paoli et al., 2018) or the breeding conditions during autumn. This suggests that wind power could produce local impacts on reindeer adding to the effect of climate change, even though they are implemented as a solution for climate change globally. These hypotheses require further investigation in long-term and multi-population studies.

In contrast to calving season and autumn, in summer reindeer selected areas near wind turbines at landscape and patch scales, both during construction and operation phases. This pattern might reflect a shift in the balance between avoidance to anthropogenic disturbance and other ecological drivers, particularly insect harassment. Insect activity is known to induce reindeer to move away from closed, forested areas towards more open and wind-exposed areas, even when these areas are associated with anthropogenic disturbance (Johnson et al., 2021; Skarin et al., 2004; Valente et al., 2020). In Malå RHC, particularly, there is no high mountains without wind turbines, and wind power development create large vegetation free areas which offer good exposure to wind. The presence of the fence along the Lapland border may also have contributed to this selection pattern by constraining movements and

increasing the use of certain areas, particularly around the Åmliden wind power plant (see Fig. 2). Despite this increased use, the wind power plants still hindered the movements of reindeer when trying to cross them during operation phase in summer, as also observed for calving season here and previously (Skarin et al., 2018).

The avoidance of the wind power plants and the mine in autumn further affected the reindeer possibility to select high-quality pastures, such as mires, to build up the energy reserves for the coming winter (Storeheier et al., 2003). This is especially important during years with increased insect harassment, when the time for grazing already might have been substantially reduced (Skarin et al., 2010; Valente et al., 2020; Witter et al., 2012). Furthermore, disturbance for grazing during autumn might affect breeding, leading to potential populational consequences in the following year.

We found clear evidence of cumulative impacts across different types of infrastructure. The combined effects of the mine, wind power plants, and other anthropogenic features such as roads indicate that reindeer respond to a landscape shaped by multiple, co-occurring disturbances. The mine showed strong and consistent effects across all seasons, causing large ZOIs and indicating clear avoidance patterns, including reduced use of areas for calving sites. Compared to wind power plants, which showed more variable effects, the mine represents a more permanent and intensive disturbance, which may explain its stronger influence. These results indicate that cumulative impacts arise not only from several features of the same type but also from the interaction of different infrastructure types, reinforcing the need for integrated assessments across development projects and sectors (Hodgson et al., 2019).

Our analyses are based on habitat selection and movement responses, which reflect relative patterns of space use rather than direct measures of habitat quality or fitness. While these metrics provide valuable insight into behavioural responses and spatial impacts, caution is needed when extrapolating to population-level consequences (Boyce et al., 2016; Matthiopoulos et al., 2015). Ideally, behavioural responses should be evaluated in combination with physiological and demographic responses, to create more comprehensive understanding of cumulative impacts on animal health and survival (Hodgson et al., 2019). In a reindeer husbandry context, using records of slaughter weight in autumn before and after wind power construction could potentially provide such an opportunity (cf. Lundqvist et al., 2009). Likewise, increased stress and movement in summer reduce foraging time, having a direct impact on growth and build-up of energy storage necessary for survival in winter (Åhman and White, 2018; Weladji and Holand, 2003), what could be further explored by integrating habitat and population data and models.

4.2 Relevance for impact assessment and land-use planning

Our findings have direct implications for environmental impact assessments and land-use planning processes. Current practices are often project-based and local in scope (Gillingham et al., 2016; Noble et al., 2017; Österlin and Raitio, 2020), which limits the ability to capture cumulative impacts across landscapes. In addition, earlier efforts to map cumulative impacts often end up with geographical location and the structural distribution of potential disturbance sources (Fohringer et al., 2021; Larsen et al., 2016; Stoessel et al., 2022), not evaluating functionally the dimensions of the impacts (Niebuhr et al., 2023b). The framework presented here provides a practical approach to address this limitation by quantifying both the spatial extent and the accumulation of impacts from multiple disturbances. By explicitly quantifying ZOIs and testing for cumulative impacts across infrastructure types, this approach makes it possible to move beyond single-project assessments and evaluate how multiple existing and planned developments interact across space. Furthermore, our approach provides a framework towards understanding the additional impacts new features contribute with when added into an already impacted landscape. This is of course the most common situation today as more development features is added into already complex landscape situations.

The large ZOIs and the cumulative impacts observed here indicate that the effective area influenced by industrial development can be several times larger than the area directly occupied by infrastructure, especially when multiple infrastructure occurs in proximity to each other. This highlights the need to account for indirect habitat loss, existing disturbance, and multiple ongoing projects in land-use planning processes. More broadly, the approach is transferrable to other species and systems and can support more comprehensive assessments in contexts such as renewable energy expansion, mining, and transportation networks. The framework also has potential to support predictive assessments by evaluating alternative development scenarios and identifying contexts and areas where cumulative impacts are likely to be highest (Dorber et al., 2023; Zhu et al., 2026).

Conclusion

While our work focus on spatial impacts on habitat suitability, impacts can also accumulate over time and across levels of ecological organization, from individual organisms to populations, landscapes, and ecosystems (Hodgson and Halpern, 2019; Matthiopoulos et al., 2015; Van Moorter et al., 2023). Likewise, zones of influence and cumulative impacts can have consequences for human communities and social-ecological livelihoods (Fan et al., 2022; Gillingham et al., 2016). Furthermore, in addition to new infrastructures, species and ecosystems are increasingly subject to other stressors such as climate change and altered vegetation dynamics, which interact to shape responses on animals and humans. Advancing cumulative impact assessment will therefore require both methodological developments and changes in policy and planning processes to move beyond project-based assessments toward integrated, landscape-scale and interdisciplinary approaches.

Sámi reindeer husbandry represents a social–ecological system in which animals, landscapes, and human practices are tightly interconnected (Holand et al., 2022). In reindeer husbandry, cumulative impacts affect not only animal behaviour but also reindeer herding activities and the ability of Sámi reindeer people to exercise their culture. Our study shows how combining movement and environmental data, as well as long-term experience and observations by reindeer herders that provide context to analyses, might help quantify these impacts and support the maintenance of reindeer husbandry and other social-ecological systems.

Acknowledgements

We thank the reindeer herders from Malå Sámi reindeer herding community for sharing their data and knowledge with us, what allowed the current assessment to be made. We also thank Naturvårdsverket, Energimyndgheten, and a panel of reviewers and followers for insightful discussions and suggestions in previous versions of the analysis and text, and Holger Dettki, Debora Arlt, and the WRAM team for support with the GPS database. BBN, MA, PS, and AS were supported by a grant from the Swedish Energy Agency within the research programme Vindval (grant no. 46780- 1). BBN, EC, PS, AS were funded by project MineDeer (Vinnova project no. 2019-05191). BBN, MP, BVM received support from the Research Council of Norway through the projects OneImpact (no. 287925) and GreenPlan (no. 326979). AS, LD were funded by Formas REINFORCE-project (Dnr 2021-01046). PS was also funded by Formas ScalingUp project (Dnr 2021-00044).

Author contributions. (CRediT)

Conceptualization: BBN, EC, LD, MA, MP, BMV, PS, AS. Funding acquisition, project administration, and supervision: AS, PS. Data curation, resources: BBN, EC, LD, PS, AS. Methodology: BBN, MA, MP, BVM, PS, AS. Software: BBN, BVM, PS, AS. Investigation, formal analysis, visualization: BBN, EC, LD, MA, PS, AS. Writing – original draft: BBN, EC, LD. Writing – review and editing: BBN, EC, LD, MA, MP, BVM, PS, AS.

Data statement

The GPS data is stored on the Wireless Remote Animal Movement Database (WRAM). All environmental data was retrieved from public sources, as detailed in Appendix A. The scripts for data

processing, GPS data cleaning, model fitting and model interpretation are documented publicly in a GitHub repository (https://github.com/SLU-Reindeer-Group/cumulative_impacts_mala), to be made public upon acceptance of the article.

Declaration of competing interests

The authors declare no competing interests that might have affected the present study.

Declaration of generative AI use

During the preparation of this work the authors used ChatGPT, v. 5.3 in order to find repetitions and places where the text writing could be improved, for the sake of clarity. No text presented in the article was directly generated by AI. The authors take full responsibility for the content of the published article.

References

Åhman, B., White, R.G., 2018. Rangifer Diet and Nutritional Needs, in: Reindeer and Caribou. CRC Press.

Avgar, T., Lele, S.R., Keim, J.L., Boyce, M.S., 2017. Relative Selection Strength: Quantifying effect size in habitat- and step-selection inference. Ecol Evol 7, 5322–5330. https://doi.org/10.1002/ece3.3122

Avgar, T., Potts, J.R., Lewis, M.A., Boyce, M.S., 2016. Integrated step selection analysis: bridging the gap between resource selection and animal movement. Methods Ecol Evol 7, 619–630. https://doi.org/10.1111/2041-210X.12528

Barraquand, F., Benhamou, S., 2008. Animal Movements in Heterogeneous Landscapes: Identifying Profitable Places and Homogeneous Movement Bouts. Ecology 89, 3336–3348. https://doi.org/10.1890/08-0162.1

Barrio, I.C., Vuorinen, K.E.M., Barbero-Palacios, L., Defourneaux, M., Bon, M.P., Greer, E.A., Anderson, H.B., Horstkotte, T., Lecomte, N., Windirsch, T., Ferraro, K., Forbes, B.C., Forbey, J.S., García Criado, M., Hagenberg, L., Hik, D.S., Kater, I., Macek, P., Moen, J., Sundqvist, M.K., Szejgis, J., Villoslada, M., Zaja, E., Berthelot, F., Björnsdóttir, K., Cunow, J., Den Herder, M., Eskelinen, A., Hayes, K., Hollister, R.D., Í Haraldsstovu, K., Jónsdóttir, I.S., Kristensen, J.A., Lameris, T.K., Oksanen, L., Oksanen, T., Olofsson, J., Park, T., Pedersen, Å.Ø., Ramirez, J.I., Ravolainen, V.T., Roy, A., Ryde, I., Schmidt, N.M., Schrofner-Brunner, B., Skarin, A., Speed, J.D.M., Te Beest, M., Simmonds, M., Torres, R.T., Traylor, W., Virtanen, R., Wheeler, H.C., Alatalo, J.M., Axmacher, J.C., Bartolomé Filella, J., Cooper, E.J., Geange, S.R., Gilg, O., Grogan, P., Hernández-Castellano, C., Høye, T.T., Kerby, J.T., Klanderud, K., Koltz, A.M., Lang, J., Le Moullec, M., Loonen, M.J.J.E., Macias-Fauria, M., Post, E., Serrano, E., Siewert, M., Sokolov, A., Sokolova, N., Suominen, O., Tamayo, M., Terekhina, A., Volkovitskiy, A., Kamenova, S., 2025. Emerging priorities in terrestrial herbivory research in the Arctic. Arctic Science 11, 1–26. https://doi.org/10.1139/as-2024-0080

Benítez-López, A., Alkemade, R., Verweij, P.A., 2010. The impacts of roads and other infrastructure on mammal and bird populations: A meta-analysis. Biological Conservation 143, 1307–1316. https://doi.org/10.1016/j.biocon.2010.02.009

Bischof, R., Loe, L.E., Meisingset, E.L., Zimmermann, B., Van Moorter, B., Mysterud, A., 2012. A Migratory Northern Ungulate in the Pursuit of Spring: Jumping or Surfing the Green Wave? The American Naturalist 180, 407–424. https://doi.org/10.1086/667590

Bjørneraas, K., Moorter, B.V., Rolandsen, C.M., Herfindal, I., 2010. Screening Global Positioning System Location Data for Errors Using Animal Movement Characteristics. wild 74, 1361–1366. https://doi.org/10.2193/2009-405

Boulanger, J., Kite, R., Campbell, M., Shaw, J., Lee, D., Atkinson, S., 2024. Estimating the effects of roads on migration: a barren-ground caribou case study. Canadian Journal of Zoology 102, 476–493. https://doi.org/10.1139/cjz-2023-0121

Boulanger, J., Poole, K.G., Gunn, A., Adamczewski, J., Wierzchowski, J., 2021. Estimation of trends in zone of influence of mine sites on barren-ground caribou populations in the Northwest

Territories, Canada, using new methods. Wildlife Biology 2021. https://doi.org/10.2981/wlb.00719
Boyce, M.S., Johnson, C.J., Merrill, E.H., Nielsen, S.E., Solberg, E.J., van Moorter, B., 2016. Can habitat selection predict abundance? Journal of Animal Ecology 85, 11–20. https://doi.org/10.1111/1365-2656.12359
Bracis, C., Bildstein, K.L., Mueller, T., 2018. Revisitation analysis uncovers spatio-temporal patterns in animal movement data. Ecography 41, 1801–1811. https://doi.org/10.1111/ecog.03618
Burnham, K.P., Anderson, D.R., 2002. Model selection and multimodel inference: a practical information-theoretic approach, 2nd ed. ed. Springer, New York.
Calenge, C., Dray, contributions from S., Royer, M., 2023. adehabitatLT: Analysis of Animal Movements.
Cambou, D., Sandström, P., Skarin, A., Borg, E., 2021. Reindeer husbandry vs. wind energy, in: Indigenous Peoples, Natural Resources and Governance. Routledge, London, pp. 39–58. https://doi.org/10.4324/9781003131274-3
Couriot, O.H., Cameron, M.D., Joly, K., Adamczewski, J., Campbell, M.W., Davison, T., Gunn, A., Kelly, A.P., Leblond, M., Williams, J., Fagan, W.F., Brose, A., Gurarie, E., 2023. Continental synchrony and local responses: Climatic effects on spatiotemporal patterns of calving in a social ungulate. Ecosphere 14, e4399. https://doi.org/10.1002/ecs2.4399
Cowan, M.A., Forrest, S.W., Setterfield, S.A., Dunlop, J.A., Gibson, L.A., Nimmo, D.G., 2025. The impact of mining on animal movement and landscape connectivity revealed through simulations and scenarios. Ecological Applications 35, e70134. https://doi.org/10.1002/eap.70134
Dorber, M., Panzacchi, M., Strand, O., van Moorter, B., 2023. New indicator of habitat functionality reveals high risk of underestimating trade-offs among sustainable development goals: The case of wild reindeer and hydropower. Ambio 52, 757–768. https://doi.org/10.1007/s13280-022-01824-x
Eftestøl, S., Flydal, K., Tsegaye, D., Colman, J.E., 2019. Mining activity disturbs habitat use of reindeer in Finnmark, Northern Norway. Polar Biol 42, 1849–1858. https://doi.org/10.1007/s00300-019-02563-8
Eftestøl, S., Tsegaye, D., Flydal, K., Colman, J., 2023. Effects of Wind Power Development on Reindeer: Global Positioning System Monitoring and Herders' Experience. Rangeland Ecology & Management 87, 55–68. https://doi.org/10.1016/j.rama.2022.11.011
Engen, S., Hausner, V.H., Fauchald, P., Ruud, A., Broderstad, E.G., 2023. Small hydropower, large obstacle? Exploring land use conflict, Indigenous opposition and acceptance in the Norwegian Arctic. Energy Research & Social Science 95, 102888. https://doi.org/10.1016/j.erss.2022.102888
Fan, P., Cho, M.S., Lin, Z., Ouyang, Z., Qi, J., Chen, J., Moran, E.F., 2022. Recently constructed hydropower dams were associated with reduced economic production, population, and greenness in nearby areas. Proc. Natl. Acad. Sci. U.S.A. 119, e2108038119. https://doi.org/10.1073/pnas.2108038119
Fieberg, J., Signer, J., Smith, B., Avgar, T., 2021. A 'How to' guide for interpreting parameters in habitat-selection analyses. J Anim Ecol 90, 1027–1043. https://doi.org/10.1111/1365-2656.13441
Fohringer, C., Rosqvist, G., Inga, N., Singh, N.J., 2021. Reindeer husbandry in peril?—How extractive industries exert multiple pressures on an Arctic pastoral ecosystem. People and Nature 3, 872–886. https://doi.org/10.1002/pan3.10234
Foley, M.M., Mease, L.A., Martone, R.G., Prahler, E.E., Morrison, T.H., Murray, C.C., Wojcik, D., 2017. The challenges and opportunities in cumulative effects assessment. Environmental Impact Assessment Review 62, 122–134. https://doi.org/10.1016/j.eiar.2016.06.008
Gillingham, M.P., Halseth, G.R., Johnson, C.J., Parkes, M.W. (Eds.), 2016. The Integration Imperative: cumulative environmental, community and health effects of multiple natural resource developments. Springer International Publishing, Cham. https://doi.org/10.1007/978-3-319-22123-6
Gundersen, V., Myrvold, K.M., Kaltenborn, B.P., Strand, O., Kofinas, G., 2022. A review of reindeer (*Rangifer tarandus tarandus*) disturbance research in Northern Europe: towards a social-

ecological framework? Landscape Research 1–17. https://doi.org/10.1080/01426397.2022.2078486
Halpern, B.S., McLeod, K.L., Rosenberg, A.A., Crowder, L.B., 2008. Managing for cumulative impacts in ecosystem-based management through ocean zoning. Ocean & Coastal Management 51, 203–211. https://doi.org/10.1016/j.ocecoaman.2007.08.002
Helldin, J.O., Jung, J., Neumann, W., Olsson, M., Skarin, A., Widemo, F., 2012. The impacts of wind power on terrestrial mammals: a synthesis (No. 6510), VindVal. Naturvårdsverket, Stockholm.
Hirzel, A.H., Le Lay, G., 2008. Habitat suitability modelling and niche theory. Journal of Applied Ecology 45, 1372–1381. https://doi.org/10.1111/j.1365-2664.2008.01524.x
Hodgson, E.E., Halpern, B.S., 2019. Investigating cumulative effects across ecological scales. Conservation Biology 33, 22–32. https://doi.org/10.1111/cobi.13125
Hodgson, E.E., Halpern, B.S., Essington, T.E., 2019. Moving Beyond Silos in Cumulative Effects Assessment. Front. Ecol. Evol. 7. https://doi.org/10.3389/fevo.2019.00211
Holand, Ø., Horstkotte, T., Kumpula, J., Moen, J., 2022. Reindeer pastoralism in Fennoscandia, in: Horstkotte, T., Holand, Ø., Kumpula, J., Moen, J. (Eds.), Reindeer Husbandry and Global Environmental Change. Routledge, London, pp. 7–47. https://doi.org/10.4324/9781003118565-3
Horstkotte, T., Kumpula, J., Sandström, P., Tømmervik, H., Kivinen, S., Skarin, A., Moen, J., Sandström, S., 2022. Pastures under pressure: Effects of other land users and the environment, in: Reindeer Husbandry and Global Environmental Change. Routledge.
Inga, B., 2007. Reindeer (Rangifer tarandus tarandus) feeding on lichens and mushrooms: traditional ecological knowledge among reindeer-herding Sami in northern Sweden. Rangifer 27, 93–106. https://doi.org/10.7557/2.27.2.163
James, G., Witten, D., Hastie, T., Tibshirani, R., 2021. An introduction to statistical learning: with applications in R, Second edition. ed, Springer texts in statistics. Springer, New York.
Johnson, C.J., Boyce, M.S., Case, R.L., Cluff, H.D., Gau, R.J., Gunn, A., Mulders, R., 2005. Cumulative effects of human developments on Arctic wildlife. Wildlife Monographs 160, 1–36.
Johnson, D.H., 1980. The Comparison of Usage and Availability Measurements for Evaluating Resource Preference. Ecology 61, 65–71. https://doi.org/10.2307/1937156
Johnson, H.E., Golden, T.S., Adams, L.G., Gustine, D.D., Lenart, E.A., Barboza, P.S., 2021. Dynamic selection for forage quality and quantity in response to phenology and insects in an Arctic ungulate. Ecology and Evolution 11, 11664–11688. https://doi.org/10.1002/ece3.7852
Katzner, T.E., Nelson, D.M., Marques, A.T., Voigt, C.C., Lambertucci, S.A., Rebolo, N., Bernard, E., Diehl, R., Murgatroyd, M., 2025. Impacts of onshore wind energy production on biodiversity. Nat. Rev. Biodivers. 1, 567–580. https://doi.org/10.1038/s44358-025-00078-1
Klich, D., Łopucki, R., Ścibior, A., Gołębiowska, D., Wojciechowska, M., 2020. Roe deer stress response to a wind farms: Methodological and practical implications. Ecological Indicators 117, 106658. https://doi.org/10.1016/j.ecolind.2020.106658
Kong, D., McVicar, T.R., Xiao, M., Zhang, Y., Peña-Arancibia, J.L., Filippa, G., Xie, Y., Gu, X., 2022. *phenofit* : A R package for extracting vegetation phenology from time series remote sensing. Methods Ecol Evol 2041–210X.13870. https://doi.org/10.1111/2041-210X.13870
Larsen, R.K., Raitio, K., Sandström, P., Skarin, A., Stinnerbom, M., Wik-Karlsson, J., Sandström, S., Österlin, C., Buhot, Y., 2016. Kumulativa effekter av exploateringar på renskötseln: vad behöver göras inom tillståndsprocesser (No. 6722), Naturvårdsverket Rapport. Naturvårdsverket, Stockholm.
Lundqvist, H., Norell, L., Danell, Ö., 2009. Relationships between biotic and abiotic range characteristics and productivity of reindeer husbandry in Sweden. Rangifer 29, 1–24. https://doi.org/10.7557/2.29.1.198
Martin, A.E., 2018. The Spatial Scale of a Species' Response to the Landscape Context Depends on which Biological Response You Measure. Curr Landscape Ecol Rep 3, 23–33. https://doi.org/10.1007/s40823-018-0030-z
Matthiopoulos, J., Fieberg, J., Aarts, G., Beyer, H.L., Morales, J.M., Haydon, D.T., 2015. Establishing the link between habitat selection and animal population dynamics. Ecological Monographs 85, 413–436. https://doi.org/10.1890/14-2244.1

Matthiopoulos, J., Fieberg, J.R., Aarts, G., 2023. Species-Habitat Associations: Spatial data, predictive models, and ecological insights, 2nd Edition. University of Minnesota Libraries Publishing. https://doi.org/10.24926/2020.081320

Moreau, G., Fortin, D., Couturier, S., Duchesne, T., 2012. Multi-level functional responses for wildlife conservation: the case of threatened caribou in managed boreal forests. Journal of Applied Ecology 49, 611–620. https://doi.org/10.1111/j.1365-2664.2012.02134.x

Moreira, E.F., Boscolo, D., Viana, B.F., 2015. Spatial Heterogeneity Regulates Plant-Pollinator Networks across Multiple Landscape Scales. PLoS ONE 10, e0123628. https://doi.org/10.1371/journal.pone.0123628

Naturvårdsverket, 2020. National Land Cover Database (NMD) – Product Description. Swedish Environmental Protection Agency (Naturvårdsverket). https://geodata.naturvardsverket.se/nedladdning/marktacke/NMD2018/NMD2018_ProductDescription_ENG.pdf [2026-02-23].

Niebuhr, B.B., Panzacchi, M., Van Moorter, B., 2023a. Oneimpact package version 0.1.1: Tools for the assessment of the cumulative impacts of anthropogenic features in ecological studies.

Niebuhr, B.B., Sant'Ana, D., Panzacchi, M., Van Moorter, B., Sandström, P., Morato, R.G., Skarin, A., 2022. Renewable energy infrastructure impacts biodiversity beyond the area it occupies. Proc. Natl. Acad. Sci. U.S.A. 119, e2208815119. https://doi.org/10.1073/pnas.2208815119

Niebuhr, B.B., Van Moorter, B., Stien, A., Tveraa, T., Strand, O., Langeland, K., Sandström, P., Alam, M., Skarin, A., Panzacchi, M., 2023b. Estimating the cumulative impact and zone of influence of anthropogenic features on biodiversity. Methods in Ecology and Evolution 14, 2362–2375. https://doi.org/10.1111/2041-210X.14133

Noble, B., Liu, J., Hackett, P., 2017. The Contribution of Project Environmental Assessment to Assessing and Managing Cumulative Effects: Individually and Collectively Insignificant? Environmental Management 59, 531–545. https://doi.org/10.1007/s00267-016-0799-7

Österlin, C., Raitio, K., 2020. Fragmented Landscapes and Planscapes—The Double Pressure of Increasing Natural Resource Exploitation on Indigenous Sámi Lands in Northern Sweden. Resources 9, 104. https://doi.org/10.3390/resources9090104

Panzacchi, M., Van Moorter, B., Strand, O., 2013. A road in the middle of one of the last wild reindeer migration routes in Norway: crossing behaviour and threats to conservation. Rangifer 15–26. https://doi.org/10.7557/2.33.2.2521

Panzacchi, M., van Moorter, B., Strand, O., Loe, L.E., Reimers, E., 2015. Searching for the fundamental niche using individual-based habitat selection modelling across populations. Ecography 38, 659–669. https://doi.org/10.1111/ecog.01075

Panzacchi, M., Van Moorter, B., Strand, O., Saerens, M., Kivimäki, I., St. Clair, C.C., Herfindal, I., Boitani, L., 2016. Predicting the *continuum* between corridors and barriers to animal movements using Step Selection Functions and Randomized Shortest Paths. J Anim Ecol 85, 32–42. https://doi.org/10.1111/1365-2656.12386

Paoli, A., Weladji, R.B., Holand, Ø., Kumpula, J., 2018. Winter and spring climatic conditions influence timing and synchrony of calving in reindeer. PLOS ONE 13, e0195603. https://doi.org/10.1371/journal.pone.0195603

Pease, B.S., 2024. Ecological scales of effect vary across space and time. Ecography 2024, e07163. https://doi.org/10.1111/ecog.07163

Pinard, V., Dussault, C., Ouellet, J.-P., Fortin, D., Courtois, R., 2012. Calving rate, calf survival rate, and habitat selection of forest-dwelling caribou in a highly managed landscape. The Journal of Wildlife Management 76, 189–199. https://doi.org/10.1002/jwmg.217

Plante, S., Dussault, C., Richard, J.H., Côté, S.D., 2018. Human disturbance effects and cumulative habitat loss in endangered migratory caribou. Biological Conservation 224, 129–143. https://doi.org/10.1016/j.biocon.2018.05.022

Polfus, J.L., Hebblewhite, M., Heinemeyer, K., 2011. Identifying indirect habitat loss and avoidance of human infrastructure by northern mountain woodland caribou. Biological Conservation 144, 2637–2646. https://doi.org/10.1016/j.biocon.2011.07.023

Prokopenko, C.M., Boyce, M.S., Avgar, T., 2017. Characterizing wildlife behavioural responses to roads using integrated step selection analysis. J Appl Ecol 54, 470–479. https://doi.org/10.1111/1365-2664.12768

R Core Team, 2024. R: A Language and Environment for Statistical Computing. R Foundation for Statistical Computing, Vienna, Austria.
Rio-Maior, H., Nakamura, M., Álvares, F., Beja, P., 2019. Designing the landscape of coexistence: Integrating risk avoidance, habitat selection and functional connectivity to inform large carnivore conservation. Biological Conservation 235, 178–188. https://doi.org/10.1016/j.biocon.2019.04.021
Sametinget, 2022. RenGIS 2.0, https://www.sametinget.se/renGIS.
Signer, J., Fieberg, J., Avgar, T., 2019. Animal movement tools (amt): R package for managing tracking data and conducting habitat selection analyses. Ecol Evol 9, 880–890. https://doi.org/10.1002/ece3.4823
Sih, A., 1980. Optimal Behavior: Can Foragers Balance Two Conflicting Demands? Science 210, 1041–3. https://doi.org/10.1126/science.210.4473.1041
Skarin, A., Åhman, B., 2014. Do human activity and infrastructure disturb domesticated reindeer? The need for the reindeer's perspective. Polar Biol 37, 1041–1054. https://doi.org/10.1007/s00300-014-1499-5
Skarin, A., Alam, M., 2017. Reindeer habitat use in relation to two small wind farms, during preconstruction, construction, and operation. Ecol Evol 7, 3870–3882. https://doi.org/10.1002/ece3.2941
Skarin, A., Danell, Ö., Bergström, R., Moen, J., 2010. Reindeer movement patterns in alpine summer ranges. Polar Biol 33, 1263–1275. https://doi.org/10.1007/s00300-010-0815-y
Skarin, A., Danell, Ö., Bergström, R., Moen, J., 2004. Insect avoidance may override human disturbances in reindeer habitat selection. Rangifer 24, 95–103. https://doi.org/10.7557/2.24.2.306
Skarin, A., Kumpula, J., Tveraa, T., Åhman, B., 2022a. Reindeer behavioural ecology and use of pastures in pastoral livelihoods, in: Reindeer Husbandry and Global Environmental Change. Routledge.
Skarin, A., Nellemann, C., Rönnegård, L., Sandström, P., Lundqvist, H., 2015. Wind farm construction impacts reindeer migration and movement corridors. Landscape Ecol 30, 1527–1540. https://doi.org/10.1007/s10980-015-0210-8
Skarin, A., Niebuhr, B.B., Sandström, P., Tømmervik, H., 2022b. Den ekologiska bevisföringen i Fosenmålet - Analys av renens användning av vinterbetesmarkerna och konsekvenser av vindkraftutbyggnad. Tidsskriftet Utmark 2022–1, 1–9.
Skarin, A., Sandström, P., Alam, M., 2018. Out of sight of wind turbines-Reindeer response to wind farms in operation. Ecol Evol 8, 9906–9919. https://doi.org/10.1002/ece3.4476
Skarin, A., Sandström, P., Niebuhr, B.B., Alam, M., Adler, S., 2021. Renar, renskötsel och vindkraft: vinter- och barmarksbete. Naturvårdsverket, Stockholm.
Sonter, L.J., Dade, M.C., Watson, J.E.M., Valenta, R.K., 2020. Renewable energy production will exacerbate mining threats to biodiversity. Nat Commun 11, 4174. https://doi.org/10.1038/s41467-020-17928-5
Stoessel, M., Moen, J., Lindborg, R., 2022. Mapping cumulative pressures on the grazing lands of northern Fennoscandia. Sci Rep 12, 16044. https://doi.org/10.1038/s41598-022-20095-w
Storeheier, P.V., Sehested, J., Diernæs, L., Sundset, M.A., Mathiesen, S.D., 2003. Effects of seasonal changes in food quality and food intake on the transport of sodium and butyrate across ruminal epithelium of reindeer. J Comp Physiol B 173, 391–399. https://doi.org/10.1007/s00360-003-0345-9
Torres, A., Jaeger, J.A.G., Alonso, J.C., 2016. Assessing large-scale wildlife responses to human infrastructure development. Proc Natl Acad Sci USA 113, 8472–8477. https://doi.org/10.1073/pnas.1522488113
Valente, S., Skarin, A., Ciucci, P., Uboni, A., 2020. Attacked from two fronts: Interactive effects of anthropogenic and biotic disturbances generate complex movement patterns. Arctic, Antarctic, and Alpine Research 52, 27–40. https://doi.org/10.1080/15230430.2019.1698251
Van Moorter, B., Kivimäki, I., Panzacchi, M., Saura, S., Niebuhr, B.B., Strand, O., Saerens, M., 2023. Habitat functionality: Integrating environmental and geographic space in niche modeling for conservation planning. Ecology 104, e4105. https://doi.org/10.1002/ecy.4105

Vistnes, I., Nellemann, C., 2008. The matter of spatial and temporal scales: a review of reindeer and caribou response to human activity. Polar Biol 9.

Weiss, A.D., 2001. Topographic Position and Landforms Analysis. Presented at the ESRI User Conference.

Weladji, R.B., Holand, Ø., 2003. Sex ratio variation in reindeer Rangifer tarandus: a test of the extrinsic modification hypothesis. Wildlife Biology 9, 29–36. https://doi.org/10.2981/wlb.2003.005

Witter, L.A., Johnson, C.J., Croft, B., Gunn, A., Gillingham, M.P., 2012. Behavioural trade-offs in response to external stimuli: time allocation of an Arctic ungulate during varying intensities of harassment by parasitic flies. Journal of Animal Ecology 81, 284–295. https://doi.org/10.1111/j.1365-2656.2011.01905.x

Wolfe, S.A., Griffith, B., Wolfe, C.A.G., 2000. Response of reindeer and caribou to human activities. Polar Research 19, 63–73. https://doi.org/10.1111/j.1751-8369.2000.tb00329.x

Zhu, Z., Yang, W., Cai, W., Peng, W., Wu, C., 2026. Scenario-based cumulative impacts assessment on iconic species habitats under marine spatial planning and fishing policies in the Yangtze River Estuary. Environmental Impact Assessment Review 119, 108356. https://doi.org/10.1016/j.eiar.2026.108356

Appendices

Figure 1

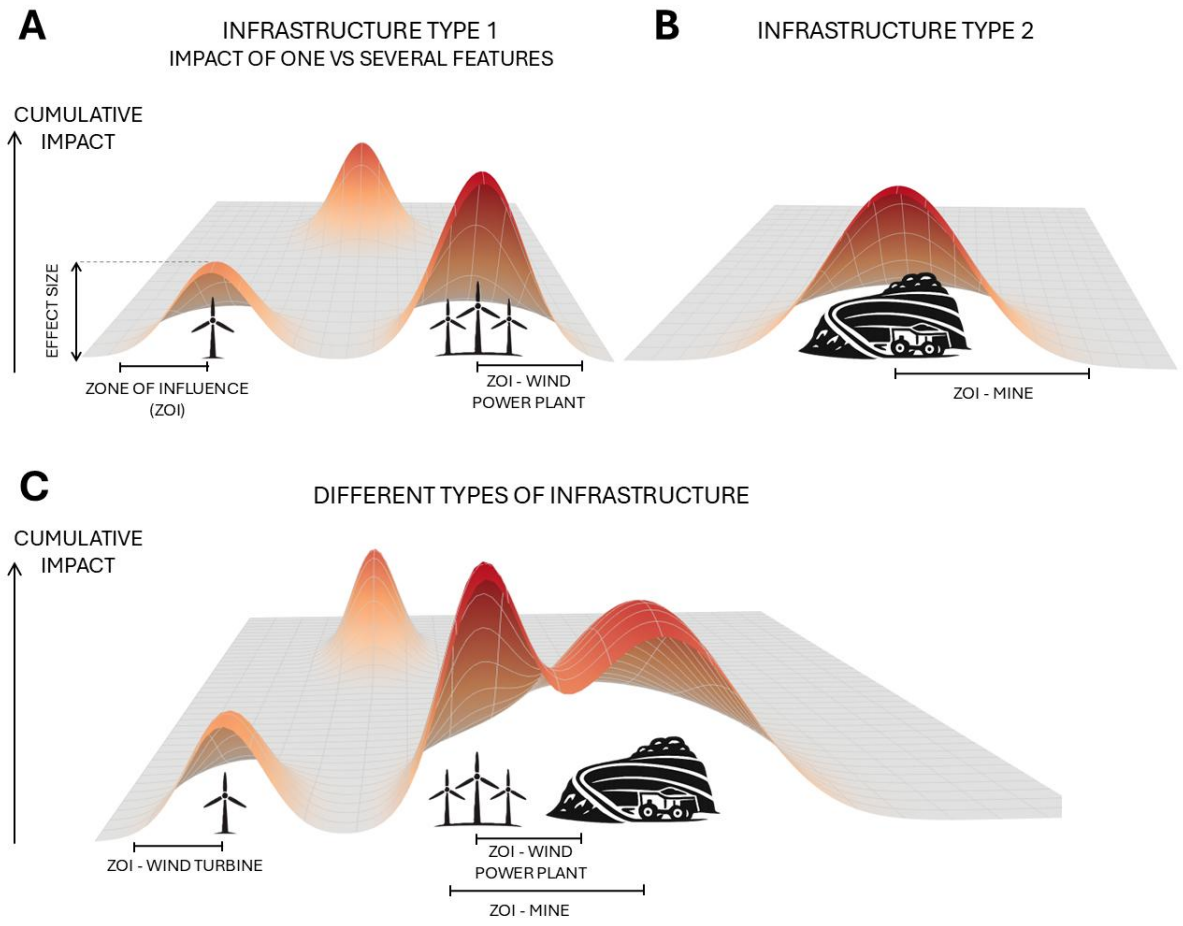

Figure 1. Illustration of the multiple dimensions of the impacts measured in this study. The total cumulative impact is defined by the combination of effect size and spatial extent of overlapping zones of influence. It is shown as the volume under the surface and varies in space depending on the distribution of infrastructure. (A) The impact of one single wind turbine is defined by the effect size and the zone of influence (ZOI) radius. When several wind turbines lie together in a wind power plant, the cumulative impact is larger than the impact for one single turbine. (B) The impact of a mine has an effect size and ZOI radius, different from those of wind turbines. (C) When wind turbines and mines are close together, their ZOIs overlap and the total, cumulative impact is locally higher. The figure uses wind turbines and mine as examples, but the principle can be applied to any other infrastructure or disturbance.

896 Figure 2

897

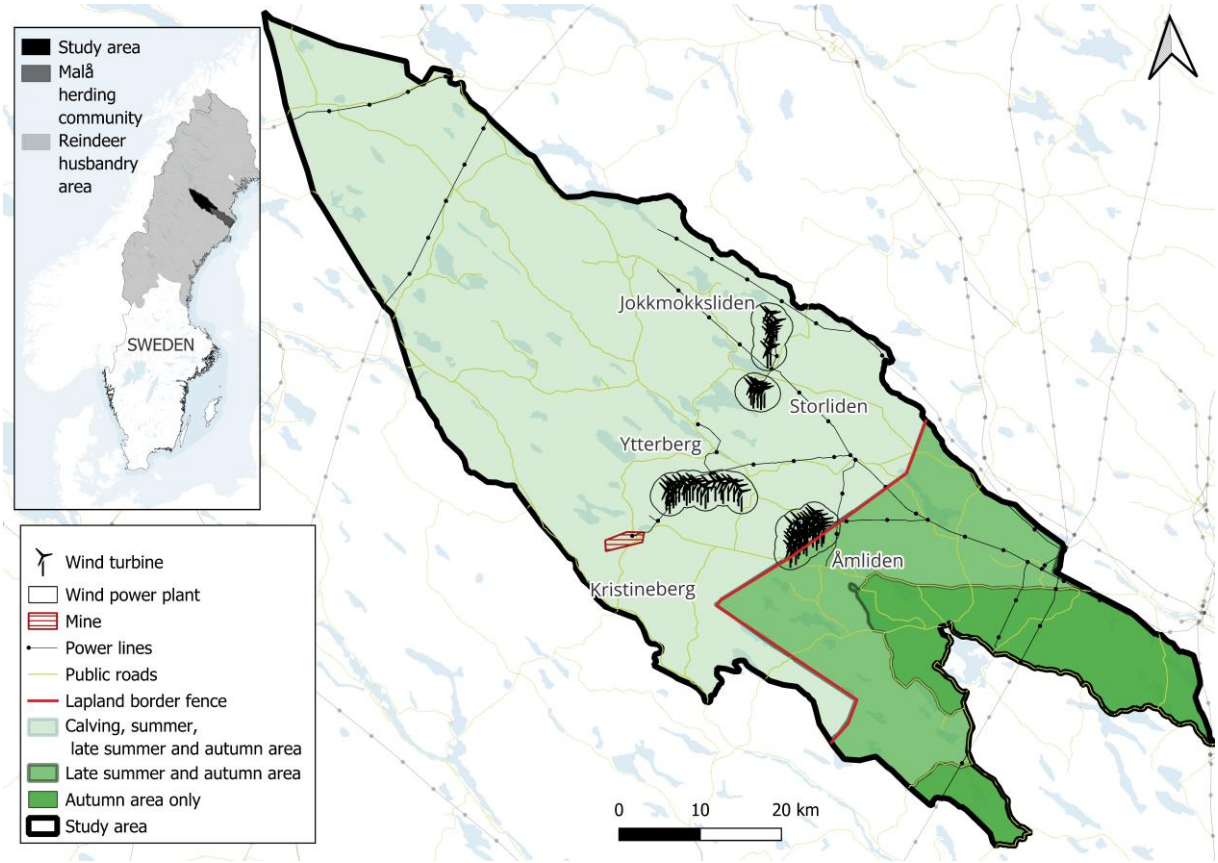

898

899 Figure 2. Illustration of the study area in Malå Sámi reindeer herding community in Sweden, with the
900 main infrastructure highlighted (wind power plants, mine, power lines, and public roads). The upper
901 left inset shows the location of the study area within the reindeer husbandry area in Sweden. The area
902 is crossed by a fence along the border of Lapland, which limits the area available for reindeer in
903 calving and early summer.

904 Figure 3

905

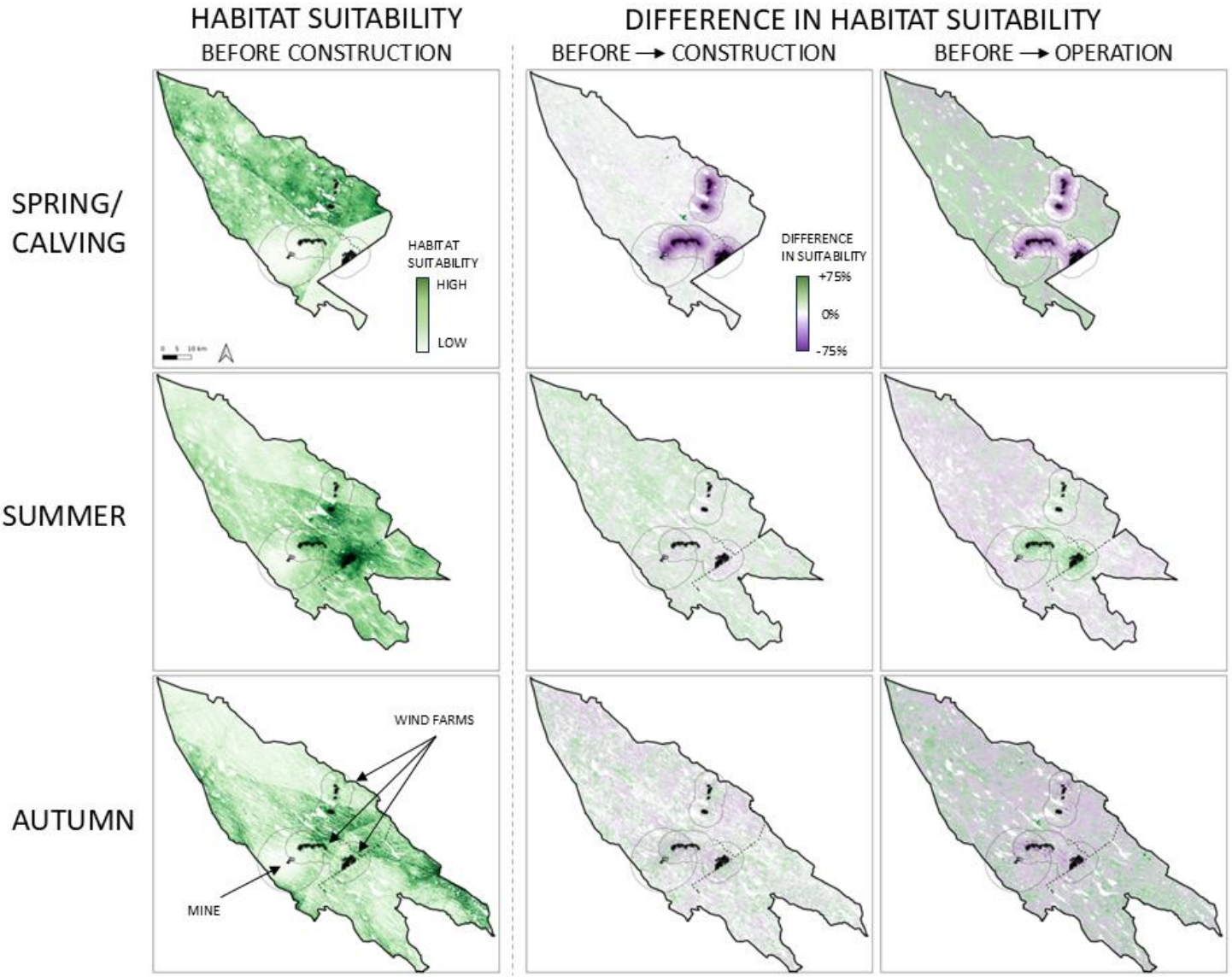

906 Figure 3. Predicted habitat suitability of reindeer at the landscape-scale within each season. A buffer of
907 10 km around the mine and 5 km around the wind power plants is added, for reference, and the
908 Lapland border fence is shown as a dashed line. The first column shows the predicted habitat
909 suitability in the pre-construction period, before the construction of the wind power plants (2008-
910 2009). The other two columns show the proportional difference between the pre-construction habitat
911 suitability and the suitability during the construction (2010-2011) and the operation (2015-2018) of the
912 four wind power plants. Note that the mine was already present from the beginning and was avoided in
913 all seasons.

914

915 Figure 4

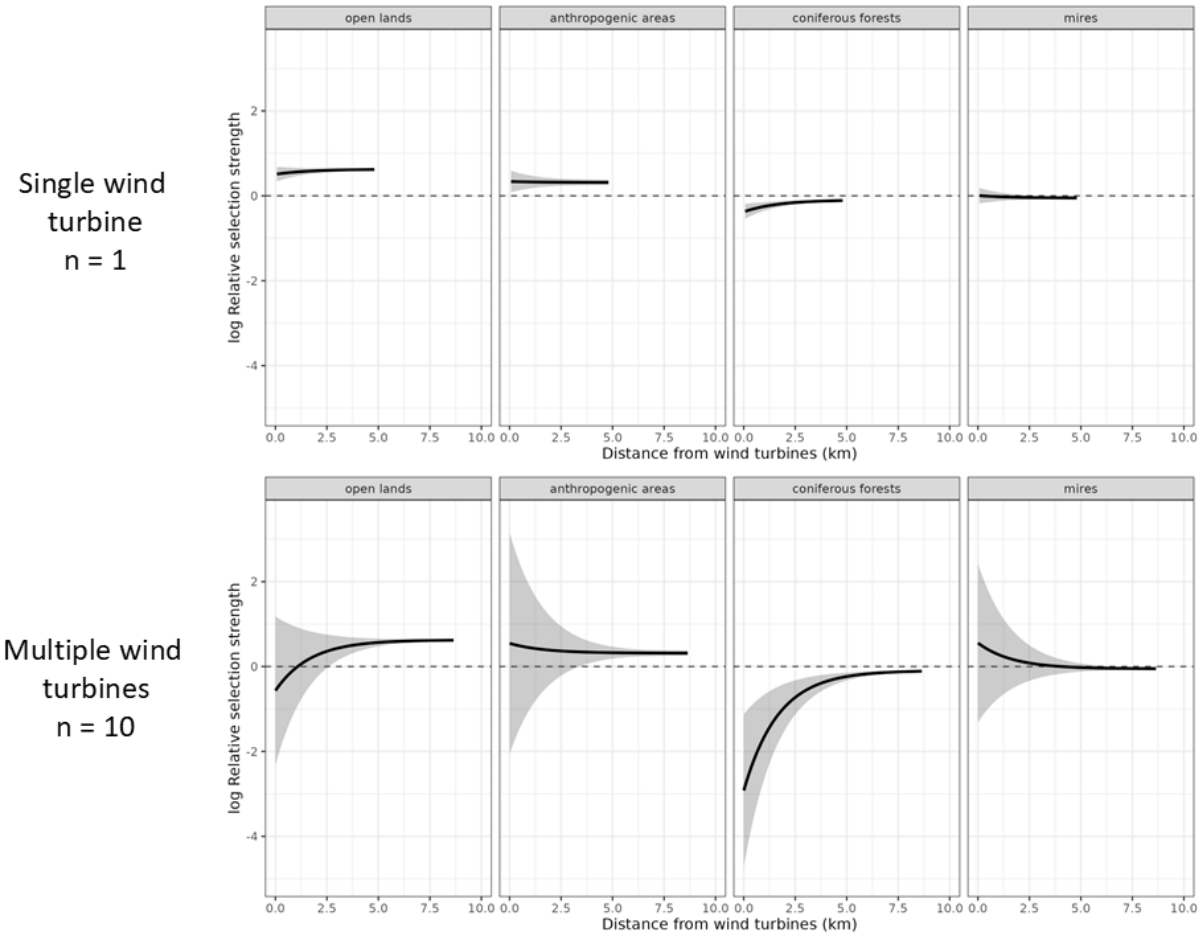

916

917 Figure 4. Illustration of the impact of a single wind turbine (upper row) and the cumulative impact of
918 several turbines (bottom row) on patch-scale habitat selection (iSSA) in calving during the
919 construction phase, with ZOI of 5 km. The response curves show the mean (and 95% confidence
920 interval) predicted relative selection strength (in log scale) against the distance to wind turbines in
921 different land use classes, using deciduous forest as a reference and keeping all other variables
922 constant. Smaller relative selection strength values indicate relative avoidance.

923

924 Figure 5

925

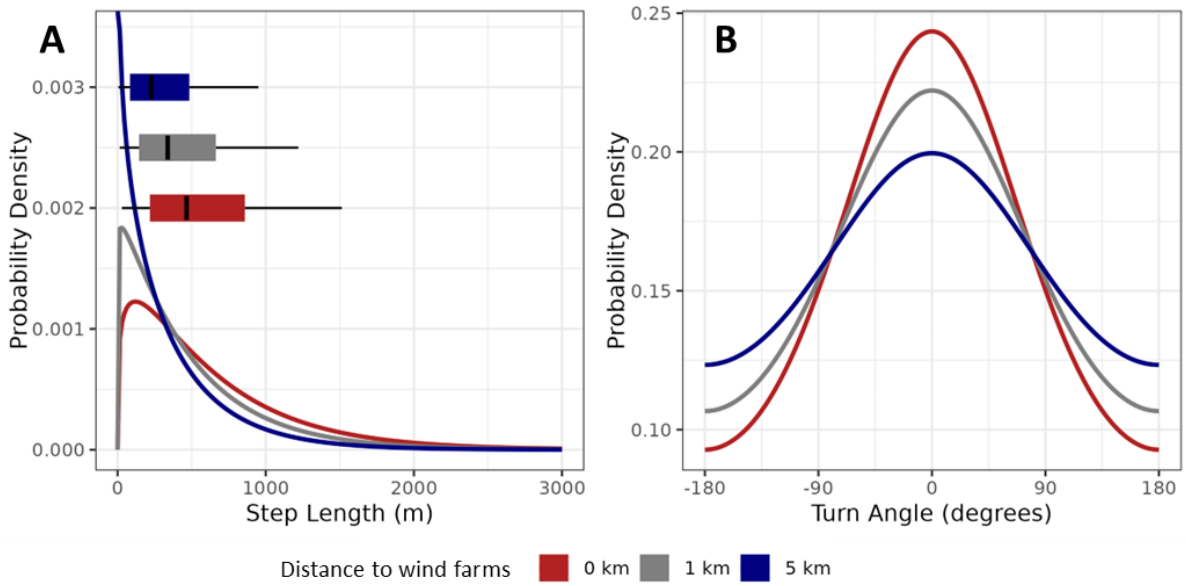

926

927 Figure 5. Prediction of the (A) step lengths (distance walked every 2 h) and (B) turn angles (between
928 subsequent displacements) for reindeer in calving during the construction of the wind power plants in
929 Malå RHC. Higher step lengths and lower turn angles indicate faster and more directional movement
930 when reindeer were close to the wind turbines (distance = 0) in comparison to when they are far
931 (distance = 1 or 5 km).

932

Appendix A. Study area details and environmental data sources

In this document we provide details on the study area and sources of environmental data used to analyze the cumulative impacts of a mine and wind power plants on reindeer in the Malå Sámi reindeer herding community (RHC) in Northern Sweden. More specifically, we: (i) detail the definition of the seasons in each year for which we used GPS data; (ii) describe all the environmental data used in the study, pointing to sources, geographical information, thematic resolution, and details on the processing and preparation of the data layers; (iii) present a summary statistics of the values for the environmental variables for the study area.

Table of contents

1 Seasons

Table A1 shows the dates of start and end of each season for each year, defined based on information from the reindeer herders in the Malå RHC.

Year	Phase	Calving	Summer	Autumn
2008	Before construction	2008-05-12 to 2008-06-18	2008-07-15 to 2008-09-15	2008-09-16 to 2008-11-18
2009	Before construction	2009-05-02 to 2009-06-19	2009-07-14 to 2009-09-15	2009-09-16 to 2009-11-07

(continued)

Year	Phase	Calving	Summer	Autumn
2010	Construction	2010-05-10 to 2010-06-24	2010-07-14 to 2010-09-15	2010-09-16 to 2010-11-05
2011	Construction	2011-05-10 to 2011-06-22	2011-07-09 to 2011-09-15	2011-09-16 to 2011-11-30
2015	Operation	2015-05-01 to 2015-06-25	2015-07-15 to 2015-09-15	2015-09-16 to 2015-11-13
2016	Operation	2016-05-05 to 2016-06-23	2016-07-15 to 2016-09-15	2016-09-16 to 2016-11-30
2017	Operation	2017-05-03 to 2017-06-28	2017-07-08 to 2017-09-15	2017-09-16 to 2017-11-15
2018	Operation	2018-05-05 to 2018-06-26	2018-07-12 to 2018-09-15	2018-09-16 to 2018-11-30

Table A1. Dates of the calving, summer, and autumn seasons in each of the years of reindeer monitoring.

2 Environmental data

All environmental data was processed in GRASS GIS environment, version 7.8 (GRASS Development Team, 2017), in SWEREF99 (EPSG:3006) coordinate reference system. All vector data was rasterized with resolution 10 m to be processed and used in the analyses. Environmental variables, data sources, and data processing are described in Table A2.

Layer	Description	Image type	Year	Original resolution	Institution	Source
Land use and land cover	National Land Cover Database (NMD). Land cover map over Sweden with 25 thematic classes. Classified using Snetinel-2 satellite images and LIDAR data as well as existing national maps like soil maps, hydography, roads and buildings. The original classes are: 111 – Pine forest not on wetlands, 112 – Spruce forest not on wetlands, 113 – Mixed coniferous forest not on wetlands, 114 – Broadleaved forest not on wetlands, 115 – Mixed forest not on wetlands, 116 – Temporarily non-forest (clear-cuts etc.) not on wetlands, 121 – Pine forest on wetlands, 122 – Spruce forest on wetlands, 123 – Mixed coniferous forest on wetlands, 124 – Broadleaved forest on wetlands, 125 – Mixed forest on wetlands, 126 – Temporarily non-forest (clear-cuts etc.) on wetlands, 211 – Arable land, 212 – Grassland, 221 – Artificial surfaces, 231 – Bare rock and other areas with sparse vegetation, 241 – Open wetlands, 242 – Forested wetlands, 251 – Natural grasslands, 252 – Alpine heaths, 253 – Alpine meadows, 261 – Glaciers and permanent snow, 271 – Inland water, 272 – Marine water. The classes were re-classified as: deciduous forest (114, 124), coniferous forest (111, 112, 113, 115, 121, 122, 123), open areas (116, 211, 212, 231, 251, 252, 253), mires (125, 241, 242), and anthropogenic areas (221). Classes 261 and 272 were not present in the study area, and class 271 was removed because few GPS position were found within water.	Raster	2018	10 m	Swedish Environmental Protection Agency (Naturvårdsverket)	[1]
Clear cuts	Final fellings data from the Forest Attribute Map (Digital Open Forest Data), consisting of polygons and corresponding year of cut. Clear cuts year was compared with the acquisition time of GPS positions and land use classes were updated for those positions when the acquisition time occurred after the clear cut year.	Vector	2020	NA	The Swedish Forest Agency	[2]
Start of season (SOS), end of season (EOS), and instantaneous rate of green-up (IRG)	Derived from Normalized Difference Vegetation Index (NDVI) downloaded from Google Earth Engine (MOD13Q1.061 Terra Vegetation Indices 16-Day Global 250 m) using the R package phenofit (https://github.com/eco-hydro/phenofit).	Raster	2022	250 m	Google Earth Engine	[3]
Elevation	Terrain model of Sweden	Raster	NA	1 m, resampled to 10 m	Lantmäteriet (Swedish mapping, cadastral and land registration authority)	[4]
Slope, aspect	Derived from elevation using the module r.slope.aspect in GRASS GIS 7.8.	Raster	NA	10 m	Computed for this study	Derived data

(continued)

Layer	Description	Image type	Year	Original resolution	Institution	Source
Terrain position index (TPI)	Computed based on the elevation, with neighborhood sizes 150 m, 250 m, and 510 m. TPI was reclassified following the approach from Weiss (2001) into six categories: valley, lower slope, flat, middle slope, upper slope, ridge. Reference: Weiss, A.D., 2001. Topographic Position and Landforms Analysis. ESRI User Conference.	NA	NA	10 m	Computed for this study	Derived data
Wind turbines	Position for each wind turbine, not used directly in the analysis	Vector	2019	NA	County administrative boards and Swedish Energy Agency	[5]
Zone of influence (ZOI) of wind turbines	Either the density of wind turbines of and the decay-distance to the nearest wind turbine, computed at scales 100 m, 250 m, 500 m, 1 km, 2.5 km, 5 km, and 10 km. ZOIs were computed using an exponential distance decay shape using the oneimpact package in R (https://github.com/NINAnor/oneimpact/).	NA	2019	10 m	Computed for this study	Derived data
Mines	Active mining areas	Vector	NA	NA	The Geological Survey of Sweden (SGU)	[6]
Zone of influence (ZOI) of mine	Computed considering an exponential decay distance to the mine, with ZOI radius 100 m, 250 m, 500 m, 1 km, 2.5 km, 5 km, and 10 km. ZOIs were computed using the oneimpact package in R (https://github.com/NINAnor/oneimpact/).	NA	NA	10 m	Computed for this study	Derived data
Public roads	Public (main) roads. Used to compute the (log) distance to the nearest feature, used in the statistical models.	Vector	2019	NA	Lantmäteriet (Swedish mapping, cadastral and land registration authority)	[7]
Private roads	Private roads (mostly private and forestry roads). Used to compute the (log) distance to the nearest feature as input for the statistical models.	Vector	2019	NA	Lantmäteriet (Swedish mapping, cadastral and land registration authority)	[7]
Trails	Tourist trails. Used to compute the (log) distance to the nearest feature as input for the statistical models.	Vector	2019	NA	Lantmäteriet (Swedish mapping, cadastral and land registration authority)	[7]

(continued)

Layer	Description	Image type	Year	Original resolution	Institution	Source
Power lines	Power lines. Used to compute the (log) distance to the nearest feature as input for the statistical models.	Vector	2019	NA	Lantmäteriet (Swedish mapping, cadastral and land registration authority)	[7]
Houses	Houses and associated building. Used to compute the (log) distance to the nearest feature as input for the statistical models.	Vector	2019	NA	Lantmäteriet (Swedish mapping, cadastral and land registration authority)	[7]

Table A2. Description of the environmental variables used for estimating reindeer habitat selection and movement patterns.

3 Summary statistics of environmental variables

Variable	Average (range) or proportion
Elevation (m)	370 (231 - 648)
Slope (degrees)	3 (0 - 63)
Start of season (doy)	136 (103 - 247)
End of season (doy)	302 (259 - 331)
Distance to public roads (m)	2107 (0 - 10890)
Distance to private roads (m)	453 (0 - 4924)
Distance to wind turbines (m)	21928 (0 - 72341)
Distance to power lines (m)	6893 (0 - 22152)
Deciduous forests	14.46%
Open lands	20.01%
Anthropogenic areas	1.49%
Coniferous forests	43.12%
Mires	20.92%

Table A3. Summary statistics (mean and range, or proportion of land use classes) of the environmental variables used for estimating reindeer habitat selection and movement patterns.

4 Data source references

[1] https://www.naturvardsverket.se/en/services-and-permits/maps-and-map-services/national-land-cover-database/

[2] https://www.skogsstyrelsen.se/en/digital-open-forest-data/

[3] https://developers.google.com/earth-engine/datasets/catalog/MODIS_061_MOD13Q1

[4] https://www.lantmateriet.se/en/geodata/our-products/product-list/elevation-model-download/

[5] https://ext-webbgis.lansstyrelsen.se/vbk/

[6] https://apps.sgu.se/kartvisare/kartvisare-mineralrattigheter.html

[7] https://www.lantmateriet.se/en/geodata/our-products/product-list/topography-10-download-vector/

5 References

GRASS Development Team. (2017). Geographic Resources Analysis Support System (GRASS GIS) Software, Version 7.8. Open Source Geospatial Foundation. http://grass.osgeo.org

Appendix B. Cumulative impacts of mining and wind power development on reindeer: landscape-scale habitat selection analysis (HSA)

Here we provide supplementary information regarding the landscape-scale (2nd order) assessment of reindeer selection for grazing sites in the Malå reindeer herding community, Sweden, under the presence of mining and wind power development, for the three snow-free seasons: calving, summer, and autumn. We present, for each season: (i) the setup of the habitat selection models; (ii) the best-ranged habitat selection models; (iii) the model selection tables; (iv) the tables of coefficients; (v) figures illustrating the impacts of mining and wind turbines; (vi) maps with the predicted habitat suitability and GPS data across the three wind power development phases.

Table of contents

1 Text B1: Statistical modeling of the HSA

As described in the main text, the landscape-scale HSA followed a habitat selection function setup. The overall model structure we fitted was the following:

```
base_formula <- case_ ~
  # habitat selection
  scale(dem) + I(scale(dem)^2) + scale(slope) + cos_aspect +
  scale(sos) +
  log(power_lines_dist+1) + log(priv_road_dist+1) + log(public_road_dist+1) +
  log(trails_dist+1) +
  log(house_dist+1) +
  # mining habitat selection
  scale(mining_Krist_nearestXXX) +
  # wind habitat selection
  wf_name +
  landcover*phase*scale(wind_turbines_ZZZ) +
  # tpi habitat selection
  tpi_scale_TTT
```

where the terms are:

- `case_`: our response variable (0/1);

- `dem`: elevation, we include a linear and a quadratic term;
- `slope`: slope;
- `cos_aspect`: cosine of the aspect;
- `tpi_scale_TTT`: topographic position index (TPI) computed at a certain scale, classified in 6 levels: flat, lower slope, medium slope, upper slope, ridge, valley;
- `sos`: start of season (used for calving and summer), replaced by `eos`, end of season, for autumn;
- `phase`: wind power development phase, with 3 categories: before construction, during construction, operation;
- `wf_name`: name of the wind power plant closest to each point, with four categories, added as a fixed effect to control for differential effects close to the Åmliden wind park, which lies along a large fenced area;
- `landcover`: land cover, with 5 categories: deciduous forest, coniferous forest, open areas, mires, and anthropogenic areas;
- `log(public_road_dist+1)`, `log(priv_road_dist+1)`, `log(trails_dist+1)`, `log(house_dist+1)`, `log(power_lines_dist+1)`: logarithm of the distance to the nearest infrastructure for public roads, private roads, trails, houses, and power lines;
- `mining_Krist_nearestXXX`: ZOI (exponential decay distance) of the mine, computed considering a certain ZOI radius;
- `wind_turbines_ZZZ`: ZOI of wind turbines (considering either the density or the nearest infrastructure only), computed considering a certain ZOI radius.

The terms `XXX`, `ZZZ`, and `TTT` in the model structure above represent scales or variables that varied across models fitted. To evaluate the most likely ZOI for the mine and the wind turbines, whether there was a cumulative impact of multiple wind power plants, and at which scale the TPI most affected reindeer habitat selection, we replaced these variables in the model structure above using each possible combination of ZOI radii and type (cumulative vs. nearest; Fig. B1) for wind power and the different ZOI radii for the mine, together with different scales for the TPI. Models were compared through Akaike information criterion (AIC), as described in the main text. The scales included were:

- Mining (`XXX`): 100 m, 250 m, 500 m, 1 km, 2.5 km, 5 km, 10 km.
- Wind turbines (`ZZZ`): density of turbines or distance to the nearest turbine, with ZOI radii 100 m, 250 m, 500 m, 1 km, 2.5 km, 5 km, 10 km.
- TPI: 150 m, 250 m, 510 m.

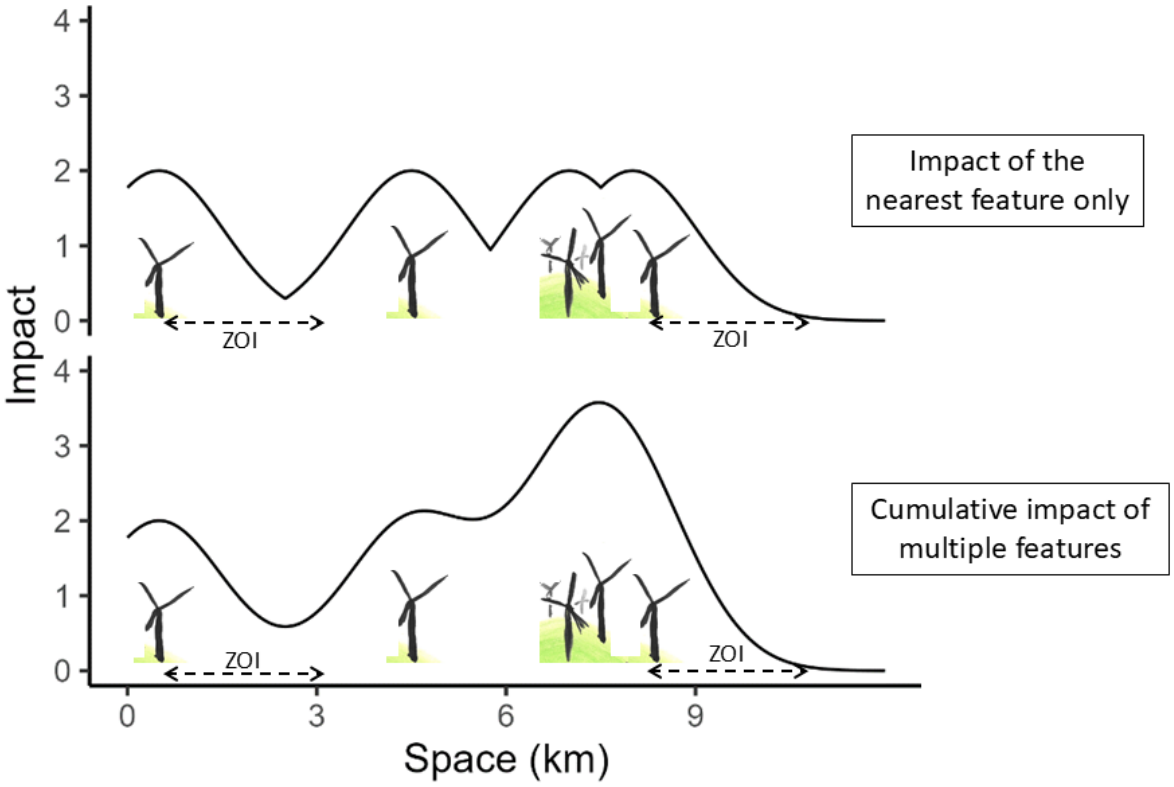

Figure B1. Illustration of two types of measures used to represent the influence of wind turbines in our study. The upper row shows the expected impact if we consider the effect of the nearest wind turbine only, which is similar whether one gets closer to one isolated turbine or a whole wind park. The bottom row shows the density of wind turbines, which captures the cumulative impact of multiple wind turbines and is larger when one gets closer to a wind park than to an isolated wind turbine. These two types of variables were used as predictors in the statistical models to estimate whether there were cumulative impacts of features of the same type.

2 Text B2: Best-ranked habitat selection models

This is the structure of the best-ranked HSA model selected for each season.

Summary of best ranked models:

- **Calving. Impact of the nearest wind turbine, ZOI radius = 5 km; ZOI of the mine with radius 10 km:**
  case_ ~ scale(dem) + I(scale(dem)^2) + scale(slope) + cos_aspect + scale(sos) + log(power_lines_dist + 1) + log(priv_road_dist + 1) + log(public_road_dist + 1) + log(trails_dist + 1) + log(house_dist + 1) + wf_name + tpi_cat_s150m +

scale(mining_Krist_nearest10000) + landcover_cc_grouped + phase + scale(wind_turbines_nearest5000) + landcover_cc_grouped:phase + landcover_cc_grouped:scale(wind_turbines_nearest5000) + phase:scale(wind_turbines_nearest5000) + landcover_cc_grouped:phase:scale(wind_turbines_nearest500

- **Summer. Cumulative impact of wind turbines, ZOI radius = 10 km; ZOI of the mine with radius 10 km:**
  case_ ~ scale(dem) + I(scale(dem)^2) + scale(slope) + cos_aspect + scale(sos) + log(power_lines_dist + 1) + log(priv_road_dist + 1) + log(public_road_dist + 1) + log(trails_dist + 1) + log(house_dist + 1) + wf_name + tpi_cat_s510m + scale(mining_Krist_nearest10000) + landcover_cc_grouped + phase + scale(wind_turbines_cumulative100 + landcover_cc_grouped:phase + landcover_cc_grouped:scale(wind_turbines_cumulative10000) + phase:scale(wind_turbines_cumulative10000) + landcover_cc_grouped:phase:scale(wind_turbines_cumu
- **Autumn. Impact of the nearest wind turbine, ZOI radius = 10 km; ZOI of the mine with radius 10 km:**
  case_ ~ scale(dem) + I(scale(dem)^2) + scale(slope) + cos_aspect + scale(eos) + log(power_lines_dist + 1) + log(priv_road_dist + 1) + log(public_road_dist + 1) + log(trails_dist + 1) + log(house_dist + 1) + wf_name + tpi_cat_s510m + scale(mining_Krist_nearest10000) + landcover_cc_grouped + phase + scale(wind_turbines_nearest10000) + landcover_cc_grouped:phase + landcover_cc_grouped:scale(wind_turbines_nearest10000) + phase:scale(wind_turbines_nearest10000) + landcover_cc_grouped:phase:scale(wind_turbines_nearest10

3 Table B1: Model selection table in calving

Table B1 was truncated to show only the first 10 models, to avoid an overly long table.

Mining ZOI radius	Wind turbine ZOI radius	TPI	AIC	dAIC	formula
10000	nearest5000	150m	636451.8	0.00	case_ ~ scale(dem) + I(scale(dem)^2) + scale(slope) + cos_aspect + scale(sos) + log(power_lines_dist + 1) + log(priv_road_dist + 1) + log(public_road_dist + 1) + log(trails_dist + 1) + log(house_dist + 1) + wf_name + tpi_cat_s150m + scale(mining_Krist_nearest10000) + landcover_cc + phase + scale(wind_turbines_nearest5000) + landcover_cc:phase + landcover_cc:scale(wind_turbines_nearest5000) + phase:scale(wind_turbines_nearest5000) + landcover_cc:phase:scale(wind_turbines_nearest5000)
10000	nearest10000	150m	636535.5	83.66	case_ ~ scale(dem) + I(scale(dem)^2) + scale(slope) + cos_aspect + scale(sos) + log(power_lines_dist + 1) + log(priv_road_dist + 1) + log(public_road_dist + 1) + log(trails_dist + 1) + log(house_dist + 1) + wf_name + tpi_cat_s150m + scale(mining_Krist_nearest10000) + landcover_cc + phase + scale(wind_turbines_nearest10000) + landcover_cc:phase + landcover_cc:scale(wind_turbines_nearest10000) + phase:scale(wind_turbines_nearest10000) + landcover_cc:phase:scale(wind_turbines_nearest10000)

(continued)

Mining ZOI radius	Wind turbine ZOI radius	TPI	AIC	dAIC	formula
10000	nearest5000	250m	636536.9	85.05	case_ ~ scale(dem) + I(scale(dem)^2) + scale(slope) + cos_aspect + scale(sos) + log(power_lines_dist + 1) + log(priv_road_dist + 1) + log(public_road_dist + 1) + log(trails_dist + 1) + log(house_dist + 1) + wf_name + tpi_cat_s250m + scale(mining_Krist_nearest10000) + landcover_cc + phase + scale(wind_turbines_nearest5000) + landcover_cc:phase + landcover_cc:scale(wind_turbines_nearest5000) + phase:scale(wind_turbines_nearest5000) + landcover_cc:phase:scale(wind_turbines_nearest5000)
10000	nearest2500	150m	636570.4	118.61	case_ ~ scale(dem) + I(scale(dem)^2) + scale(slope) + cos_aspect + scale(sos) + log(power_lines_dist + 1) + log(priv_road_dist + 1) + log(public_road_dist + 1) + log(trails_dist + 1) + log(house_dist + 1) + wf_name + tpi_cat_s150m + scale(mining_Krist_nearest10000) + landcover_cc + phase + scale(wind_turbines_nearest2500) + landcover_cc:phase + landcover_cc:scale(wind_turbines_nearest2500) + phase:scale(wind_turbines_nearest2500) + landcover_cc:phase:scale(wind_turbines_nearest2500)
10000	nearest10000	250m	636614.4	162.52	case_ ~ scale(dem) + I(scale(dem)^2) + scale(slope) + cos_aspect + scale(sos) + log(power_lines_dist + 1) + log(priv_road_dist + 1) + log(public_road_dist + 1) + log(trails_dist + 1) + log(house_dist + 1) + wf_name + tpi_cat_s250m + scale(mining_Krist_nearest10000) + landcover_cc + phase + scale(wind_turbines_nearest10000) + landcover_cc:phase + landcover_cc:scale(wind_turbines_nearest10000) + phase:scale(wind_turbines_nearest10000) + landcover_cc:phase:scale(wind_turbines_nearest10000)
10000	cumulative5000	150m	636623.7	171.82	case_ ~ scale(dem) + I(scale(dem)^2) + scale(slope) + cos_aspect + scale(sos) + log(power_lines_dist + 1) + log(priv_road_dist + 1) + log(public_road_dist + 1) + log(trails_dist + 1) + log(house_dist + 1) + wf_name + tpi_cat_s150m + scale(mining_Krist_nearest10000) + landcover_cc + phase + scale(wind_turbines_cumulative5000) + landcover_cc:phase + landcover_cc:scale(wind_turbines_cumulative5000) + phase:scale(wind_turbines_cumulative5000) + landcover_cc:phase:scale(wind_turbines_cumulative5000)
10000	nearest5000	510m	636649.7	197.86	case_ ~ scale(dem) + I(scale(dem)^2) + scale(slope) + cos_aspect + scale(sos) + log(power_lines_dist + 1) + log(priv_road_dist + 1) + log(public_road_dist + 1) + log(trails_dist + 1) + log(house_dist + 1) + wf_name + tpi_cat_s510m + scale(mining_Krist_nearest10000) + landcover_cc + phase + scale(wind_turbines_nearest5000) + landcover_cc:phase + landcover_cc:scale(wind_turbines_nearest5000) + phase:scale(wind_turbines_nearest5000) + landcover_cc:phase:scale(wind_turbines_nearest5000)

(continued)

Mining ZOI radius	Wind turbine ZOI radius	TPI	AIC	dAIC	formula
10000	nearest2500	250m	636658.9	207.06	case_ ~ scale(dem) + I(scale(dem)^2) + scale(slope) + cos_aspect + scale(sos) + log(power_lines_dist + 1) + log(priv_road_dist + 1) + log(public_road_dist + 1) + log(trails_dist + 1) + log(house_dist + 1) + wf_name + tpi_cat_s250m + scale(mining_Krist_nearest10000) + landcover_cc + phase + scale(wind_turbines_nearest2500) + landcover_cc:phase + landcover_cc:scale(wind_turbines_nearest2500) + phase:scale(wind_turbines_nearest2500) + landcover_cc:phase:scale(wind_turbines_nearest2500)
10000	cumulative2500	150m	636691.9	240.03	case_ ~ scale(dem) + I(scale(dem)^2) + scale(slope) + cos_aspect + scale(sos) + log(power_lines_dist + 1) + log(priv_road_dist + 1) + log(public_road_dist + 1) + log(trails_dist + 1) + log(house_dist + 1) + wf_name + tpi_cat_s150m + scale(mining_Krist_nearest10000) + landcover_cc + phase + scale(wind_turbines_cumulative2500) + landcover_cc:phase + landcover_cc:scale(wind_turbines_cumulative2500) + phase:scale(wind_turbines_cumulative2500) + landcover_cc:phase:scale(wind_turbines_cumulative2500)
10000	cumulative10000	150m	636703.8	251.96	case_ ~ scale(dem) + I(scale(dem)^2) + scale(slope) + cos_aspect + scale(sos) + log(power_lines_dist + 1) + log(priv_road_dist + 1) + log(public_road_dist + 1) + log(trails_dist + 1) + log(house_dist + 1) + wf_name + tpi_cat_s150m + scale(mining_Krist_nearest10000) + landcover_cc + phase + scale(wind_turbines_cumulative10000) + landcover_cc:phase + landcover_cc:scale(wind_turbines_cumulative10000) + phase:scale(wind_turbines_cumulative10000) + landcover_cc:phase:scale(wind_turbines_cumulative10000)

Table B1. Table of model selection for the HSA models for calving. Columns are zone of influence (ZOI) radius for mining and wind turbines, scale for the topographic position index (TPI), AIC of the model, dAIC of each model in relation to the most parsimonious model, and the formula with each model's structure.

4 Table B2: Model selection table in summer

Table B2 was truncated to show only the first 10 models, to avoid an overly long table.

Mining ZOI radius	Wind turbine ZOI radius	TPI	AIC	dAIC	formula
10000	cumulative10000	510m	685857.2	0.00	case_ ~ scale(dem) + I(scale(dem)^2) + scale(slope) + cos_aspect + scale(sos) + log(power_lines_dist + 1) + log(priv_road_dist + 1) + log(public_road_dist + 1) + log(trails_dist + 1) + log(house_dist + 1) + wf_name + tpi_cat_s510m + scale(mining_Krist_nearest10000) + landcover_cc_grouped + phase + scale(wind_turbines_cumulative10000) + landcover_cc_grouped:phase + landcover_cc_grouped:scale(wind_turbines_cumulative10000) + phase:scale(wind_turbines_cumulative10000) + landcover_cc_grouped:phase:scale(wind_turbines_cumulative10000)
5000	cumulative10000	510m	686161.3	304.06	case_ ~ scale(dem) + I(scale(dem)^2) + scale(slope) + cos_aspect + scale(sos) + log(power_lines_dist + 1) + log(priv_road_dist + 1) + log(public_road_dist + 1) + log(trails_dist + 1) + log(house_dist + 1) + wf_name + tpi_cat_s510m + scale(mining_Krist_nearest5000) + landcover_cc_grouped + phase + scale(wind_turbines_cumulative10000) + landcover_cc_grouped:phase + landcover_cc_grouped:scale(wind_turbines_cumulative10000) + phase:scale(wind_turbines_cumulative10000) + landcover_cc_grouped:phase:scale(wind_turbines_cumulative10000)
10000	nearest10000	510m	686179.6	322.39	case_ ~ scale(dem) + I(scale(dem)^2) + scale(slope) + cos_aspect + scale(sos) + log(power_lines_dist + 1) + log(priv_road_dist + 1) + log(public_road_dist + 1) + log(trails_dist + 1) + log(house_dist + 1) + wf_name + tpi_cat_s510m + scale(mining_Krist_nearest10000) + landcover_cc_grouped + phase + scale(wind_turbines_nearest10000) + landcover_cc_grouped:phase + landcover_cc_grouped:scale(wind_turbines_nearest10000) + phase:scale(wind_turbines_nearest10000) + landcover_cc_grouped:phase:scale(wind_turbines_nearest10000)
10000	cumulative10000	250m	686297.5	440.30	case_ ~ scale(dem) + I(scale(dem)^2) + scale(slope) + cos_aspect + scale(sos) + log(power_lines_dist + 1) + log(priv_road_dist + 1) + log(public_road_dist + 1) + log(trails_dist + 1) + log(house_dist + 1) + wf_name + tpi_cat_s250m + scale(mining_Krist_nearest10000) + landcover_cc_grouped + phase + scale(wind_turbines_cumulative10000) + landcover_cc_grouped:phase + landcover_cc_grouped:scale(wind_turbines_cumulative10000) + phase:scale(wind_turbines_cumulative10000) + landcover_cc_grouped:phase:scale(wind_turbines_cumulative10000)
10000	cumulative10000	150m	686318.4	461.13	case_ ~ scale(dem) + I(scale(dem)^2) + scale(slope) + cos_aspect + scale(sos) + log(power_lines_dist + 1) + log(priv_road_dist + 1) + log(public_road_dist + 1) + log(trails_dist + 1) + log(house_dist + 1) + wf_name + tpi_cat_s150m + scale(mining_Krist_nearest10000) + landcover_cc_grouped + phase + scale(wind_turbines_cumulative10000) + landcover_cc_grouped:phase + landcover_cc_grouped:scale(wind_turbines_cumulative10000) + phase:scale(wind_turbines_cumulative10000) + landcover_cc_grouped:phase:scale(wind_turbines_cumulative10000)

(continued)

Mining ZOI radius	Wind turbine ZOI radius	TPI	AIC	dAIC	formula
5000	nearest10000	510m	686367.2	510.01	case_ ~ scale(dem) + I(scale(dem)^2) + scale(slope) + cos_aspect + scale(sos) + log(power_lines_dist + 1) + log(priv_road_dist + 1) + log(public_road_dist + 1) + log(trails_dist + 1) + log(house_dist + 1) + wf_name + tpi_cat_s510m + scale(mining_Krist_nearest5000) + landcover_cc_grouped + phase + scale(wind_turbines_nearest10000) + landcover_cc_grouped:phase + landcover_cc_grouped:scale(wind_turbines_nearest10000) + phase:scale(wind_turbines_nearest10000) + landcover_cc_grouped:phase:scale(wind_turbines_nearest10000)
10000	nearest10000	250m	686509.5	652.24	case_ ~ scale(dem) + I(scale(dem)^2) + scale(slope) + cos_aspect + scale(sos) + log(power_lines_dist + 1) + log(priv_road_dist + 1) + log(public_road_dist + 1) + log(trails_dist + 1) + log(house_dist + 1) + wf_name + tpi_cat_s250m + scale(mining_Krist_nearest10000) + landcover_cc_grouped + phase + scale(wind_turbines_nearest10000) + landcover_cc_grouped:phase + landcover_cc_grouped:scale(wind_turbines_nearest10000) + phase:scale(wind_turbines_nearest10000) + landcover_cc_grouped:phase:scale(wind_turbines_nearest10000)
10000	nearest10000	150m	686513.4	656.12	case_ ~ scale(dem) + I(scale(dem)^2) + scale(slope) + cos_aspect + scale(sos) + log(power_lines_dist + 1) + log(priv_road_dist + 1) + log(public_road_dist + 1) + log(trails_dist + 1) + log(house_dist + 1) + wf_name + tpi_cat_s150m + scale(mining_Krist_nearest10000) + landcover_cc_grouped + phase + scale(wind_turbines_nearest10000) + landcover_cc_grouped:phase + landcover_cc_grouped:scale(wind_turbines_nearest10000) + phase:scale(wind_turbines_nearest10000) + landcover_cc_grouped:phase:scale(wind_turbines_nearest10000)
5000	cumulative10000	250m	686571.5	714.27	case_ ~ scale(dem) + I(scale(dem)^2) + scale(slope) + cos_aspect + scale(sos) + log(power_lines_dist + 1) + log(priv_road_dist + 1) + log(public_road_dist + 1) + log(trails_dist + 1) + log(house_dist + 1) + wf_name + tpi_cat_s250m + scale(mining_Krist_nearest5000) + landcover_cc_grouped + phase + scale(wind_turbines_cumulative10000) + landcover_cc_grouped:phase + landcover_cc_grouped:scale(wind_turbines_cumulative10000) + phase:scale(wind_turbines_cumulative10000) + landcover_cc_grouped:phase:scale(wind_turbines_cumulative10000)

(continued)

Mining ZOI radius	Wind turbine ZOI radius	TPI	AIC	dAIC	formula
5000	cumulative10000	150m	686578.8	721.55	case_ ~ scale(dem) + I(scale(dem)^2) + scale(slope) + cos_aspect + scale(sos) + log(power_lines_dist + 1) + log(priv_road_dist + 1) + log(public_road_dist + 1) + log(trails_dist + 1) + log(house_dist + 1) + wf_name + tpi_cat_s150m + scale(mining_Krist_nearest5000) + landcover_cc_grouped + phase + scale(wind_turbines_cumulative10000) + landcover_cc_grouped:phase + landcover_cc_grouped:scale(wind_turbines_cumulative10000) + phase:scale(wind_turbines_cumulative10000) + landcover_cc_grouped:phase:scale(wind_turbines_cumulative10000)

Table B2. Table of model selection for the HSA models for summer. Columns are zone of influence (ZOI) radius for mining and wind turbines, scale for the topographic position index (TPI), AIC of the model, dAIC of each model in relation to the most parsimonious model, and the formula with each model's structure.

5 Table B3: Model selection table in autumn

Table B3 was truncated to show only the first 10 models, to avoid an overly long table.

Mining ZOI radius	Wind turbine ZOI radius	TPI	AIC	dAIC	formula
10000	nearest10000	510m	499872.5	0.00	case_ ~ scale(dem) + I(scale(dem)^2) + scale(slope) + cos_aspect + scale(eos) + log(power_lines_dist + 1) + log(priv_road_dist + 1) + log(public_road_dist + 1) + log(trails_dist + 1) + log(house_dist + 1) + wf_name + tpi_cat_s510m + scale(mining_Krist_nearest10000) + landcover_cc + phase + scale(wind_turbines_nearest10000) + landcover_cc:phase + landcover_cc:scale(wind_turbines_nearest10000) + phase:scale(wind_turbines_nearest10000) + landcover_cc:phase:scale(wind_turbines_nearest10000)
10000	cumulative10000	510m	500263.4	390.95	case_ ~ scale(dem) + I(scale(dem)^2) + scale(slope) + cos_aspect + scale(eos) + log(power_lines_dist + 1) + log(priv_road_dist + 1) + log(public_road_dist + 1) + log(trails_dist + 1) + log(house_dist + 1) + wf_name + tpi_cat_s510m + scale(mining_Krist_nearest10000) + landcover_cc + phase + scale(wind_turbines_cumulative10000) + landcover_cc:phase + landcover_cc:scale(wind_turbines_cumulative10000) + phase:scale(wind_turbines_cumulative10000) + landcover_cc:phase:scale(wind_turbines_cumulative10000)

(continued)

Mining ZOI radius	Wind turbine ZOI radius	TPI	AIC	dAIC	formula
10000	nearest5000	510m	500547.7	675.26	case_ ~ scale(dem) + I(scale(dem)^2) + scale(slope) + cos_aspect + scale(eos) + log(power_lines_dist + 1) + log(priv_road_dist + 1) + log(public_road_dist + 1) + log(trails_dist + 1) + log(house_dist + 1) + wf_name + tpi_cat_s510m + scale(mining_Krist_nearest10000) + landcover_cc + phase + scale(wind_turbines_nearest5000) + landcover_cc:phase + landcover_cc:scale(wind_turbines_nearest5000) + phase:scale(wind_turbines_nearest5000) + landcover_cc:phase:scale(wind_turbines_nearest5000)
10000	cumulative5000	510m	500710.7	838.27	case_ ~ scale(dem) + I(scale(dem)^2) + scale(slope) + cos_aspect + scale(eos) + log(power_lines_dist + 1) + log(priv_road_dist + 1) + log(public_road_dist + 1) + log(trails_dist + 1) + log(house_dist + 1) + wf_name + tpi_cat_s510m + scale(mining_Krist_nearest10000) + landcover_cc + phase + scale(wind_turbines_cumulative5000) + landcover_cc:phase + landcover_cc:scale(wind_turbines_cumulative5000) + phase:scale(wind_turbines_cumulative5000) + landcover_cc:phase:scale(wind_turbines_cumulative5000)
10000	cumulative2500	510m	500848.9	976.46	case_ ~ scale(dem) + I(scale(dem)^2) + scale(slope) + cos_aspect + scale(eos) + log(power_lines_dist + 1) + log(priv_road_dist + 1) + log(public_road_dist + 1) + log(trails_dist + 1) + log(house_dist + 1) + wf_name + tpi_cat_s510m + scale(mining_Krist_nearest10000) + landcover_cc + phase + scale(wind_turbines_cumulative2500) + landcover_cc:phase + landcover_cc:scale(wind_turbines_cumulative2500) + phase:scale(wind_turbines_cumulative2500) + landcover_cc:phase:scale(wind_turbines_cumulative2500)
10000	nearest2500	510m	500870.4	997.95	case_ ~ scale(dem) + I(scale(dem)^2) + scale(slope) + cos_aspect + scale(eos) + log(power_lines_dist + 1) + log(priv_road_dist + 1) + log(public_road_dist + 1) + log(trails_dist + 1) + log(house_dist + 1) + wf_name + tpi_cat_s510m + scale(mining_Krist_nearest10000) + landcover_cc + phase + scale(wind_turbines_nearest2500) + landcover_cc:phase + landcover_cc:scale(wind_turbines_nearest2500) + phase:scale(wind_turbines_nearest2500) + landcover_cc:phase:scale(wind_turbines_nearest2500)
10000	cumulative1000	510m	500951.9	1079.43	case_ ~ scale(dem) + I(scale(dem)^2) + scale(slope) + cos_aspect + scale(eos) + log(power_lines_dist + 1) + log(priv_road_dist + 1) + log(public_road_dist + 1) + log(trails_dist + 1) + log(house_dist + 1) + wf_name + tpi_cat_s510m + scale(mining_Krist_nearest10000) + landcover_cc + phase + scale(wind_turbines_cumulative1000) + landcover_cc:phase + landcover_cc:scale(wind_turbines_cumulative1000) + phase:scale(wind_turbines_cumulative1000) + landcover_cc:phase:scale(wind_turbines_cumulative1000)

(continued)

Mining ZOI radius	Wind turbine ZOI radius	TPI	AIC	dAIC	formula
10000	nearest1000	510m	500996.1	1123.63	case_ ~ scale(dem) + I(scale(dem)^2) + scale(slope) + cos_aspect + scale(eos) + log(power_lines_dist + 1) + log(priv_road_dist + 1) + log(public_road_dist + 1) + log(trails_dist + 1) + log(house_dist + 1) + wf_name + tpi_cat_s510m + scale(mining_Krist_nearest10000) + landcover_cc + phase + scale(wind_turbines_nearest1000) + landcover_cc:phase + landcover_cc:scale(wind_turbines_nearest1000) + phase:scale(wind_turbines_nearest1000) + landcover_cc:phase:scale(wind_turbines_nearest1000)
10000	cumulative500	510m	501059.6	1187.16	case_ ~ scale(dem) + I(scale(dem)^2) + scale(slope) + cos_aspect + scale(eos) + log(power_lines_dist + 1) + log(priv_road_dist + 1) + log(public_road_dist + 1) + log(trails_dist + 1) + log(house_dist + 1) + wf_name + tpi_cat_s510m + scale(mining_Krist_nearest10000) + landcover_cc + phase + scale(wind_turbines_cumulative500) + landcover_cc:phase + landcover_cc:scale(wind_turbines_cumulative500) + phase:scale(wind_turbines_cumulative500) + landcover_cc:phase:scale(wind_turbines_cumulative500)
10000	nearest500	510m	501080.5	1208.05	case_ ~ scale(dem) + I(scale(dem)^2) + scale(slope) + cos_aspect + scale(eos) + log(power_lines_dist + 1) + log(priv_road_dist + 1) + log(public_road_dist + 1) + log(trails_dist + 1) + log(house_dist + 1) + wf_name + tpi_cat_s510m + scale(mining_Krist_nearest10000) + landcover_cc + phase + scale(wind_turbines_nearest500) + landcover_cc:phase + landcover_cc:scale(wind_turbines_nearest500) + phase:scale(wind_turbines_nearest500) + landcover_cc:phase:scale(wind_turbines_nearest500)

Table B3. Table of model selection for the HSA models for autumn. Columns are zone of influence (ZOI) radius for mining and wind turbines, scale for the topographic position index (TPI), AIC of the model, dAIC of each model in relation to the most parsimonious model, and the formula with each model's structure.

6 Text B3: Disturbance effects on habitat selection

Here we present the coefficients of the HSA models. Even though all results come from the same models, we split the way we present the parts of the resulting model, to ease its interpretation. In this section we restrict ourselves on presenting the coefficients of all infrastructure and landscape covariates, without going into details regarding the impact of wind turbines on habitat selection.

In Table B4 we show the coefficient estimates for all the infrastructure types, excluding wind turbines which present interactions in the model structure and are explored further down. The

estimates are put together for different seasons in Table B4 to make it easy to compare the effects between them.

A summary of the results:

- The mine was strongly avoided in all seasons, especially during calving, with a large ZOI radius of 10 km;
- Public roads were avoided in all seasons;
- Private roads and trails were avoided during calving and summer, but were selected in autumn;
- Power lines were avoided only during calving and were selected in the other seasons;
- Houses were avoided during autumn, but were select during calving and summer;
- Areas with a later start of season and a later end of season timing were selected during calving and autumn, respectively; in contrast, areas with an earlier start of seasons were selected during summer.

season	term	estimate	std.error	p	select
calving	log(house_dist + 1)	-0.187	0.004	<0.001	selection/positive
summer	log(house_dist + 1)	-0.052	0.005	<0.001	selection/positive
autumn	log(house_dist + 1)	0.014	0.005	0.007	avoidance/negative
calving	log(power_lines_dist + 1)	0.097	0.003	<0.001	avoidance/negative
summer	log(power_lines_dist + 1)	-0.096	0.003	<0.001	selection/positive
autumn	log(power_lines_dist + 1)	-0.123	0.003	<0.001	selection/positive
calving	log(priv_road_dist + 1)	0.017	0.003	<0.001	avoidance/negative
summer	log(priv_road_dist + 1)	0.052	0.003	<0.001	avoidance/negative
autumn	log(priv_road_dist + 1)	-0.041	0.004	<0.001	selection/positive
calving	log(public_road_dist + 1)	0.040	0.003	<0.001	avoidance/negative
summer	log(public_road_dist + 1)	0.137	0.003	<0.001	avoidance/negative
autumn	log(public_road_dist + 1)	0.076	0.004	<0.001	avoidance/negative
calving	log(trails_dist + 1)	0.057	0.004	<0.001	avoidance/negative
summer	log(trails_dist + 1)	0.146	0.004	<0.001	avoidance/negative
autumn	log(trails_dist + 1)	-0.072	0.004	<0.001	selection/positive
autumn	scale(eos)	0.062	0.004	<0.001	selection/positive
calving	scale(mining_Krist_nearest10000)	-1.019	0.017	<0.001	avoidance/negative
summer	scale(mining_Krist_nearest10000)	-0.317	0.006	<0.001	avoidance/negative
autumn	scale(mining_Krist_nearest10000)	-0.453	0.009	<0.001	avoidance/negative
calving	scale(sos)	0.027	0.004	<0.001	selection/positive
summer	scale(sos)	-0.060	0.004	<0.001	avoidance/negative

Table B4. Coefficient estimates for the infrastructure types and the start/end of season on habitat selection for all three seasons. The complete table of coefficient estimates for each season is shown in Tables B5-B7.

7 Table B5: Coefficients - calving

term	estimate	std.error	p	select
(Intercept)	-2.545	0.050	<0.001	avoidance/negative
scale(dem)	-0.287	0.005	<0.001	avoidance/negative
I(scale(dem)^2)	-0.089	0.003	<0.001	avoidance/negative
scale(slope)	-0.096	0.005	<0.001	avoidance/negative
cos_aspect	0.002	0.005	0.707	no effect
scale(sos)	0.027	0.004	<0.001	selection/positive
log(power_lines_dist + 1)	0.097	0.003	<0.001	avoidance/negative
log(priv_road_dist + 1)	0.017	0.003	<0.001	avoidance/negative
log(public_road_dist + 1)	0.040	0.003	<0.001	avoidance/negative
log(trails_dist + 1)	0.057	0.004	<0.001	avoidance/negative
log(house_dist + 1)	-0.187	0.004	<0.001	selection/positive
wf_namestorliden	0.103	0.011	<0.001	selection/positive
wf_nameytteberg	-0.493	0.010	<0.001	avoidance/negative
wf_nameamliden	-2.255	0.024	<0.001	avoidance/negative
tpi_cat_s150mlower slope	-0.131	0.012	<0.001	avoidance/negative
tpi_cat_s150mmedium slope	0.144	0.009	<0.001	selection/positive
tpi_cat_s150mridge	0.129	0.013	<0.001	selection/positive
tpi_cat_s150mupper slope	0.076	0.012	<0.001	selection/positive
tpi_cat_s150mvalley	-0.136	0.015	<0.001	avoidance/negative
scale(mining_Krist_nearest10000)	-1.019	0.017	<0.001	avoidance/negative
landcover_cc_groupedopen lands	0.695	0.021	<0.001	selection/positive
landcover_cc_groupedanthropogenic areas	0.082	0.055	0.135	no effect
landcover_cc_groupedconiferous forests	-0.029	0.020	0.145	no effect
landcover_cc_groupedmires	0.209	0.021	<0.001	selection/positive
phaseConstruction	0.053	0.026	0.041	selection/positive
phaseOperation	-0.121	0.024	<0.001	avoidance/negative
scale(wind_turbines_nearest5000)	0.102	0.023	<0.001	selection/positive
landcover_cc_groupedopen lands:phaseConstruction	-0.154	0.031	<0.001	avoidance/negative
landcover_cc_groupedanthropogenic areas:phaseConstruction	1.097	0.070	<0.001	selection/positive
landcover_cc_groupedconiferous forests:phaseConstruction	-0.144	0.030	<0.001	avoidance/negative
landcover_cc_groupedmires:phaseConstruction	-0.076	0.032	0.017	avoidance/negative
landcover_cc_groupedopen lands:phaseOperation	0.212	0.028	<0.001	selection/positive
landcover_cc_groupedanthropogenic areas:phaseOperation	0.274	0.071	<0.001	selection/positive
landcover_cc_groupedconiferous forests:phaseOperation	0.201	0.027	<0.001	selection/positive
landcover_cc_groupedmires:phaseOperation	-0.219	0.030	<0.001	avoidance/negative
landcover_cc_groupedopen lands:scale(wind_turbines_nearest5000)	-0.041	0.026	0.121	no effect
landcover_cc_groupedanthropogenic areas:scale(wind_turbines_nearest5000)	-0.194	0.073	0.008	avoidance/negative
landcover_cc_groupedconiferous forests:scale(wind_turbines_nearest5000)	-0.086	0.026	0.001	avoidance/negative
landcover_cc_groupedmires:scale(wind_turbines_nearest5000)	0.128	0.028	<0.001	selection/positive
phaseConstruction:scale(wind_turbines_nearest5000)	-0.216	0.041	<0.001	avoidance/negative
phaseOperation:scale(wind_turbines_nearest5000)	0.016	0.031	0.619	no effect
landcover_cc_groupedopen lands:phaseConstruction:scale(wind_turbines_nearest5000)	0.017	0.047	0.724	no effect
landcover_cc_groupedanthropogenic areas:phaseConstruction:scale(wind_turbines_nearest5000)	-0.300	0.124	0.015	avoidance/negative
landcover_cc_groupedconiferous forests:phaseConstruction:scale(wind_turbines_nearest5000)	-0.037	0.048	0.439	no effect
landcover_cc_groupedmires:phaseConstruction:scale(wind_turbines_nearest50	-0.015	0.050	0.76	no effect
landcover_cc_groupedopen lands:phaseOperation:scale(wind_turbines_nearest5000)	-0.235	0.037	<0.001	avoidance/negative

(continued)

term	estimate	std.error	p	select
landcover_cc_groupedanthropogenic areas:phaseOperation:scale(wind_turbines_nearest5000)	-0.154	0.106	0.145	no effect
landcover_cc_groupedconiferous forests:phaseOperation:scale(wind_turbines_nearest5000)	-0.243	0.037	<0.001	avoidance/negative
landcover_cc_groupedmires:phaseOperation:scale(wind_turbines_nearest5000)	-0.133	0.040	0.001	avoidance/negative

Table B5. Complete table with coefficient estimates for the best-ranked landscape-scale habitat selection functions during calving.

8 Table B6: Coefficients - summer

term	estimate	std.error	p	select
(Intercept)	-3.954	0.050	<0.001	avoidance/negative
scale(dem)	-0.103	0.006	<0.001	avoidance/negative
I(scale(dem)^2)	-0.107	0.003	<0.001	avoidance/negative
scale(slope)	-0.070	0.004	<0.001	avoidance/negative
cos_aspect	-0.002	0.005	0.629	no effect
scale(sos)	-0.060	0.004	<0.001	avoidance/negative
log(power_lines_dist + 1)	-0.096	0.003	<0.001	selection/positive
log(priv_road_dist + 1)	0.052	0.003	<0.001	avoidance/negative
log(public_road_dist + 1)	0.137	0.003	<0.001	avoidance/negative
log(trails_dist + 1)	0.146	0.004	<0.001	avoidance/negative
log(house_dist + 1)	-0.052	0.005	<0.001	selection/positive
wf_namestorliden	0.701	0.013	<0.001	selection/positive
wf_nameytteberg	0.498	0.011	<0.001	selection/positive
wf_nameamliden	0.553	0.013	<0.001	selection/positive
tpi_cat_s510mlower slope	0.028	0.011	0.01	selection/positive
tpi_cat_s510mmedium slope	0.080	0.009	<0.001	selection/positive
tpi_cat_s510mridge	0.310	0.012	<0.001	selection/positive
tpi_cat_s510mupper slope	0.113	0.012	<0.001	selection/positive
tpi_cat_s510mvalley	0.020	0.014	0.136	no effect
scale(mining_Krist_nearest10000)	-0.317	0.006	<0.001	avoidance/negative
landcover_cc_groupedopen lands	0.200	0.018	<0.001	selection/positive
landcover_cc_groupedanthropogenic areas	0.856	0.037	<0.001	selection/positive
landcover_cc_groupedconiferous forests	0.217	0.016	<0.001	selection/positive
landcover_cc_groupedmires	-0.505	0.021	<0.001	avoidance/negative
phaseConstruction	-0.057	0.024	0.015	avoidance/negative
phaseOperation	0.030	0.021	0.148	no effect
scale(wind_turbines_cumulative10000)	0.313	0.011	<0.001	selection/positive
landcover_cc_groupedopen lands:phaseConstruction	-0.040	0.030	0.182	no effect
landcover_cc_groupedanthropogenic areas:phaseConstruction	-0.331	0.064	<0.001	avoidance/negative
landcover_cc_groupedconiferous forests:phaseConstruction	0.133	0.026	<0.001	selection/positive
landcover_cc_groupedmires:phaseConstruction	0.118	0.034	<0.001	selection/positive
landcover_cc_groupedopen lands:phaseOperation	-0.021	0.027	0.44	no effect
landcover_cc_groupedanthropogenic areas:phaseOperation	-0.283	0.056	<0.001	avoidance/negative
landcover_cc_groupedconiferous forests:phaseOperation	-0.127	0.024	<0.001	avoidance/negative

(continued)

term	estimate	std.error	p	select
landcover_cc_groupedmires:phaseOperation	0.107	0.030	<0.001	selection/positive
landcover_cc_groupedopen lands:scale(wind_turbines_cumulative10000)	0.007	0.013	0.599	no effect
landcover_cc_groupedanthropogenic areas:scale(wind_turbines_cumulative10000)	0.055	0.029	0.055	no effect
landcover_cc_groupedconiferous forests:scale(wind_turbines_cumulative10000)	-0.037	0.012	0.003	avoidance/negative
landcover_cc_groupedmires:scale(wind_turbines_cumulative10000)	-0.011	0.016	0.505	no effect
phaseConstruction:scale(wind_turbines_cumulative10000)	-0.055	0.018	0.003	avoidance/negative
phaseOperation:scale(wind_turbines_cumulative10000)	0.140	0.015	<0.001	selection/positive
landcover_cc_groupedopen lands:phaseConstruction:scale(wind_turbines_cumulative10000)	0.038	0.023	0.096	no effect
landcover_cc_groupedanthropogenic areas:phaseConstruction:scale(wind_turbines_cumulative10000)	0.063	0.049	0.199	no effect
landcover_cc_groupedconiferous forests:phaseConstruction:scale(wind_turbines_cumulative10000)	0.020	0.021	0.338	no effect
landcover_cc_groupedmires:phaseConstruction:scale(wind_turbines_cumulativ	0.084	0.027	0.002	selection/positive
landcover_cc_groupedopen lands:phaseOperation:scale(wind_turbines_cumulative10000)	-0.038	0.019	0.041	avoidance/negative
landcover_cc_groupedanthropogenic areas:phaseOperation:scale(wind_turbines_cumulative10000)	-0.115	0.040	0.004	avoidance/negative
landcover_cc_groupedconiferous forests:phaseOperation:scale(wind_turbines_cumulative10000)	-0.076	0.017	<0.001	avoidance/negative
landcover_cc_groupedmires:phaseOperation:scale(wind_turbines_cumulative1(	-0.102	0.023	<0.001	avoidance/negative

Table B6. Complete table with coefficient estimates for the best-ranked landscape-scale habitat selection functions during summer.

9 Table B7: Coefficients - autumn

term	estimate	std.error	p	select
(Intercept)	-2.720	0.053	<0.001	avoidance/negative
scale(dem)	-0.571	0.006	<0.001	avoidance/negative
I(scale(dem)^2)	0.112	0.003	<0.001	selection/positive
scale(slope)	-0.057	0.004	<0.001	avoidance/negative
cos_aspect	0.007	0.005	0.174	no effect
scale(eos)	0.062	0.004	<0.001	selection/positive
log(power_lines_dist + 1)	-0.123	0.003	<0.001	selection/positive
log(priv_road_dist + 1)	-0.041	0.004	<0.001	selection/positive
log(public_road_dist + 1)	0.076	0.004	<0.001	avoidance/negative
log(trails_dist + 1)	-0.072	0.004	<0.001	selection/positive
log(house_dist + 1)	0.014	0.005	0.007	avoidance/negative
wf_namestorliden	0.700	0.017	<0.001	selection/positive
wf_nameytteberg	0.744	0.014	<0.001	selection/positive
wf_nameamliden	-0.044	0.016	0.005	avoidance/negative
tpi_cat_s510mlower slope	-0.031	0.014	0.025	avoidance/negative
tpi_cat_s510mmedium slope	0.328	0.010	<0.001	selection/positive

(continued)

term	estimate	std.error	p	select
tpi_cat_s510mridge	0.770	0.014	<0.001	selection/positive
tpi_cat_s510mupper slope	0.603	0.013	<0.001	selection/positive
tpi_cat_s510mvalley	-0.256	0.018	<0.001	avoidance/negative
scale(mining_Krist_nearest10000)	-0.453	0.009	<0.001	avoidance/negative
landcover_cc_groupedopen lands	1.282	0.024	<0.001	selection/positive
landcover_cc_groupedanthropogenic areas	0.494	0.052	<0.001	selection/positive
landcover_cc_groupedconiferous forests	0.932	0.023	<0.001	selection/positive
landcover_cc_groupedmires	0.387	0.028	<0.001	selection/positive
phaseConstruction	-0.148	0.044	0.001	avoidance/negative
phaseOperation	0.021	0.033	0.527	no effect
scale(wind_turbines_nearest10000)	0.281	0.019	<0.001	selection/positive
landcover_cc_groupedopen lands:phaseConstruction	0.325	0.048	<0.001	selection/positive
landcover_cc_groupedanthropogenic areas:phaseConstruction	0.194	0.097	0.046	selection/positive
landcover_cc_groupedconiferous forests:phaseConstruction	0.159	0.047	0.001	selection/positive
landcover_cc_groupedmires:phaseConstruction	-0.040	0.057	0.477	no effect
landcover_cc_groupedopen lands:phaseOperation	0.230	0.036	<0.001	selection/positive
landcover_cc_groupedanthropogenic areas:phaseOperation	0.506	0.071	<0.001	selection/positive
landcover_cc_groupedconiferous forests:phaseOperation	-0.234	0.035	<0.001	avoidance/negative
landcover_cc_groupedmires:phaseOperation	-0.310	0.043	<0.001	avoidance/negative
landcover_cc_groupedopen lands:scale(wind_turbines_nearest10000)	-0.089	0.020	<0.001	avoidance/negative
landcover_cc_groupedanthropogenic areas:scale(wind_turbines_nearest10000)	-0.060	0.045	0.184	no effect
landcover_cc_groupedconiferous forests:scale(wind_turbines_nearest10000)	-0.168	0.020	<0.001	avoidance/negative
landcover_cc_groupedmires:scale(wind_turbines_nearest10000)	-0.074	0.025	0.003	avoidance/negative
phaseConstruction:scale(wind_turbines_nearest10000)	-0.112	0.042	0.007	avoidance/negative
phaseOperation:scale(wind_turbines_nearest10000)	-0.087	0.029	0.003	avoidance/negative
landcover_cc_groupedopen lands:phaseConstruction:scale(wind_turbines_nearest10000)	0.079	0.045	0.077	no effect
landcover_cc_groupedanthropogenic areas:phaseConstruction:scale(wind_turbines_nearest10000)	0.053	0.090	0.557	no effect
landcover_cc_groupedconiferous forests:phaseConstruction:scale(wind_turbines_nearest10000)	0.138	0.044	0.002	selection/positive
landcover_cc_groupedmires:phaseConstruction:scale(wind_turbines_nearest10	0.089	0.056	0.108	no effect
landcover_cc_groupedopen lands:phaseOperation:scale(wind_turbines_nearest10000)	0.059	0.032	0.064	no effect
landcover_cc_groupedanthropogenic areas:phaseOperation:scale(wind_turbines_nearest10000)	-0.280	0.073	<0.001	avoidance/negative
landcover_cc_groupedconiferous forests:phaseOperation:scale(wind_turbines_nearest10000)	0.109	0.032	0.001	selection/positive
landcover_cc_groupedmires:phaseOperation:scale(wind_turbines_nearest1000(	-0.065	0.043	0.131	no effect

Table B7. Complete table with coefficient estimates for the best-ranked landscape-scale habitat selection functions during autumn.

10 Figure B2: Impacts of mining on habitat selection in calving

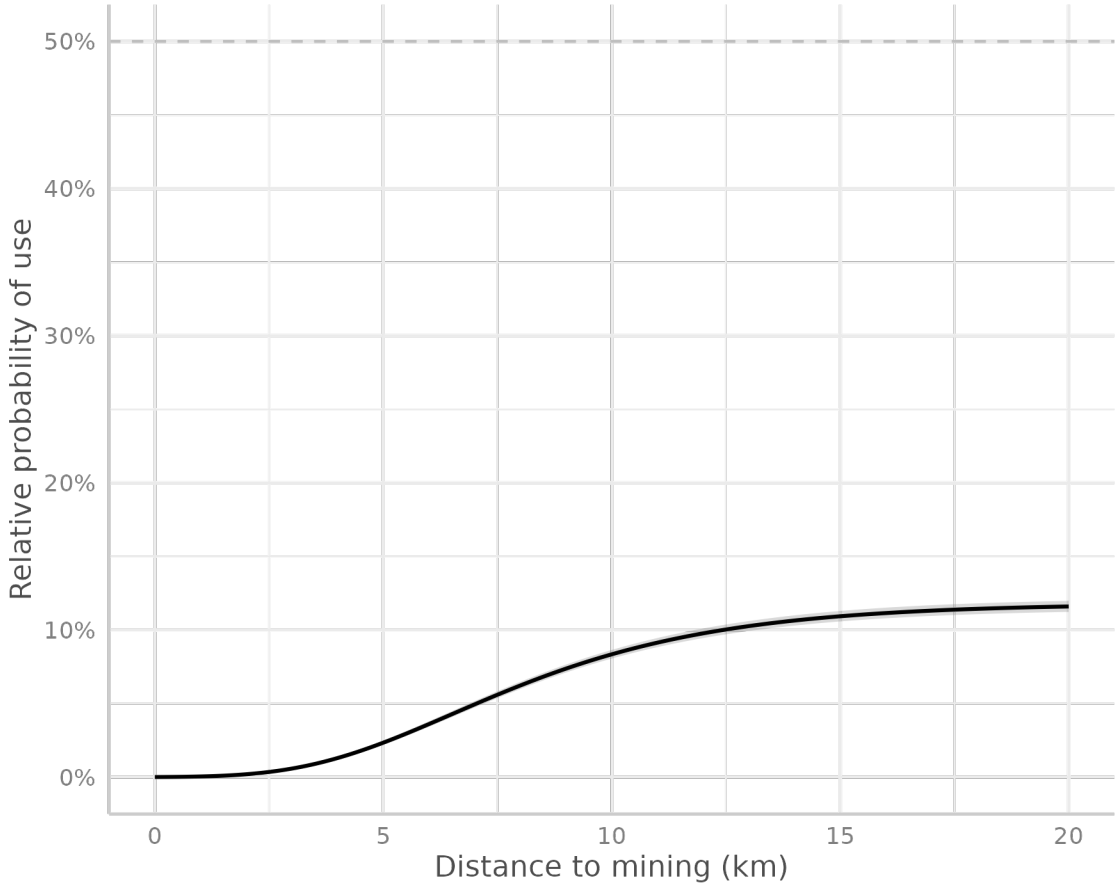

Figure B2. Relative predicted probability of use of areas as a function of the distance to the mine in Kristineberget in calving. Areas close to the mine are avoided up to ca. 10 km.

11 Figure B3: Impacts of wind power on habitat selection in calving

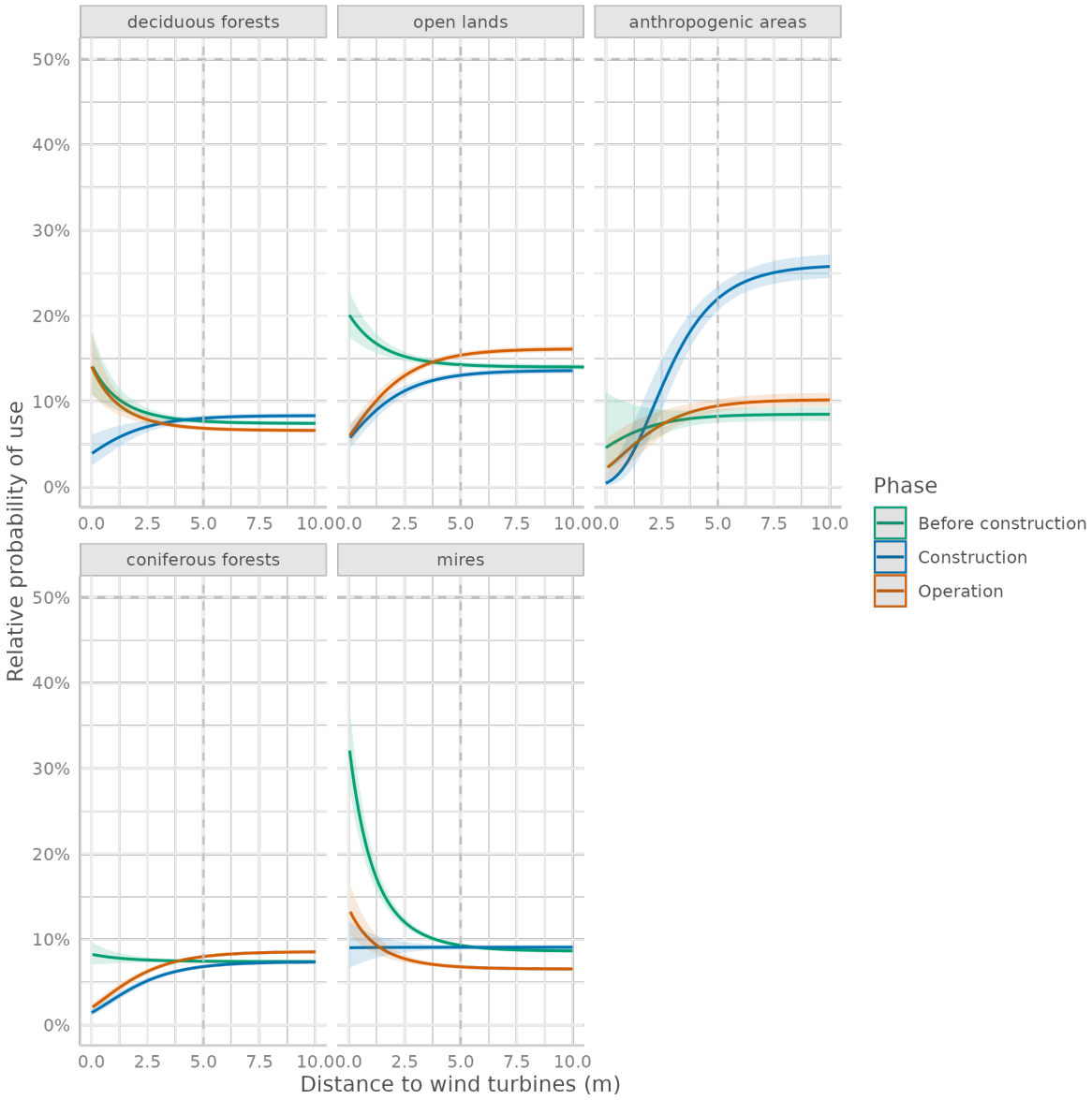

Figure B3. Relative predicted probability of use of areas as a function of the distance to the nearest wind turbine in calving, using Ytterberg wind park as a reference.

12 Figure B4: Predicted habitat suitability in calving

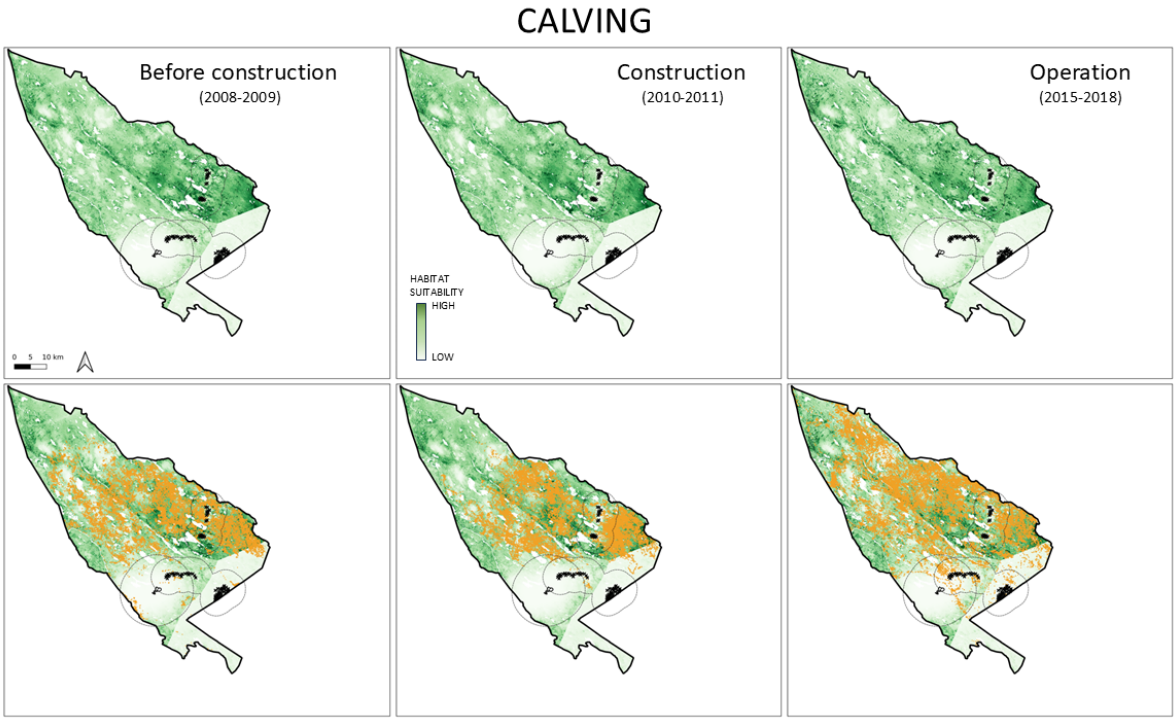

Figure B4. Predicted habitat suitability for reindeer in calving before the construction (left), during the construction (center), and during operation of the wind power plants (right). The top row shows the habitat suitability, in a gradient from 0 (white) to 1 (green), and shows the location of the wind turbines and the mine. It also highlights a buffer of 5 km around the wind power plants and 10 km around the mine, just as a reference for interpretation. The bottom row shows the GPS data for each phase superimposed over the habitat suitabiltiy predictions.

13 Figure B5: Impacts of mining on habitat selection in summer

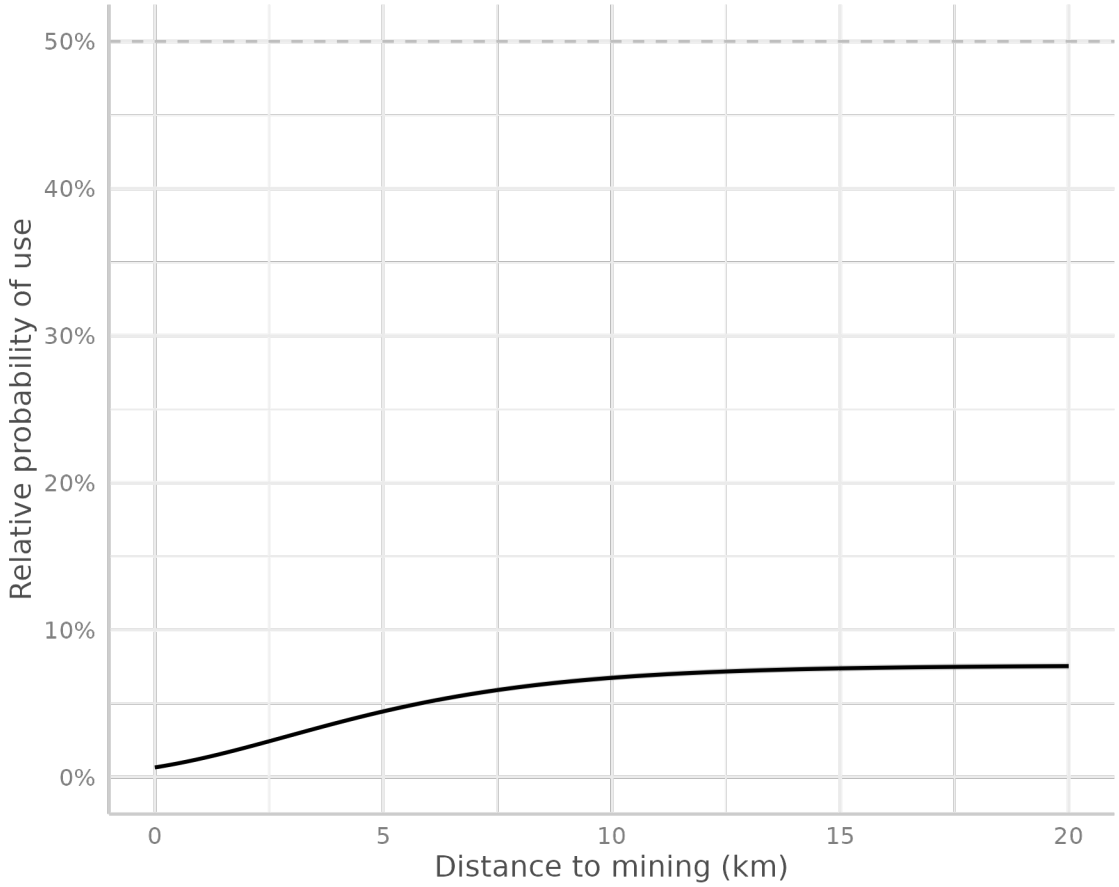

Figure B5. Relative predicted probability of use of areas as a function of the distance to the mine in Kristineberget in summer. Areas close to the mine are avoided up to ca. 10 km.

14 Figure B6: Impacts of wind power on habitat selection in summer

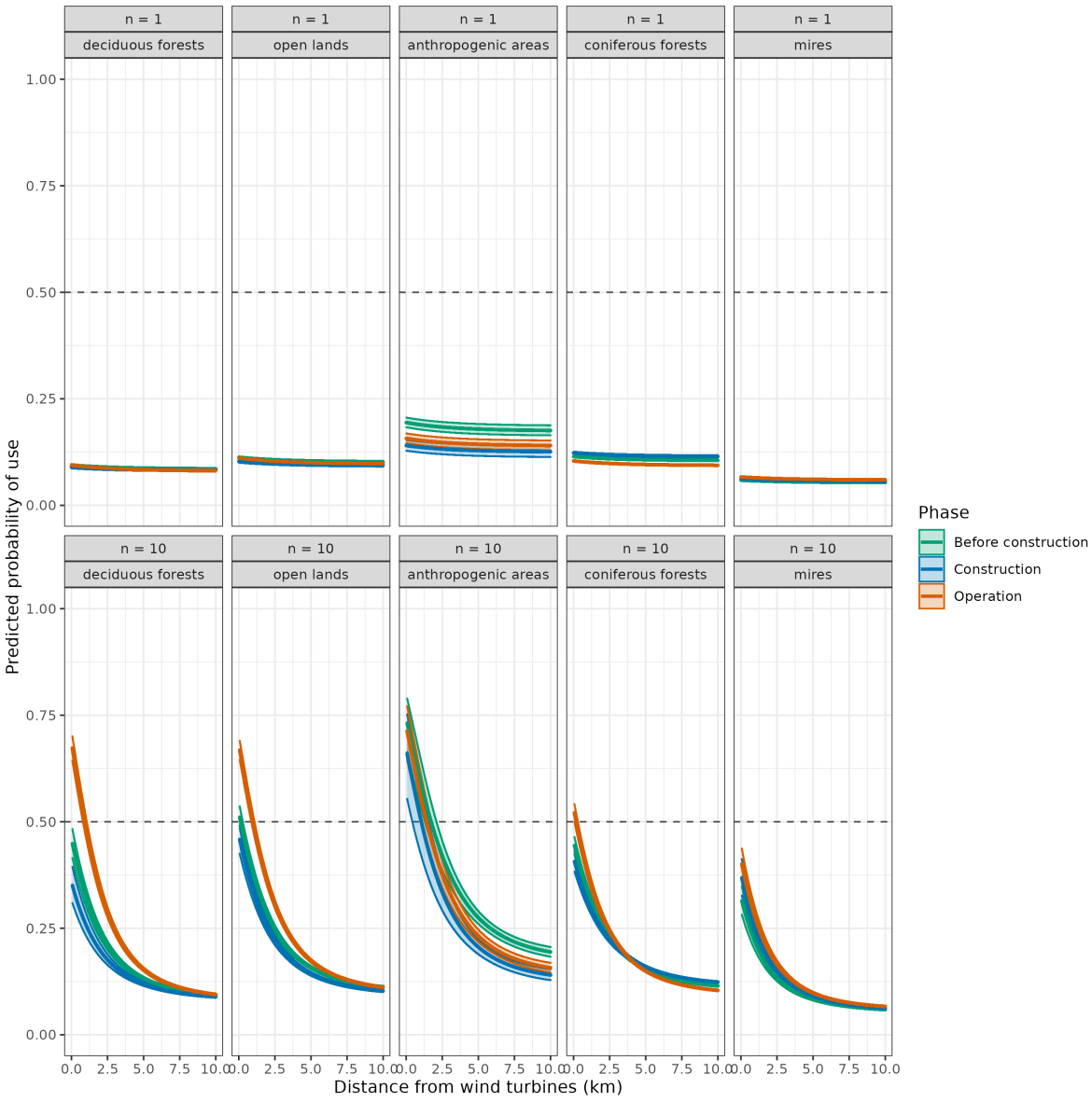

Figure B6. Relative predicted probability of use of areas versus the distance to the nearest wind turbine in summer, using Ytterberg wind park as a reference. Top row shows the (hypothetical) prediction if the wind park was composed only by n = 1 wind turbine - a small impact. The bottom row shows a cumulative impact of n = 10 wind turbines, which gets much larger.

15 Figure B7: Predicted habitat suitability in summer

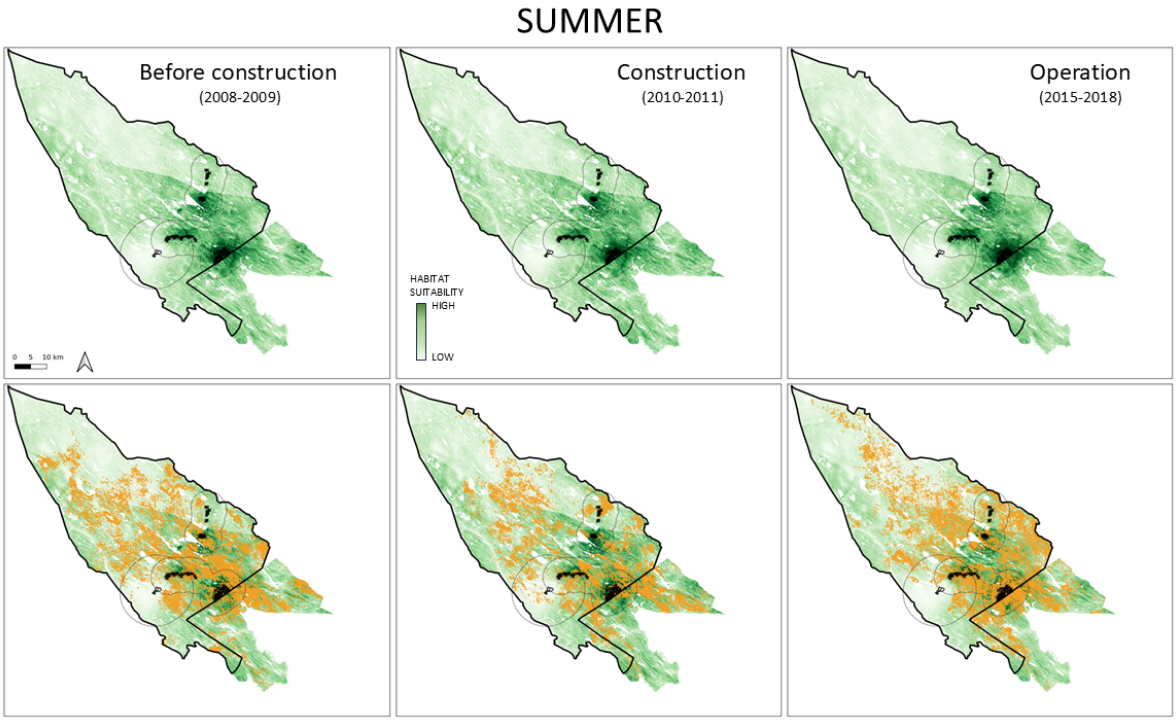

Figure B7. Predicted habitat suitability for reindeer in summer before the construction (left), during the construction (center), and during operation of the wind power plants (right). The top row shows the habitat suitability, in a gradient from 0 (white) to 1 (green), and shows the location of the wind turbines and the mine. It also highlights a buffer of 5 km around the wind power plants and 10 km around the mine, just as a reference for interpretation. The bottom row shows the GPS data for each phase superimposed over the habitat suitabiltiy predictions.

16 Figure B8: Impacts of mining on habitat selection in autumn

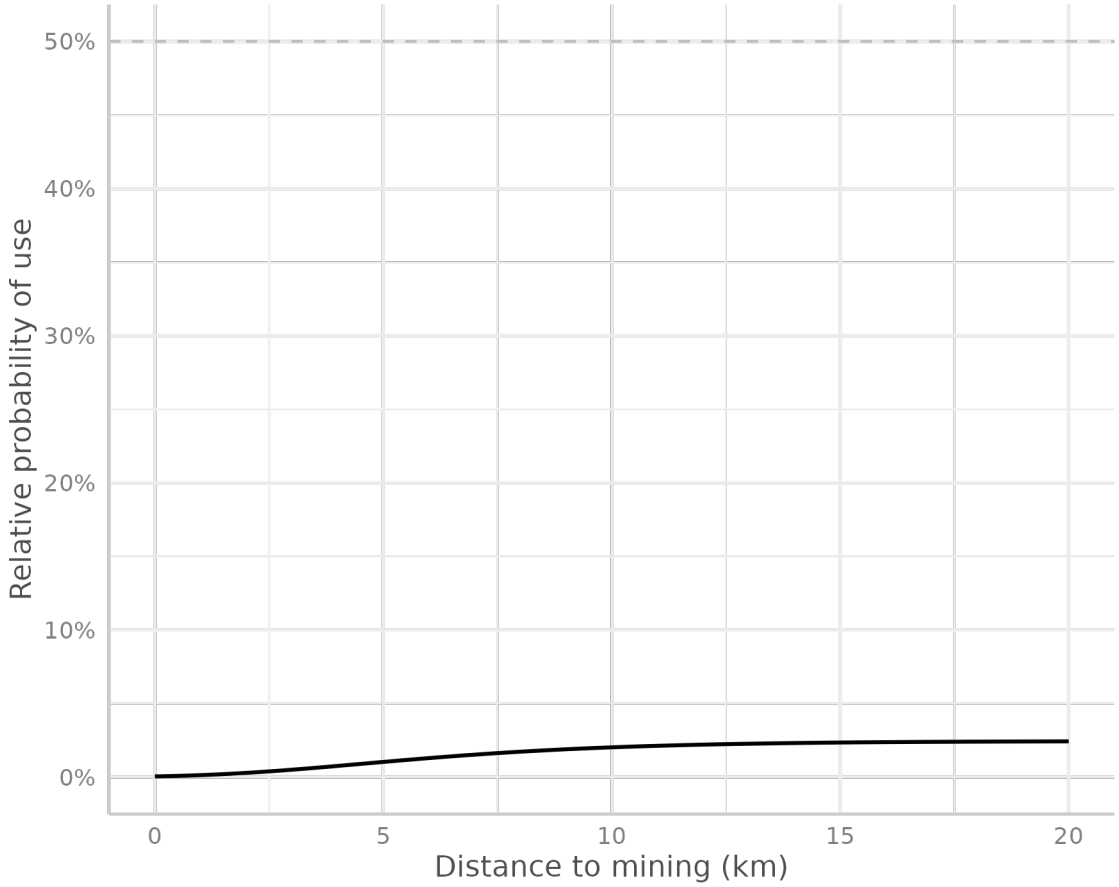

Figure B8. Relative predicted probability of use of areas as a function of the distance to the mine in Kristineberget in autumn. Areas close to the mine are avoided up to ca. 10 km.

17 Figure B9: Impacts of wind power on habitat selection in autumn

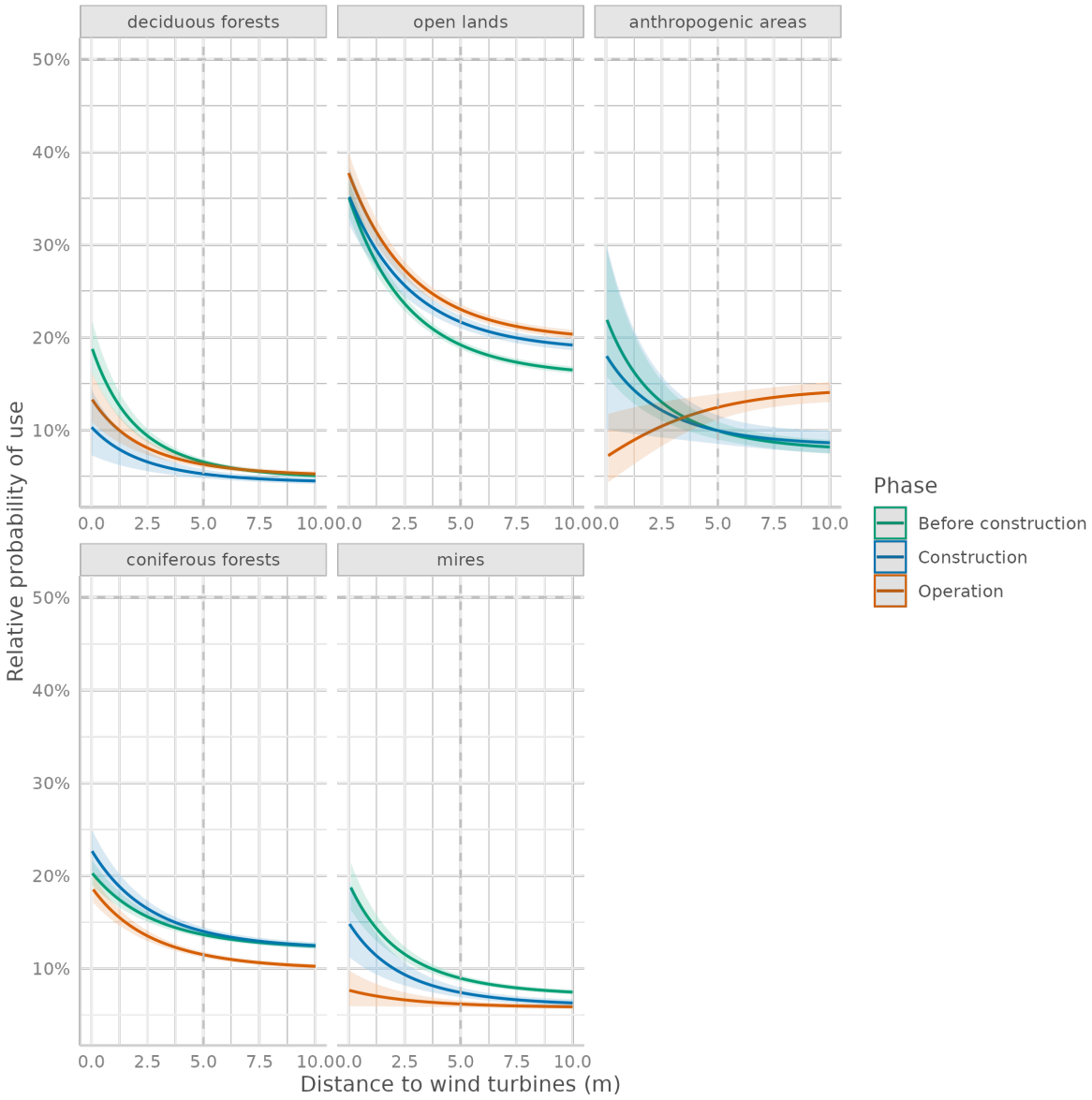

Figure B9. Relative predicted probability of use of areas as a function of the distance to the nearest wind turbine in autumn, using Ytterberg wind park as a reference.

18 Figure B10: Predicted habitat suitability in autumn

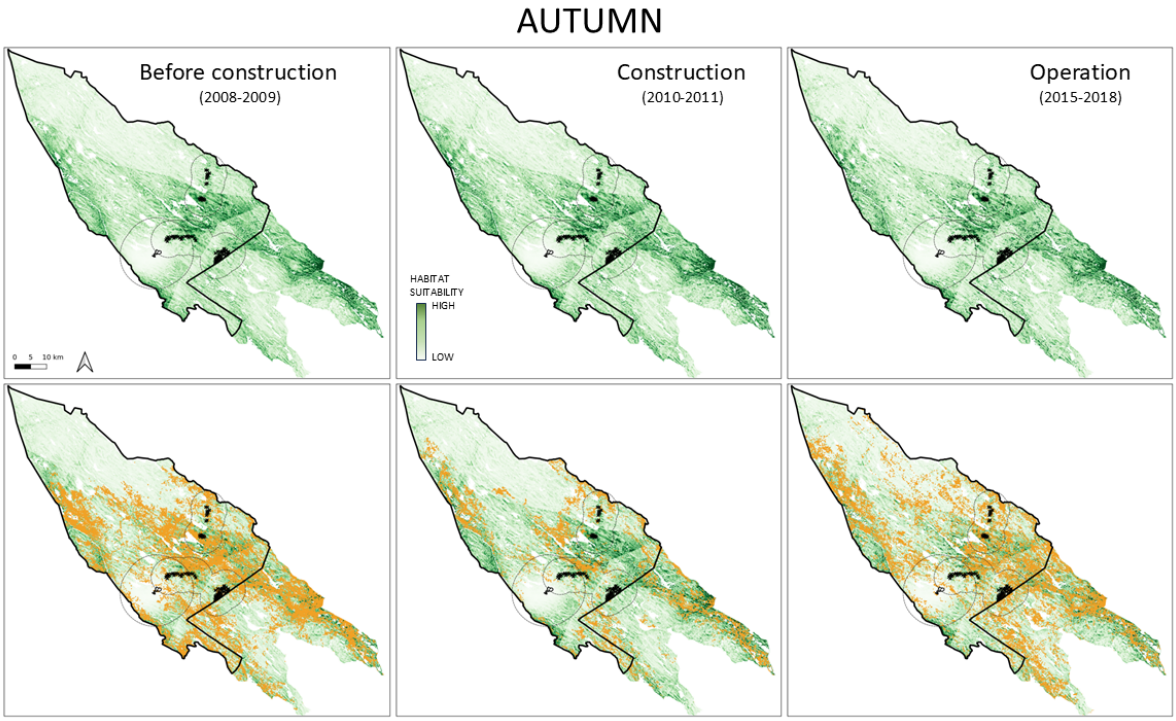

Figure B10. Predicted habitat suitability for reindeer in autumn before the construction (left), during the construction (center), and during operation of the wind power plants (right). The top row shows the habitat suitability, in a gradient from 0 (white) to 1 (green), and shows the location of the wind turbines and the mine. It also highlights a buffer of 5 km around the wind power plants and 10 km around the mine, just as a reference for interpretation. The bottom row shows the GPS data for each phase superimposed over the habitat suitabiltiy predictions.

Appendix C. Cumulative impacts of mining and wind power development on reindeer: habitat selection and movement at patch scale (integrated step selection analysis, iSSA)

Here we provide supplementary information regarding the assessment of reindeer habitat selection for grazing sites and movement patterns in the Malå reindeer herding community, Sweden, under the presence of mining and wind power development, for the three snow-free seasons: calving, summer, and autumn. The analysis consisted of an integrated step-selection analysis [iSSA; Avgar et al. (2016)] to simultaneously quantify effects on habitat selection at the foraging patch scale and on movement parameters. We present, for each season: (i) the reindeer GPS data used for the analyses; (ii) the setup of the iSSA models; (iii) the best-ranged iSSA models; (iv) the model selection tables; (v) the tables of coefficients; (vi) figures illustrating the impacts of mining and wind turbines.

Table of contents

1 Table C1: GPS data used in the iSSA analysis

Year	Phase	Calving	Summer	Autumn
2008	Before construction	47 (17360)	42 (25157)	39 (23666)
2009	Before construction	34 (14370)	33 (16469)	39 (13947)
2010	Construction	40 (17416)	43 (20416)	27 (9833)
2011	Construction	14 (5847)	12 (5143)	9 (4037)
2015	Operation	40 (22767)	38 (19777)	37 (19011)
2016	Operation	31 (11576)	19 (6936)	12 (2825)
2017	Operation	5 (2431)	7 (4092)	11 (4630)
2018	Operation	7 (3180)	6 (3023)	2 (1134)

Table C1. Number of reindeer monitored (number of GPS positions recorded, in parenthesis) in each year and season, used for the integrated step selection analysis. The numbers are sometimes lower than those used in the regional-scale habitat selection analysis.

2 Text C1: Statistical modeling of the iSSA

As described in the main text, the patch-scale habitat selection analysis followed a iSSA. The overall model structure we fitted was the following:

```r
base_formula <- case_ ~ strata(step_id_) +
  # movement
  sl_ + log_sl + cos_ta +
  wind_turbines_YYY_start_construction_scaled:(sl_ + log_sl + cos_ta) +
  wind_turbines_ZZZ_start_operation_scaled:(sl_ + log_sl + cos_ta) +
  landcover_start:(sl_ + log_sl + cos_ta) +
  # habitat selection
  dem_end_scaled + I(dem_end_scaled^2) + slope_end_scaled +
  sos_end_scaled +
  log_power_lines_dist_end + log_priv_road_dist_end + log_public_road_dist_end +
  log_house_dist_end +
  landcover_end +
  # minig habitat selection
  mining_Krist_nearestXXX_end_scaled +
  # wind habitat selection
  wf_name_end +
  wind_turbines_YYY_end_construction_scaled +
  wind_turbines_ZZZ_end_operation_scaled +
  landcover_end:wind_turbines_YYY_end_construction_scaled +
  landcover_end:wind_turbines_ZZZ_end_operation_scaled +
  # tpi habitat selection
  tpi_scale_TTT +
  # barriers to movement (along the steps)
  public_road_nearest100_cross +
  wind_turbines_nearest500_cross_construction +
  wind_turbines_nearest500_cross_operation
```

where:

- the terms `start`, `end`, and `cross` refer to variables extracted at the start or end points of a step, or along a step. Variables representing habitat selection were selected at the end points of steps, and variables in interaction with movement parameters were extracted at the starting point of steps. Variables with `cross` represented whether an infrastructure was crossed or not along a step and are used to estimate the barrier effect of that infrastructure type;
- terms with `scaled` were scaled to mean = 0 and standard deviation = 1;
- `case_`: our response variable (0/1);
- `dem`: elevation, we include a linear and a quadratic term;
- `slope`: slope;
- `cos_aspect`: cosine of the aspect;
- `tpi_scale_TTT`: topographic position index (TPI) computed at a certain scale, classified in 6 levels: flat (reference level), lower slope, medium slope, upper slope, ridge, valley;

- `sos`: start of season (used for calving and summer), replaced by `eos`, end of season, for autumn;
- `wf_name`: name of the wind power plant closest to each point, with four categories, added as a fixed effect to control for differential effects close to the Åmliden wind park, which lies along a large fenced area;
- `landcover`: land cover, with 5 categories: deciduous forest (reference category), coniferous forest, open areas, mires, and anthropogenic areas;
- `log_public_road_dist`, `log_priv_road_dist`, `log_house_dist`, `log_power_lines_dist`: logarithm of the distance to the nearest infrastructure for public roads, private roads, houses, and power lines;
- `mining_Krist_nearestXXX`: ZOI (exponential decay distance) of the mine, computed considering a certain ZOI radius;
- `sl_`, `log_sl` and `cos_ta`: movement parameters (step length, log(step length), and cosine of the turning angle, respectively).
- `wind_turbines_YYY_end_construction` and `wind_turbines_YYY_end_operation`: variables representing the ZOI of wind turbines. These variables assume a value equal to the wind turbine influence (density or nearest, with a corresponding ZOI radius) at the construction and operation phases, respectively, and were zero for other development phases;
- `public_road_nearest100_cross`: binary variable (0/1) representing whether a certain step crossed or not a public road;
- `wind_turbines_nearest500_cross_construction` and `wind_turbines_nearest500_cross_operation`: binary variables (0/1) representing whether a certain step crossed or not a buffer of 500 m around any wind turbines, during construction and operation.

The model structure contains the movement parameters, including its interaction with the effects of land cover and wind turbines; habitat selection considering the effects of wind turbines in each phase (construction, operation) in interaction with land cover; and main effects of other infrastructure and landscape variables.

The terms `XXX`, `YYY`, `ZZZ`, and `TTT` in the model structure above represent scales or variables that varied across models fitted. To evaluate the most likely ZOI for the mine and the wind turbines, whether there was a cumulative impact of multiple wind power plants, and at which scale the TPI most affected reindeer habitat selection and movement, we replaced these variables in the model structure above using each possible combination of ZOI radii and type (cumulative vs. nearest) for wind power and the different ZOI radii for mining, together with different scales for the TPI (see Fig. B1 in Appendix B). Models were compared through Akaike information criterion (AIC), as described in the main text. The scales included were:

- Mining (`XXX`): 100 m, 250 m, 500 m, 1 km, 2.5 km, 5 km, 10 km.
- Wind turbines (`ZZZ`): density of turbines or distance to the nearest turbine, with ZOI radii 100 m, 250 m, 500 m, 1 km, 2.5 km, 5 km, 10 km.
- TPI: 150 m, 250 m, 510 m.

3 Text C2: Best-ranked integrated step-selection models

This is the structure of the best-ranked iSSA model selected for each season.

Summary of best ranked models:

- **Calving. Cumulative impact of wind turbines, ZOI radius = 5 km; no significant effect of the mine:**
  case_ ~ strata(step_id_) + sl_ + log_sl + cos_ta + wind_turbines_cumulative5000_start_construction_s
  + log_sl + cos_ta) + wind_turbines_cumulative5000_start_operation_scaled:(sl_
  + log_sl + cos_ta) + landcover_cc_grouped_start:(sl_ + log_sl + cos_ta) +
  dem_end_scaled + I(dem_end_scaled^2) + slope_end_scaled + sos_end_scaled +
  log_power_lines_dist_end + log_priv_road_dist_end + log_public_road_dist_end +
  log_house_dist_end + mining_Krist_nearest250_end_scaled + wf_name_end + land-
  cover_cc_grouped_end + wind_turbines_cumulative5000_end_construction_scaled +
  wind_turbines_cumulative5000_end_operation_scaled + landcover_cc_grouped_end:wind_turbines_cum
  + landcover_cc_grouped_end:wind_turbines_cumulative5000_end_operation_scaled
  + public_road_nearest100_cross + wind_turbines_nearest500_cross_construction +
  wind_turbines_nearest500_cross_operation + tpi_cat_s150m_end
- **Summer. ZOI of the nearest wind turbine, radius = 5 km; ZOI of the mine with radius 10 km:**
  case_ ~ strata(step_id_) + sl_ + log_sl + cos_ta + wind_turbines_nearest5000_start_construction_scale
  + log_sl + cos_ta) + wind_turbines_nearest5000_start_operation_scaled:(sl_ +
  log_sl + cos_ta) + landcover_cc_grouped_start:(sl_ + log_sl + cos_ta) +
  dem_end_scaled + I(dem_end_scaled^2) + slope_end_scaled + sos_end_scaled +
  log_power_lines_dist_end + log_priv_road_dist_end + log_public_road_dist_end
  + log_house_dist_end + mining_Krist_nearest5000_end_scaled + wf_name_end +
  landcover_cc_grouped_end + wind_turbines_nearest5000_end_construction_scaled +
  wind_turbines_nearest5000_end_operation_scaled + landcover_cc_grouped_end:wind_turbines_nearest
  + landcover_cc_grouped_end:wind_turbines_nearest5000_end_operation_scaled +
  public_road_nearest100_cross + wind_turbines_nearest500_cross_construction +
  wind_turbines_nearest500_cross_operation + tpi_cat_s150m_end
- **Autumn. Cumulative ZOI of wind turbines, radius = 10km; no significant effect of the mine:**
  case_ ~ strata(step_id_) + sl_ + log_sl + cos_ta + dem_end_scaled +
  I(dem_end_scaled^2) + slope_end_scaled + eos_end_scaled + log_power_lines_dist_end
  + log_priv_road_dist_end + log_public_road_dist_end + log_house_dist_end
  + log_mining_Krist_dist_end + wf_name_end + landcover_cc_grouped_end +
  wind_turbines_cumulative10000_end_construction_scaled + wind_turbines_cumulative10000_end_opera
  + public_road_nearest100_cross + wind_turbines_nearest500_cross_construction +
  wind_turbines_nearest500_cross_operation + tpi_cat_s510m_end + sl_:wind_turbines_cumulative10000
  + log_sl:wind_turbines_cumulative10000_start_construction_scaled + cos_ta:wind_turbines_cumulative

+ sl_:wind_turbines_cumulative10000_start_operation_scaled + log_sl:wind_turbines_cumulative10000_
+ cos_ta:wind_turbines_cumulative10000_start_operation_scaled + sl_:landcover_cc_grouped_start
+ log_sl:landcover_cc_grouped_start + cos_ta:landcover_cc_grouped_start + land-
cover_cc_grouped_end:wind_turbines_cumulative10000_end_construction_scaled +
landcover_cc_grouped_end:wind_turbines_cumulative10000_end_operation_scaled

4 Table C2: Model selection table in calving

Table C2 was truncated to show only the first 10 models, to avoid an overly long table.

Mining ZOI radius	Wind turbine ZOI radius	TPI	AIC	dAIC	formula
250	cumulative5000	150m_end	442154.7	0.00	case_ ~ strata(step_id_) + sl_ + log_sl + cos_ta + wind_turbines_cumulative5000_start_construction_scaled:(sl_ + log_sl + cos_ta) + wind_turbines_cumulative5000_start_operation_scaled:(sl_ + log_sl + cos_ta) + landcover_cc_grouped_start:(sl_ + log_sl + cos_ta) + dem_end_scaled + I(dem_end_scaled^2) + slope_end_scaled + sos_end_scaled + log_power_lines_dist_end + log_priv_road_dist_end + log_public_road_dist_end + log_house_dist_end + mining_Krist_nearest250_end_scaled + wf_name_end + landcover_cc_grouped_end + wind_turbines_cumulative5000_end_construction_scaled + wind_turbines_cumulative5000_end_operation_scaled + land-cover_cc_grouped_end:wind_turbines_cumulative5000_end_construct + land-cover_cc_grouped_end:wind_turbines_cumulative5000_end_operation + public_road_nearest100_cross + wind_turbines_nearest500_cross_construction + wind_turbines_nearest500_cross_operation + tpi_cat_s150m_end

(continued)

Mining ZOI radius	Wind turbine ZOI radius	TPI	AIC	dAIC	formula
10000	cumulative5000	150m_end	442155.0	0.30	case_ ~ strata(step_id_) + sl_ + log_sl + cos_ta + wind_turbines_cumulative5000_start_construction_scaled:(sl_ + log_sl + cos_ta) + wind_turbines_cumulative5000_start_operation_scaled:(sl_ + log_sl + cos_ta) + landcover_cc_grouped_start:(sl_ + log_sl + cos_ta) + dem_end_scaled + I(dem_end_scaled^2) + slope_end_scaled + sos_end_scaled + log_power_lines_dist_end + log_priv_road_dist_end + log_public_road_dist_end + log_house_dist_end + mining_Krist_nearest10000_end_scaled + wf_name_end + landcover_cc_grouped_end + wind_turbines_cumulative5000_end_construction_scaled + wind_turbines_cumulative5000_end_operation_scaled + landcover_cc_grouped_end:wind_turbines_cumulative5000_end_construct + landcover_cc_grouped_end:wind_turbines_cumulative5000_end_operation + public_road_nearest100_cross + wind_turbines_nearest500_cross_construction + wind_turbines_nearest500_cross_operation + tpi_cat_s150m_end
500	cumulative5000	150m_end	442156.4	1.68	case_ ~ strata(step_id_) + sl_ + log_sl + cos_ta + wind_turbines_cumulative5000_start_construction_scaled:(sl_ + log_sl + cos_ta) + wind_turbines_cumulative5000_start_operation_scaled:(sl_ + log_sl + cos_ta) + landcover_cc_grouped_start:(sl_ + log_sl + cos_ta) + dem_end_scaled + I(dem_end_scaled^2) + slope_end_scaled + sos_end_scaled + log_power_lines_dist_end + log_priv_road_dist_end + log_public_road_dist_end + log_house_dist_end + mining_Krist_nearest500_end_scaled + wf_name_end + landcover_cc_grouped_end + wind_turbines_cumulative5000_end_construction_scaled + wind_turbines_cumulative5000_end_operation_scaled + landcover_cc_grouped_end:wind_turbines_cumulative5000_end_construct + landcover_cc_grouped_end:wind_turbines_cumulative5000_end_operation + public_road_nearest100_cross + wind_turbines_nearest500_cross_construction + wind_turbines_nearest500_cross_operation + tpi_cat_s150m_end

(continued)

Mining ZOI radius	Wind turbine ZOI radius	TPI	AIC	dAIC	formula
1000	cumulative5000	150m_end	442158.2	3.51	case_ ~ strata(step_id_) + sl_ + log_sl + cos_ta + wind_turbines_cumulative5000_start_construction_scaled:(sl_ + log_sl + cos_ta) + wind_turbines_cumulative5000_start_operation_scaled:(sl_ + log_sl + cos_ta) + landcover_cc_grouped_start:(sl_ + log_sl + cos_ta) + dem_end_scaled + I(dem_end_scaled^2) + slope_end_scaled + sos_end_scaled + log_power_lines_dist_end + log_priv_road_dist_end + log_public_road_dist_end + log_house_dist_end + mining_Krist_nearest1000_end_scaled + wf_name_end + landcover_cc_grouped_end + wind_turbines_cumulative5000_end_construction_scaled + wind_turbines_cumulative5000_end_operation_scaled + landcover_cc_grouped_end:wind_turbines_cumulative5000_end_construct + landcover_cc_grouped_end:wind_turbines_cumulative5000_end_operation + public_road_nearest100_cross + wind_turbines_nearest500_cross_construction + wind_turbines_nearest500_cross_operation + tpi_cat_s150m_end
2500	cumulative5000	150m_end	442158.3	3.61	case_ ~ strata(step_id_) + sl_ + log_sl + cos_ta + wind_turbines_cumulative5000_start_construction_scaled:(sl_ + log_sl + cos_ta) + wind_turbines_cumulative5000_start_operation_scaled:(sl_ + log_sl + cos_ta) + landcover_cc_grouped_start:(sl_ + log_sl + cos_ta) + dem_end_scaled + I(dem_end_scaled^2) + slope_end_scaled + sos_end_scaled + log_power_lines_dist_end + log_priv_road_dist_end + log_public_road_dist_end + log_house_dist_end + mining_Krist_nearest2500_end_scaled + wf_name_end + landcover_cc_grouped_end + wind_turbines_cumulative5000_end_construction_scaled + wind_turbines_cumulative5000_end_operation_scaled + landcover_cc_grouped_end:wind_turbines_cumulative5000_end_construct + landcover_cc_grouped_end:wind_turbines_cumulative5000_end_operation + public_road_nearest100_cross + wind_turbines_nearest500_cross_construction + wind_turbines_nearest500_cross_operation + tpi_cat_s150m_end

(continued)

Mining ZOI radius	Wind turbine ZOI radius	TPI	AIC	dAIC	formula
5000	cumulative5000	150m_end	442158.3	3.67	case_ ~ strata(step_id_) + sl_ + log_sl + cos_ta + wind_turbines_cumulative5000_start_construction_scaled:(sl_ + log_sl + cos_ta) + wind_turbines_cumulative5000_start_operation_scaled:(sl_ + log_sl + cos_ta) + landcover_cc_grouped_start:(sl_ + log_sl + cos_ta) + dem_end_scaled + I(dem_end_scaled^2) + slope_end_scaled + sos_end_scaled + log_power_lines_dist_end + log_priv_road_dist_end + log_public_road_dist_end + log_house_dist_end + mining_Krist_nearest5000_end_scaled + wf_name_end + landcover_cc_grouped_end + wind_turbines_cumulative5000_end_construction_scaled + wind_turbines_cumulative5000_end_operation_scaled + landcover_cc_grouped_end:wind_turbines_cumulative5000_end_construct + landcover_cc_grouped_end:wind_turbines_cumulative5000_end_operation + public_road_nearest100_cross + wind_turbines_nearest500_cross_construction + wind_turbines_nearest500_cross_operation + tpi_cat_s150m_end
100	cumulative5000	150m_end	442166.6	11.91	case_ ~ strata(step_id_) + sl_ + log_sl + cos_ta + wind_turbines_cumulative5000_start_construction_scaled:(sl_ + log_sl + cos_ta) + wind_turbines_cumulative5000_start_operation_scaled:(sl_ + log_sl + cos_ta) + landcover_cc_grouped_start:(sl_ + log_sl + cos_ta) + dem_end_scaled + I(dem_end_scaled^2) + slope_end_scaled + sos_end_scaled + log_power_lines_dist_end + log_priv_road_dist_end + log_public_road_dist_end + log_house_dist_end + mining_Krist_nearest100_end_scaled + wf_name_end + landcover_cc_grouped_end + wind_turbines_cumulative5000_end_construction_scaled + wind_turbines_cumulative5000_end_operation_scaled + landcover_cc_grouped_end:wind_turbines_cumulative5000_end_construct + landcover_cc_grouped_end:wind_turbines_cumulative5000_end_operation + public_road_nearest100_cross + wind_turbines_nearest500_cross_construction + wind_turbines_nearest500_cross_operation + tpi_cat_s150m_end

(continued)

Mining ZOI radius	Wind turbine ZOI radius	TPI	AIC	dAIC	formula
250	nearest5000	150m_end	442174.1	19.42	case_ ~ strata(step_id_) + sl_ + log_sl + cos_ta + wind_turbines_nearest5000_start_construction_scaled:(sl_ + log_sl + cos_ta) + wind_turbines_nearest5000_start_operation_scaled:(sl_ + log_sl + cos_ta) + landcover_cc_grouped_start:(sl_ + log_sl + cos_ta) + dem_end_scaled + I(dem_end_scaled^2) + slope_end_scaled + sos_end_scaled + log_power_lines_dist_end + log_priv_road_dist_end + log_public_road_dist_end + log_house_dist_end + mining_Krist_nearest250_end_scaled + wf_name_end + landcover_cc_grouped_end + wind_turbines_nearest5000_end_construction_scaled + wind_turbines_nearest5000_end_operation_scaled + landcover_cc_grouped_end:wind_turbines_nearest5000_end_construction_ + landcover_cc_grouped_end:wind_turbines_nearest5000_end_operation_sc + public_road_nearest100_cross + wind_turbines_nearest500_cross_construction + wind_turbines_nearest500_cross_operation + tpi_cat_s150m_end
10000	nearest5000	150m_end	442175.3	20.60	case_ ~ strata(step_id_) + sl_ + log_sl + cos_ta + wind_turbines_nearest5000_start_construction_scaled:(sl_ + log_sl + cos_ta) + wind_turbines_nearest5000_start_operation_scaled:(sl_ + log_sl + cos_ta) + landcover_cc_grouped_start:(sl_ + log_sl + cos_ta) + dem_end_scaled + I(dem_end_scaled^2) + slope_end_scaled + sos_end_scaled + log_power_lines_dist_end + log_priv_road_dist_end + log_public_road_dist_end + log_house_dist_end + mining_Krist_nearest10000_end_scaled + wf_name_end + landcover_cc_grouped_end + wind_turbines_nearest5000_end_construction_scaled + wind_turbines_nearest5000_end_operation_scaled + landcover_cc_grouped_end:wind_turbines_nearest5000_end_construction_ + landcover_cc_grouped_end:wind_turbines_nearest5000_end_operation_sc + public_road_nearest100_cross + wind_turbines_nearest500_cross_construction + wind_turbines_nearest500_cross_operation + tpi_cat_s150m_end

(continued)

Mining ZOI radius	Wind turbine ZOI radius	TPI	AIC	dAIC	formula
500	nearest5000	150m_end	442175.9	21.22	case_ ~ strata(step_id_) + sl_ + log_sl + cos_ta + wind_turbines_nearest5000_start_construction_scaled:(sl_ + log_sl + cos_ta) + wind_turbines_nearest5000_start_operation_scaled:(sl_ + log_sl + cos_ta) + landcover_cc_grouped_start:(sl_ + log_sl + cos_ta) + dem_end_scaled + I(dem_end_scaled^2) + slope_end_scaled + sos_end_scaled + log_power_lines_dist_end + log_priv_road_dist_end + log_public_road_dist_end + log_house_dist_end + mining_Krist_nearest500_end_scaled + wf_name_end + landcover_cc_grouped_end + wind_turbines_nearest5000_end_construction_scaled + wind_turbines_nearest5000_end_operation_scaled + landcover_cc_grouped_end:wind_turbines_nearest5000_end_construction_ + landcover_cc_grouped_end:wind_turbines_nearest5000_end_operation_sc + public_road_nearest100_cross + wind_turbines_nearest500_cross_construction + wind_turbines_nearest500_cross_operation + tpi_cat_s150m_end

Table C2. Table of model selection for the iSSA models for calving. Columns are zone of influence (ZOI) radius for mining and wind turbines, scale for the topographic position index (TPI), AIC of the model, dAIC of each model in relation to the most parsimonious model, and the formula with each model's structure. For impact of wind turbines, cumulative represents the density of turbines, and nearest represents the distance-decay ZOI of the nearest turbine.

5 Table C3: Model selection table in summer

Table C3 was truncated to show only the first 10 models, to avoid an overly long table.

Mining ZOI radius	Wind turbine ZOI radius	TPI	AIC	dAIC	formula
10000	nearest5000	150m	470896.2	0.00	case_ ~ strata(step_id_) + sl_ + log_sl + cos_ta + wind_turbines_nearest5000_start_construction_scaled:(sl_ + log_sl + cos_ta) + wind_turbines_nearest5000_start_operation_scaled:(sl_ + log_sl + cos_ta) + landcover_cc_grouped_start:(sl_ + log_sl + cos_ta) + dem_end_scaled + I(dem_end_scaled^2) + slope_end_scaled + sos_end_scaled + log_power_lines_dist_end + log_priv_road_dist_end + log_public_road_dist_end + log_house_dist_end + mining_Krist_nearest10000_end_scaled + wf_name_end + landcover_cc_grouped_end + wind_turbines_nearest5000_end_construction_scaled + wind_turbines_nearest5000_end_operation_scaled + landcover_cc_grouped_end:wind_turbines_nearest5000_end_construction_ + landcover_cc_grouped_end:wind_turbines_nearest5000_end_operation_sc + public_road_nearest100_cross + wind_turbines_nearest500_cross_construction + wind_turbines_nearest500_cross_operation + tpi_cat_s150m_end
10000	nearest10000	150m	470896.8	0.63	case_ ~ strata(step_id_) + sl_ + log_sl + cos_ta + wind_turbines_nearest10000_start_construction_scaled:(sl_ + log_sl + cos_ta) + wind_turbines_nearest10000_start_operation_scaled:(sl_ + log_sl + cos_ta) + landcover_cc_grouped_start:(sl_ + log_sl + cos_ta) + dem_end_scaled + I(dem_end_scaled^2) + slope_end_scaled + sos_end_scaled + log_power_lines_dist_end + log_priv_road_dist_end + log_public_road_dist_end + log_house_dist_end + mining_Krist_nearest10000_end_scaled + wf_name_end + landcover_cc_grouped_end + wind_turbines_nearest10000_end_construction_scaled + wind_turbines_nearest10000_end_operation_scaled + landcover_cc_grouped_end:wind_turbines_nearest10000_end_construction + landcover_cc_grouped_end:wind_turbines_nearest10000_end_operation_s + public_road_nearest100_cross + wind_turbines_nearest500_cross_construction + wind_turbines_nearest500_cross_operation + tpi_cat_s150m_end

(continued)

Mining ZOI radius	Wind turbine ZOI radius	TPI	AIC	dAIC	formula
5000	nearest5000	150m	470897.9	1.69	case_ ~ strata(step_id_) + sl_ + log_sl + cos_ta + wind_turbines_nearest5000_start_construction_scaled:(sl_ + log_sl + cos_ta) + wind_turbines_nearest5000_start_operation_scaled:(sl_ + log_sl + cos_ta) + landcover_cc_grouped_start:(sl_ + log_sl + cos_ta) + dem_end_scaled + I(dem_end_scaled^2) + slope_end_scaled + sos_end_scaled + log_power_lines_dist_end + log_priv_road_dist_end + log_public_road_dist_end + log_house_dist_end + mining_Krist_nearest5000_end_scaled + wf_name_end + landcover_cc_grouped_end + wind_turbines_nearest5000_end_construction_scaled + wind_turbines_nearest5000_end_operation_scaled + landcover_cc_grouped_end:wind_turbines_nearest5000_end_construction_ + landcover_cc_grouped_end:wind_turbines_nearest5000_end_operation_sc + public_road_nearest100_cross + wind_turbines_nearest500_cross_construction + wind_turbines_nearest500_cross_operation + tpi_cat_s150m_end
5000	nearest10000	150m	470898.9	2.70	case_ ~ strata(step_id_) + sl_ + log_sl + cos_ta + wind_turbines_nearest10000_start_construction_scaled:(sl_ + log_sl + cos_ta) + wind_turbines_nearest10000_start_operation_scaled:(sl_ + log_sl + cos_ta) + landcover_cc_grouped_start:(sl_ + log_sl + cos_ta) + dem_end_scaled + I(dem_end_scaled^2) + slope_end_scaled + sos_end_scaled + log_power_lines_dist_end + log_priv_road_dist_end + log_public_road_dist_end + log_house_dist_end + mining_Krist_nearest5000_end_scaled + wf_name_end + landcover_cc_grouped_end + wind_turbines_nearest10000_end_construction_scaled + wind_turbines_nearest10000_end_operation_scaled + landcover_cc_grouped_end:wind_turbines_nearest10000_end_construction + landcover_cc_grouped_end:wind_turbines_nearest10000_end_operation_s + public_road_nearest100_cross + wind_turbines_nearest500_cross_construction + wind_turbines_nearest500_cross_operation + tpi_cat_s150m_end

(continued)

Mining ZOI radius	Wind turbine ZOI radius	TPI	AIC	dAIC	formula
2500	nearest5000	150m	470902.8	6.55	case_ ~ strata(step_id_) + sl_ + log_sl + cos_ta + wind_turbines_nearest5000_start_construction_scaled:(sl_ + log_sl + cos_ta) + wind_turbines_nearest5000_start_operation_scaled:(sl_ + log_sl + cos_ta) + landcover_cc_grouped_start:(sl_ + log_sl + cos_ta) + dem_end_scaled + I(dem_end_scaled^2) + slope_end_scaled + sos_end_scaled + log_power_lines_dist_end + log_priv_road_dist_end + log_public_road_dist_end + log_house_dist_end + mining_Krist_nearest2500_end_scaled + wf_name_end + landcover_cc_grouped_end + wind_turbines_nearest5000_end_construction_scaled + wind_turbines_nearest5000_end_operation_scaled + landcover_cc_grouped_end:wind_turbines_nearest5000_end_construction_ + landcover_cc_grouped_end:wind_turbines_nearest5000_end_operation_sc + public_road_nearest100_cross + wind_turbines_nearest500_cross_construction + wind_turbines_nearest500_cross_operation + tpi_cat_s150m_end
10000	nearest2500	150m	470903.3	7.09	case_ ~ strata(step_id_) + sl_ + log_sl + cos_ta + wind_turbines_nearest2500_start_construction_scaled:(sl_ + log_sl + cos_ta) + wind_turbines_nearest2500_start_operation_scaled:(sl_ + log_sl + cos_ta) + landcover_cc_grouped_start:(sl_ + log_sl + cos_ta) + dem_end_scaled + I(dem_end_scaled^2) + slope_end_scaled + sos_end_scaled + log_power_lines_dist_end + log_priv_road_dist_end + log_public_road_dist_end + log_house_dist_end + mining_Krist_nearest10000_end_scaled + wf_name_end + landcover_cc_grouped_end + wind_turbines_nearest2500_end_construction_scaled + wind_turbines_nearest2500_end_operation_scaled + landcover_cc_grouped_end:wind_turbines_nearest2500_end_construction_ + landcover_cc_grouped_end:wind_turbines_nearest2500_end_operation_sc + public_road_nearest100_cross + wind_turbines_nearest500_cross_construction + wind_turbines_nearest500_cross_operation + tpi_cat_s150m_end

(continued)

Mining ZOI radius	Wind turbine ZOI radius	TPI	AIC	dAIC	formula
2500	nearest10000	150m	470904.2	7.99	case_ ~ strata(step_id_) + sl_ + log_sl + cos_ta + wind_turbines_nearest10000_start_construction_scaled:(sl_ + log_sl + cos_ta) + wind_turbines_nearest10000_start_operation_scaled:(sl_ + log_sl + cos_ta) + landcover_cc_grouped_start:(sl_ + log_sl + cos_ta) + dem_end_scaled + I(dem_end_scaled^2) + slope_end_scaled + sos_end_scaled + log_power_lines_dist_end + log_priv_road_dist_end + log_public_road_dist_end + log_house_dist_end + mining_Krist_nearest2500_end_scaled + wf_name_end + landcover_cc_grouped_end + wind_turbines_nearest10000_end_construction_scaled + wind_turbines_nearest10000_end_operation_scaled + landcover_cc_grouped_end:wind_turbines_nearest10000_end_construction + landcover_cc_grouped_end:wind_turbines_nearest10000_end_operation_s + public_road_nearest100_cross + wind_turbines_nearest500_cross_construction + wind_turbines_nearest500_cross_operation + tpi_cat_s150m_end
5000	nearest2500	150m	470904.9	8.68	case_ ~ strata(step_id_) + sl_ + log_sl + cos_ta + wind_turbines_nearest2500_start_construction_scaled:(sl_ + log_sl + cos_ta) + wind_turbines_nearest2500_start_operation_scaled:(sl_ + log_sl + cos_ta) + landcover_cc_grouped_start:(sl_ + log_sl + cos_ta) + dem_end_scaled + I(dem_end_scaled^2) + slope_end_scaled + sos_end_scaled + log_power_lines_dist_end + log_priv_road_dist_end + log_public_road_dist_end + log_house_dist_end + mining_Krist_nearest5000_end_scaled + wf_name_end + landcover_cc_grouped_end + wind_turbines_nearest2500_end_construction_scaled + wind_turbines_nearest2500_end_operation_scaled + landcover_cc_grouped_end:wind_turbines_nearest2500_end_construction_ + landcover_cc_grouped_end:wind_turbines_nearest2500_end_operation_sc + public_road_nearest100_cross + wind_turbines_nearest500_cross_construction + wind_turbines_nearest500_cross_operation + tpi_cat_s150m_end

(continued)

Mining ZOI radius	Wind turbine ZOI radius	TPI	AIC	dAIC	formula
100	nearest5000	150m	470905.6	9.36	case_ ~ strata(step_id_) + sl_ + log_sl + cos_ta + wind_turbines_nearest5000_start_construction_scaled:(sl_ + log_sl + cos_ta) + wind_turbines_nearest5000_start_operation_scaled:(sl_ + log_sl + cos_ta) + landcover_cc_grouped_start:(sl_ + log_sl + cos_ta) + dem_end_scaled + I(dem_end_scaled^2) + slope_end_scaled + sos_end_scaled + log_power_lines_dist_end + log_priv_road_dist_end + log_public_road_dist_end + log_house_dist_end + mining_Krist_nearest100_end_scaled + wf_name_end + landcover_cc_grouped_end + wind_turbines_nearest5000_end_construction_scaled + wind_turbines_nearest5000_end_operation_scaled + landcover_cc_grouped_end:wind_turbines_nearest5000_end_construction_ + landcover_cc_grouped_end:wind_turbines_nearest5000_end_operation_sc + public_road_nearest100_cross + wind_turbines_nearest500_cross_construction + wind_turbines_nearest500_cross_operation + tpi_cat_s150m_end
10000	cumulative10000	150m	470906.2	10.03	case_ ~ strata(step_id_) + sl_ + log_sl + cos_ta + wind_turbines_cumulative10000_start_construction_scaled:(sl_ + log_sl + cos_ta) + wind_turbines_cumulative10000_start_operation_scaled:(sl_ + log_sl + cos_ta) + landcover_cc_grouped_start:(sl_ + log_sl + cos_ta) + dem_end_scaled + I(dem_end_scaled^2) + slope_end_scaled + sos_end_scaled + log_power_lines_dist_end + log_priv_road_dist_end + log_public_road_dist_end + log_house_dist_end + mining_Krist_nearest10000_end_scaled + wf_name_end + landcover_cc_grouped_end + wind_turbines_cumulative10000_end_construction_scaled + wind_turbines_cumulative10000_end_operation_scaled + landcover_cc_grouped_end:wind_turbines_cumulative10000_end_construc + landcover_cc_grouped_end:wind_turbines_cumulative10000_end_operatio + public_road_nearest100_cross + wind_turbines_nearest500_cross_construction + wind_turbines_nearest500_cross_operation + tpi_cat_s150m_end

Table C3. Table of model selection for the iSSA models for summer. Columns are zone of influence (ZOI) radius for mining and wind turbines, scale for the topographic position index (TPI), AIC of the model, dAIC of each model in relation to the most parsimonious model, and the formula with each model's structure. For impact of wind turbines, cumulative represents the density of turbines, and nearest represents the distance-decay ZOI of the nearest turbine. Here, we selected model ranked number 3 as the most parsimonious, because delta AIC < 2 in relation to the best ranked model and we chose to be more conservative, i.e. to select the smallest ZOI radii.

6 Table C4: Model selection table in autumn

Table C4 was truncated to show only the first 10 models, to avoid an overly long table.

Mining ZOI radius	Wind turbine ZOI radius	TPI	AIC	dAIC	formula
10000	cumulative10000	510m	360554.8	0.00	case_ ~ strata(step_id_) + sl_ + log_sl + cos_ta + wind_turbines_cumulative10000_start_construction_scaled:(sl_ + log_sl + cos_ta) + wind_turbines_cumulative10000_start_operation_scaled:(sl_ + log_sl + cos_ta) + landcover_cc_grouped_start:(sl_ + log_sl + cos_ta) + dem_end_scaled + I(dem_end_scaled^2) + slope_end_scaled + eos_end_scaled + log_power_lines_dist_end + log_priv_road_dist_end + log_public_road_dist_end + log_house_dist_end + mining_Krist_nearest10000_end_scaled + wf_name_end + landcover_cc_grouped_end + wind_turbines_cumulative10000_end_construction_scaled + wind_turbines_cumulative10000_end_operation_scaled + landcover_cc_grouped_end:wind_turbines_cumulative10000_end_construc + landcover_cc_grouped_end:wind_turbines_cumulative10000_end_operatio + public_road_nearest100_cross + wind_turbines_nearest500_cross_construction + wind_turbines_nearest500_cross_operation + tpi_cat_s510m_end
5000	cumulative10000	510m	360555.4	0.55	case_ ~ strata(step_id_) + sl_ + log_sl + cos_ta + wind_turbines_cumulative10000_start_construction_scaled:(sl_ + log_sl + cos_ta) + wind_turbines_cumulative10000_start_operation_scaled:(sl_ + log_sl + cos_ta) + landcover_cc_grouped_start:(sl_ + log_sl + cos_ta) + dem_end_scaled + I(dem_end_scaled^2) + slope_end_scaled + eos_end_scaled + log_power_lines_dist_end + log_priv_road_dist_end + log_public_road_dist_end + log_house_dist_end + mining_Krist_nearest5000_end_scaled + wf_name_end + landcover_cc_grouped_end + wind_turbines_cumulative10000_end_construction_scaled + wind_turbines_cumulative10000_end_operation_scaled + landcover_cc_grouped_end:wind_turbines_cumulative10000_end_construc + landcover_cc_grouped_end:wind_turbines_cumulative10000_end_operatio + public_road_nearest100_cross + wind_turbines_nearest500_cross_construction + wind_turbines_nearest500_cross_operation + tpi_cat_s510m_end

(continued)

Mining ZOI radius	Wind turbine ZOI radius	TPI	AIC	dAIC	formula
100	cumulative10000	510m	360555.5	0.60	case_ ~ strata(step_id_) + sl_ + log_sl + cos_ta + wind_turbines_cumulative10000_start_construction_scaled:(sl_ + log_sl + cos_ta) + wind_turbines_cumulative10000_start_operation_scaled:(sl_ + log_sl + cos_ta) + landcover_cc_grouped_start:(sl_ + log_sl + cos_ta) + dem_end_scaled + I(dem_end_scaled^2) + slope_end_scaled + eos_end_scaled + log_power_lines_dist_end + log_priv_road_dist_end + log_public_road_dist_end + log_house_dist_end + mining_Krist_nearest100_end_scaled + wf_name_end + landcover_cc_grouped_end + wind_turbines_cumulative10000_end_construction_scaled + wind_turbines_cumulative10000_end_operation_scaled + land-cover_cc_grouped_end:wind_turbines_cumulative10000_end_construc + land-cover_cc_grouped_end:wind_turbines_cumulative10000_end_operatio + public_road_nearest100_cross + wind_turbines_nearest500_cross_construction + wind_turbines_nearest500_cross_operation + tpi_cat_s510m_end
250	cumulative10000	510m	360555.6	0.71	case_ ~ strata(step_id_) + sl_ + log_sl + cos_ta + wind_turbines_cumulative10000_start_construction_scaled:(sl_ + log_sl + cos_ta) + wind_turbines_cumulative10000_start_operation_scaled:(sl_ + log_sl + cos_ta) + landcover_cc_grouped_start:(sl_ + log_sl + cos_ta) + dem_end_scaled + I(dem_end_scaled^2) + slope_end_scaled + eos_end_scaled + log_power_lines_dist_end + log_priv_road_dist_end + log_public_road_dist_end + log_house_dist_end + mining_Krist_nearest250_end_scaled + wf_name_end + landcover_cc_grouped_end + wind_turbines_cumulative10000_end_construction_scaled + wind_turbines_cumulative10000_end_operation_scaled + land-cover_cc_grouped_end:wind_turbines_cumulative10000_end_construc + land-cover_cc_grouped_end:wind_turbines_cumulative10000_end_operatio + public_road_nearest100_cross + wind_turbines_nearest500_cross_construction + wind_turbines_nearest500_cross_operation + tpi_cat_s510m_end

(continued)

Mining ZOI radius	Wind turbine ZOI radius	TPI	AIC	dAIC	formula
2500	cumulative10000	510m	360555.8	0.93	case_ ~ strata(step_id_) + sl_ + log_sl + cos_ta + wind_turbines_cumulative10000_start_construction_scaled:(sl_ + log_sl + cos_ta) + wind_turbines_cumulative10000_start_operation_scaled:(sl_ + log_sl + cos_ta) + landcover_cc_grouped_start:(sl_ + log_sl + cos_ta) + dem_end_scaled + I(dem_end_scaled^2) + slope_end_scaled + eos_end_scaled + log_power_lines_dist_end + log_priv_road_dist_end + log_public_road_dist_end + log_house_dist_end + mining_Krist_nearest2500_end_scaled + wf_name_end + landcover_cc_grouped_end + wind_turbines_cumulative10000_end_construction_scaled + wind_turbines_cumulative10000_end_operation_scaled + land-cover_cc_grouped_end:wind_turbines_cumulative10000_end_construc + land-cover_cc_grouped_end:wind_turbines_cumulative10000_end_operatio + public_road_nearest100_cross + wind_turbines_nearest500_cross_construction + wind_turbines_nearest500_cross_operation + tpi_cat_s510m_end
500	cumulative10000	510m	360556.1	1.30	case_ ~ strata(step_id_) + sl_ + log_sl + cos_ta + wind_turbines_cumulative10000_start_construction_scaled:(sl_ + log_sl + cos_ta) + wind_turbines_cumulative10000_start_operation_scaled:(sl_ + log_sl + cos_ta) + landcover_cc_grouped_start:(sl_ + log_sl + cos_ta) + dem_end_scaled + I(dem_end_scaled^2) + slope_end_scaled + eos_end_scaled + log_power_lines_dist_end + log_priv_road_dist_end + log_public_road_dist_end + log_house_dist_end + mining_Krist_nearest500_end_scaled + wf_name_end + landcover_cc_grouped_end + wind_turbines_cumulative10000_end_construction_scaled + wind_turbines_cumulative10000_end_operation_scaled + land-cover_cc_grouped_end:wind_turbines_cumulative10000_end_construc + land-cover_cc_grouped_end:wind_turbines_cumulative10000_end_operatio + public_road_nearest100_cross + wind_turbines_nearest500_cross_construction + wind_turbines_nearest500_cross_operation + tpi_cat_s510m_end

(continued)

Mining ZOI radius	Wind turbine ZOI radius	TPI	AIC	dAIC	formula
1000	cumulative10000	510m	360556.8	1.94	case_ ~ strata(step_id_) + sl_ + log_sl + cos_ta + wind_turbines_cumulative10000_start_construction_scaled:(sl_ + log_sl + cos_ta) + wind_turbines_cumulative10000_start_operation_scaled:(sl_ + log_sl + cos_ta) + landcover_cc_grouped_start:(sl_ + log_sl + cos_ta) + dem_end_scaled + I(dem_end_scaled^2) + slope_end_scaled + eos_end_scaled + log_power_lines_dist_end + log_priv_road_dist_end + log_public_road_dist_end + log_house_dist_end + mining_Krist_nearest1000_end_scaled + wf_name_end + landcover_cc_grouped_end + wind_turbines_cumulative10000_end_construction_scaled + wind_turbines_cumulative10000_end_operation_scaled + land-cover_cc_grouped_end:wind_turbines_cumulative10000_end_construc + land-cover_cc_grouped_end:wind_turbines_cumulative10000_end_operatio + public_road_nearest100_cross + wind_turbines_nearest500_cross_construction + wind_turbines_nearest500_cross_operation + tpi_cat_s510m_end
10000	nearest10000	510m	360564.5	9.68	case_ ~ strata(step_id_) + sl_ + log_sl + cos_ta + wind_turbines_nearest10000_start_construction_scaled:(sl_ + log_sl + cos_ta) + wind_turbines_nearest10000_start_operation_scaled:(sl_ + log_sl + cos_ta) + landcover_cc_grouped_start:(sl_ + log_sl + cos_ta) + dem_end_scaled + I(dem_end_scaled^2) + slope_end_scaled + eos_end_scaled + log_power_lines_dist_end + log_priv_road_dist_end + log_public_road_dist_end + log_house_dist_end + mining_Krist_nearest10000_end_scaled + wf_name_end + landcover_cc_grouped_end + wind_turbines_nearest10000_end_construction_scaled + wind_turbines_nearest10000_end_operation_scaled + land-cover_cc_grouped_end:wind_turbines_nearest10000_end_construction + land-cover_cc_grouped_end:wind_turbines_nearest10000_end_operation_s + public_road_nearest100_cross + wind_turbines_nearest500_cross_construction + wind_turbines_nearest500_cross_operation + tpi_cat_s510m_end

(continued)

Mining ZOI radius	Wind turbine ZOI radius	TPI	AIC	dAIC	formula
5000	nearest10000	510m	360565.1	10.27	case_ ~ strata(step_id_) + sl_ + log_sl + cos_ta + wind_turbines_nearest10000_start_construction_scaled:(sl_ + log_sl + cos_ta) + wind_turbines_nearest10000_start_operation_scaled:(sl_ + log_sl + cos_ta) + landcover_cc_grouped_start:(sl_ + log_sl + cos_ta) + dem_end_scaled + I(dem_end_scaled^2) + slope_end_scaled + eos_end_scaled + log_power_lines_dist_end + log_priv_road_dist_end + log_public_road_dist_end + log_house_dist_end + mining_Krist_nearest5000_end_scaled + wf_name_end + landcover_cc_grouped_end + wind_turbines_nearest10000_end_construction_scaled + wind_turbines_nearest10000_end_operation_scaled + landcover_cc_grouped_end:wind_turbines_nearest10000_end_construction + landcover_cc_grouped_end:wind_turbines_nearest10000_end_operation_s + public_road_nearest100_cross + wind_turbines_nearest500_cross_construction + wind_turbines_nearest500_cross_operation + tpi_cat_s510m_end
100	nearest10000	510m	360565.3	10.50	case_ ~ strata(step_id_) + sl_ + log_sl + cos_ta + wind_turbines_nearest10000_start_construction_scaled:(sl_ + log_sl + cos_ta) + wind_turbines_nearest10000_start_operation_scaled:(sl_ + log_sl + cos_ta) + landcover_cc_grouped_start:(sl_ + log_sl + cos_ta) + dem_end_scaled + I(dem_end_scaled^2) + slope_end_scaled + eos_end_scaled + log_power_lines_dist_end + log_priv_road_dist_end + log_public_road_dist_end + log_house_dist_end + mining_Krist_nearest100_end_scaled + wf_name_end + landcover_cc_grouped_end + wind_turbines_nearest10000_end_construction_scaled + wind_turbines_nearest10000_end_operation_scaled + landcover_cc_grouped_end:wind_turbines_nearest10000_end_construction + landcover_cc_grouped_end:wind_turbines_nearest10000_end_operation_s + public_road_nearest100_cross + wind_turbines_nearest500_cross_construction + wind_turbines_nearest500_cross_operation + tpi_cat_s510m_end

Table C4. Table of model selection for the iSSA models for autumn. Columns are zone of influence (ZOI) radius for mining and wind turbines, scale for the topographic position index (TPI), AIC of the model, dAIC of each model in relation to the most parsimonious model, and the formula with each model's structure. For impact of wind turbines, cumulative represents the density of turbines, and nearest represents the distance-decay ZOI of the nearest turbine.

7 Text C3: Disturbance effects on step selection

Here we present the coefficients of the iSSA models on habitat selection at patch scale. Even though all results come from the same models, we split the way we present the parts of the resulting model, to ease its interpretation. In this section we restrict ourselves on presenting the coefficients of all infrastructure and landscape covariates, without going into details regarding the impact of wind turbines on habitat selection and on movement patterns, which are shown further down.

Table C5 shows the coefficient estimates for all the infrastructure types, excluding wind turbines. Wind turbines are only included here for the barrier effects. The estimates are put together for the different seasons in table C5 so it is easy to compare the effects between them.

A summary of the results:

- Wind power plants were barriers to reindeer movement in calving during construction (and marginally during operation; p = 0.07) and in summer during wind turbine operation;
- Public roads were barrier in all seasons;
- The mine was avoided in summer (even though very weakly, Fig. C2), but not in calving and autumn;
- Public and private roads were avoided in all seasons;
- There was no effect of power lines in calving and summer, and a slight selection for them during autumn;
- Houses were selected during calving and autumn; (*why??*)
- Start of season did not affect habitat selection during calving and summer; however, end of season was positively selected in autumn, which means animals select for areas which stay green longer in autumn.

season	term	estimate	std.error	p	select
autumn	eos_end_scaled	0.097	0.010	<0.001	selection/positive
calving	log_house_dist_end	-0.213	0.008	<0.001	selection/positive
summer	log_house_dist_end	0.010	0.009	0.279	no effect
autumn	log_house_dist_end	-0.051	0.010	<0.001	selection/positive
calving	log_power_lines_dist_end	0.005	0.012	0.705	no effect
summer	log_power_lines_dist_end	0.002	0.007	0.734	no effect
autumn	log_power_lines_dist_end	-0.023	0.008	0.004	selection/positive
calving	log_priv_road_dist_end	0.030	0.004	<0.001	avoidance/negative
summer	log_priv_road_dist_end	0.043	0.004	<0.001	avoidance/negative
autumn	log_priv_road_dist_end	0.012	0.004	0.008	avoidance/negative
calving	log_public_road_dist_end	0.066	0.007	<0.001	avoidance/negative
summer	log_public_road_dist_end	0.051	0.008	<0.001	avoidance/negative
autumn	log_public_road_dist_end	0.041	0.009	<0.001	avoidance/negative
autumn	mining_Krist_nearest10000_end_scaled	-0.042	0.030	0.162	no effect
calving	mining_Krist_nearest250_end_scaled	-1171.291	890.424	0.188	no effect
summer	mining_Krist_nearest5000_end_scaled	-0.044	0.013	0.001	avoidance/negative
calving	public_road_nearest100_cross	-0.118	0.022	<0.001	avoidance/negative
summer	public_road_nearest100_cross	-0.150	0.022	<0.001	avoidance/negative

(continued)

season	term	estimate	std.error	p	select
autumn	public_road_nearest100_cross	-0.140	0.024	<0.001	avoidance/negative
calving	sos_end_scaled	-0.001	0.009	0.922	no effect
summer	sos_end_scaled	-0.001	0.007	0.931	no effect
calving	wind_turbines_nearest500_cross_construction	-0.593	0.209	0.005	avoidance/negative
summer	wind_turbines_nearest500_cross_construction	-0.007	0.092	0.939	no effect
autumn	wind_turbines_nearest500_cross_construction	0.138	0.170	0.415	no effect
calving	wind_turbines_nearest500_cross_operation	-0.221	0.122	0.07	no effect
summer	wind_turbines_nearest500_cross_operation	-0.173	0.066	0.009	avoidance/negative
autumn	wind_turbines_nearest500_cross_operation	-0.018	0.116	0.877	no effect

Table C5. Coefficient estimates for the effects of infrastructure types and the start/end of season on habitat selection for all three seasons.

8 Table C6: Coefficients - calving

term	estimate	std.error	p	select
sl_	0.000	0.000	<0.001	no effect
log_sl	0.027	0.002	<0.001	avoidance/negative
cos_ta	-0.053	0.005	<0.001	avoidance/negative
dem_end_scaled	-0.073	0.014	<0.001	avoidance/negative
I(dem_end_scaled^2)	-0.020	0.005	<0.001	avoidance/negative
slope_end_scaled	-0.054	0.005	<0.001	avoidance/negative
sos_end_scaled	-0.001	0.009	0.922	no effect
log_power_lines_dist_end	0.005	0.012	0.705	no effect
log_priv_road_dist_end	0.030	0.004	<0.001	avoidance/negative
log_public_road_dist_end	0.066	0.007	<0.001	avoidance/negative
log_house_dist_end	-0.213	0.008	<0.001	selection/positive
mining_Krist_nearest250_end_scaled	-1171.291	890.424	0.188	no effect
wf_name_endstorliden	-0.288	0.036	<0.001	avoidance/negative
wf_name_endytteberg	-0.026	0.051	0.61	no effect
wf_name_endamliden	-0.293	0.083	<0.001	avoidance/negative
landcover_cc_grouped_endopen lands	0.621	0.009	<0.001	selection/positive
landcover_cc_grouped_endanthropogenic areas	0.313	0.028	<0.001	selection/positive
landcover_cc_grouped_endconiferous forests	-0.105	0.008	<0.001	avoidance/negative
landcover_cc_grouped_endmires	-0.051	0.009	<0.001	avoidance/negative
wind_turbines_cumulative5000_end_construction_scaled	-0.025	0.019	0.178	no effect
wind_turbines_cumulative5000_end_operation_scaled	0.017	0.020	0.413	no effect
public_road_nearest100_cross	-0.118	0.022	<0.001	avoidance/negative
wind_turbines_nearest500_cross_construction	-0.593	0.209	0.005	avoidance/negative
wind_turbines_nearest500_cross_operation	-0.221	0.122	0.07	no effect
tpi_cat_s150m_endlower slope	-0.042	0.012	<0.001	avoidance/negative
tpi_cat_s150m_endmedium slope	0.105	0.008	<0.001	selection/positive
tpi_cat_s150m_endridge	0.131	0.012	<0.001	selection/positive
tpi_cat_s150m_endupper slope	0.114	0.012	<0.001	selection/positive

(continued)

term	estimate	std.error	p	select
tpi_cat_s150m_endvalley	-0.022	0.015	0.138	no effect
sl_:wind_turbines_cumulative5000_start_construction_scaled	0.000	0.000	0.005	no effect
log_sl:wind_turbines_cumulative5000_start_construction_scaled	0.019	0.003	<0.001	avoidance/negative
cos_ta:wind_turbines_cumulative5000_start_construction_scaled	0.011	0.005	0.033	selection/positive
sl_:wind_turbines_cumulative5000_start_operation_scaled	0.000	0.000	0.051	no effect
log_sl:wind_turbines_cumulative5000_start_operation_scaled	0.006	0.003	0.02	avoidance/negative
cos_ta:wind_turbines_cumulative5000_start_operation_scaled	-0.003	0.005	0.585	no effect
sl_:landcover_cc_grouped_startopen lands	0.000	0.000	<0.001	no effect
sl_:landcover_cc_grouped_startanthropogenic areas	0.001	0.000	<0.001	selection/positive
sl_:landcover_cc_grouped_startconiferous forests	0.000	0.000	0.194	no effect
sl_:landcover_cc_grouped_startmires	0.000	0.000	0.038	no effect
log_sl:landcover_cc_grouped_startopen lands	0.081	0.004	<0.001	avoidance/negative
log_sl:landcover_cc_grouped_startanthropogenic areas	-0.006	0.014	0.687	no effect
log_sl:landcover_cc_grouped_startconiferous forests	-0.094	0.004	<0.001	selection/positive
log_sl:landcover_cc_grouped_startmires	0.002	0.006	0.71	no effect
cos_ta:landcover_cc_grouped_startopen lands	0.012	0.009	0.147	no effect
cos_ta:landcover_cc_grouped_startanthropogenic areas	-0.494	0.032	<0.001	avoidance/negative
cos_ta:landcover_cc_grouped_startconiferous forests	-0.006	0.008	0.5	no effect
cos_ta:landcover_cc_grouped_startmires	0.079	0.011	<0.001	selection/positive
landcover_cc_grouped_endopen lands:wind_turbines_cumulative5000_end_construction_scaled	0.003	0.008	0.718	no effect
landcover_cc_grouped_endanthropogenic areas:wind_turbines_cumulative5000_end_construction_scaled	0.035	0.024	0.146	no effect
landcover_cc_grouped_endconiferous forests:wind_turbines_cumulative5000_end_construction_scaled	-0.036	0.009	<0.001	avoidance/negative
landcover_cc_grouped_endmires:wind_turbines_cumulative5000_end_constru	0.041	0.010	<0.001	selection/positive
landcover_cc_grouped_endopen lands:wind_turbines_cumulative5000_end_operation_scaled	-0.039	0.008	<0.001	avoidance/negative
landcover_cc_grouped_endanthropogenic areas:wind_turbines_cumulative5000_end_operation_scaled	-0.021	0.028	0.451	no effect
landcover_cc_grouped_endconiferous forests:wind_turbines_cumulative5000_end_operation_scaled	-0.033	0.008	<0.001	avoidance/negative
landcover_cc_grouped_endmires:wind_turbines_cumulative5000_end_operati	-0.017	0.009	0.073	no effect

Table C6. Complete table with coefficient estimates for the best-ranked integrated step selection model in calving.

9 Table C7: Coefficients - summer

term	estimate	std.error	p	select
sl_	0.000	0.000	0.99	no effect
log_sl	-0.002	0.012	0.877	no effect
cos_ta	-0.055	0.013	<0.001	avoidance/negative
dem_end_scaled	0.060	0.012	<0.001	selection/positive
I_dem_end_scaled^2	-0.002	0.005	0.648	no effect
slope_end_scaled	-0.087	0.004	<0.001	avoidance/negative

(continued)

term	estimate	std.error	p	select
sos_end_scaled	-0.001	0.007	0.931	no effect
log_power_lines_dist_end	0.002	0.007	0.734	no effect
log_priv_road_dist_end	0.043	0.004	<0.001	avoidance/negative
log_public_road_dist_end	0.051	0.008	<0.001	avoidance/negative
log_house_dist_end	0.010	0.009	0.279	no effect
mining_Krist_nearest5000_end_scaled	-0.044	0.013	0.001	avoidance/negative
wf_name_endstorliden	0.106	0.048	0.028	selection/positive
wf_name_endytteberg	0.078	0.054	0.147	no effect
wf_name_endamliden	0.188	0.065	0.004	selection/positive
landcover_cc_grouped_endopen lands	0.250	0.013	<0.001	selection/positive
landcover_cc_grouped_endanthropogenic areas	0.691	0.027	<0.001	selection/positive
landcover_cc_grouped_endconiferous forests	0.076	0.011	<0.001	selection/positive
landcover_cc_grouped_endmires	-0.499	0.014	<0.001	avoidance/negative
wind_turbines_nearest5000_end_construction_scaled	0.041	0.022	0.06	no effect
wind_turbines_nearest5000_end_operation_scaled	0.073	0.020	<0.001	selection/positive
public_road_nearest100_cross	-0.150	0.022	<0.001	avoidance/negative
wind_turbines_nearest500_cross_construction	-0.007	0.092	0.939	no effect
wind_turbines_nearest500_cross_operation	-0.173	0.066	0.009	avoidance/negative
tpi_cat_s150m_endlower slope	0.083	0.012	<0.001	selection/positive
tpi_cat_s150m_endmedium slope	0.036	0.009	<0.001	selection/positive
tpi_cat_s150m_endridge	0.036	0.013	0.006	selection/positive
tpi_cat_s150m_endupper slope	0.038	0.012	0.002	selection/positive
tpi_cat_s150m_endvalley	0.079	0.014	<0.001	selection/positive
sl_:wind_turbines_nearest5000_start_construction_scaled	0.000	0.000	0.376	no effect
log_sl:wind_turbines_nearest5000_start_construction_scaled	-0.006	0.004	0.212	no effect
cos_ta:wind_turbines_nearest5000_start_construction_scaled	-0.008	0.005	0.095	no effect
sl_:wind_turbines_nearest5000_start_operation_scaled	0.000	0.000	<0.001	no effect
log_sl:wind_turbines_nearest5000_start_operation_scaled	0.021	0.005	<0.001	avoidance/negative
cos_ta:wind_turbines_nearest5000_start_operation_scaled	-0.008	0.005	0.087	no effect
sl_:landcover_cc_grouped_startopen lands	0.000	0.000	0.048	no effect
sl_:landcover_cc_grouped_startanthropogenic areas	0.001	0.000	<0.001	selection/positive
sl_:landcover_cc_grouped_startconiferous forests	0.000	0.000	0.01	no effect
sl_:landcover_cc_grouped_startmires	0.000	0.000	<0.001	no effect
log_sl:landcover_cc_grouped_startopen lands	0.008	0.014	0.573	no effect
log_sl:landcover_cc_grouped_startanthropogenic areas	-0.036	0.026	0.17	no effect
log_sl:landcover_cc_grouped_startconiferous forests	0.080	0.013	<0.001	avoidance/negative
log_sl:landcover_cc_grouped_startmires	-0.132	0.016	<0.001	selection/positive
cos_ta:landcover_cc_grouped_startopen lands	0.051	0.016	0.002	selection/positive
cos_ta:landcover_cc_grouped_startanthropogenic areas	0.001	0.033	0.964	no effect
cos_ta:landcover_cc_grouped_startconiferous forests	0.040	0.015	0.007	selection/positive
cos_ta:landcover_cc_grouped_startmires	0.053	0.019	0.005	selection/positive
landcover_cc_grouped_endopen lands:wind_turbines_nearest5000_end_construction_scaled	0.014	0.013	0.287	no effect
landcover_cc_grouped_endanthropogenic areas:wind_turbines_nearest5000_end_construction_scaled	-0.007	0.023	0.769	no effect
landcover_cc_grouped_endconiferous forests:wind_turbines_nearest5000_end_construction_scaled	0.017	0.012	0.16	no effect
landcover_cc_grouped_endmires:wind_turbines_nearest5000_end_constructio	0.042	0.016	0.008	selection/positive
landcover_cc_grouped_endopen lands:wind_turbines_nearest5000_end_operation_scaled	-0.019	0.011	0.079	no effect

(continued)

term	estimate	std.error	p	select
landcover_cc_grouped_endanthropogenic areas:wind_turbines_nearest5000_end_operation_scaled	-0.010	0.020	0.601	no effect
landcover_cc_grouped_endconiferous forests:wind_turbines_nearest5000_end_operation_scaled	-0.068	0.010	<0.001	avoidance/negative
landcover_cc_grouped_endmires:wind_turbines_nearest5000_end_operation_	-0.061	0.015	<0.001	avoidance/negative

Table C7. Complete table with coefficient estimates for the best-ranked integrated step selection model in summer.

10 Table C8: Coefficients - autumn

term	estimate	std.error	p	select
sl_	0.000	0.000	<0.001	no effect
log_sl	-0.058	0.017	<0.001	selection/positive
cos_ta	0.029	0.023	0.207	no effect
dem_end_scaled	-0.223	0.021	<0.001	avoidance/negative
I(dem_end_scaled^2)	0.077	0.007	<0.001	selection/positive
slope_end_scaled	-0.105	0.005	<0.001	avoidance/negative
eos_end_scaled	0.097	0.010	<0.001	selection/positive
log_power_lines_dist_end	-0.023	0.008	0.004	selection/positive
log_priv_road_dist_end	0.012	0.004	0.008	avoidance/negative
log_public_road_dist_end	0.041	0.009	<0.001	avoidance/negative
log_house_dist_end	-0.051	0.010	<0.001	selection/positive
mining_Krist_nearest10000_end_scaled	-0.042	0.030	0.162	no effect
wf_name_endstorliden	0.199	0.063	0.002	selection/positive
wf_name_endytteberg	0.159	0.069	0.02	selection/positive
wf_name_endamliden	0.541	0.096	<0.001	selection/positive
landcover_cc_grouped_endopen lands	1.009	0.018	<0.001	selection/positive
landcover_cc_grouped_endanthropogenic areas	0.427	0.038	<0.001	selection/positive
landcover_cc_grouped_endconiferous forests	0.482	0.018	<0.001	selection/positive
landcover_cc_grouped_endmires	0.112	0.021	<0.001	selection/positive
wind_turbines_cumulative10000_end_construction_scaled	-0.080	0.048	0.095	no effect
wind_turbines_cumulative10000_end_operation_scaled	0.068	0.044	0.121	no effect
public_road_nearest100_cross	-0.140	0.024	<0.001	avoidance/negative
wind_turbines_nearest500_cross_construction	0.138	0.170	0.415	no effect
wind_turbines_nearest500_cross_operation	-0.018	0.116	0.877	no effect
tpi_cat_s510m_endlower slope	-0.101	0.018	<0.001	avoidance/negative
tpi_cat_s510m_endmedium slope	0.135	0.017	<0.001	selection/positive
tpi_cat_s510m_endridge	0.296	0.015	<0.001	selection/positive
tpi_cat_s510m_endupper slope	0.177	0.018	<0.001	selection/positive
tpi_cat_s510m_endvalley	-0.174	0.016	<0.001	avoidance/negative
sl_:wind_turbines_cumulative10000_start_construction_scaled	0.000	0.000	<0.001	no effect
log_sl:wind_turbines_cumulative10000_start_construction_scaled	-0.011	0.004	0.002	selection/positive
cos_ta:wind_turbines_cumulative10000_start_construction_scaled	0.007	0.006	0.203	no effect
sl_:wind_turbines_cumulative10000_start_operation_scaled	0.000	0.000	0.899	no effect
log_sl:wind_turbines_cumulative10000_start_operation_scaled	0.002	0.004	0.681	no effect

(continued)

term	estimate	std.error	p	select
cos_ta:wind_turbines_cumulative10000_start_operation_scaled	0.004	0.006	0.439	no effect
sl_:landcover_cc_grouped_startopen lands	0.000	0.000	<0.001	no effect
sl_:landcover_cc_grouped_startanthropogenic areas	0.000	0.000	<0.001	no effect
sl_:landcover_cc_grouped_startconiferous forests	0.000	0.000	<0.001	no effect
sl_:landcover_cc_grouped_startmires	0.000	0.000	0.132	no effect
log_sl:landcover_cc_grouped_startopen lands	0.148	0.018	<0.001	avoidance/negative
log_sl:landcover_cc_grouped_startanthropogenic areas	0.138	0.034	<0.001	avoidance/negative
log_sl:landcover_cc_grouped_startconiferous forests	0.124	0.018	<0.001	avoidance/negative
log_sl:landcover_cc_grouped_startmires	-0.157	0.021	<0.001	selection/positive
cos_ta:landcover_cc_grouped_startopen lands	-0.026	0.025	0.3	no effect
cos_ta:landcover_cc_grouped_startanthropogenic areas	-0.102	0.050	0.04	avoidance/negative
cos_ta:landcover_cc_grouped_startconiferous forests	-0.019	0.025	0.436	no effect
cos_ta:landcover_cc_grouped_startmires	-0.019	0.030	0.526	no effect
landcover_cc_grouped_endopen lands:wind_turbines_cumulative10000_end_construction_scaled	0.040	0.019	0.035	selection/positive
landcover_cc_grouped_endanthropogenic areas:wind_turbines_cumulative10000_end_construction_scaled	0.018	0.038	0.637	no effect
landcover_cc_grouped_endconiferous forests:wind_turbines_cumulative10000_end_construction_scaled	0.032	0.019	0.099	no effect
landcover_cc_grouped_endmires:wind_turbines_cumulative10000_end_const	0.026	0.023	0.256	no effect
landcover_cc_grouped_endopen lands:wind_turbines_cumulative10000_end_operation_scaled	0.005	0.016	0.738	no effect
landcover_cc_grouped_endanthropogenic areas:wind_turbines_cumulative10000_end_operation_scaled	-0.057	0.037	0.12	no effect
landcover_cc_grouped_endconiferous forests:wind_turbines_cumulative10000_end_operation_scaled	-0.071	0.016	<0.001	avoidance/negative
landcover_cc_grouped_endmires:wind_turbines_cumulative10000_end_opera	-0.089	0.023	<0.001	avoidance/negative

Table C8. Complete table with coefficient estimates for the best-ranked integrated step selection model in autumn.

11 Figure C1: Impacts of wind power on habitat selection in calving during operation phase

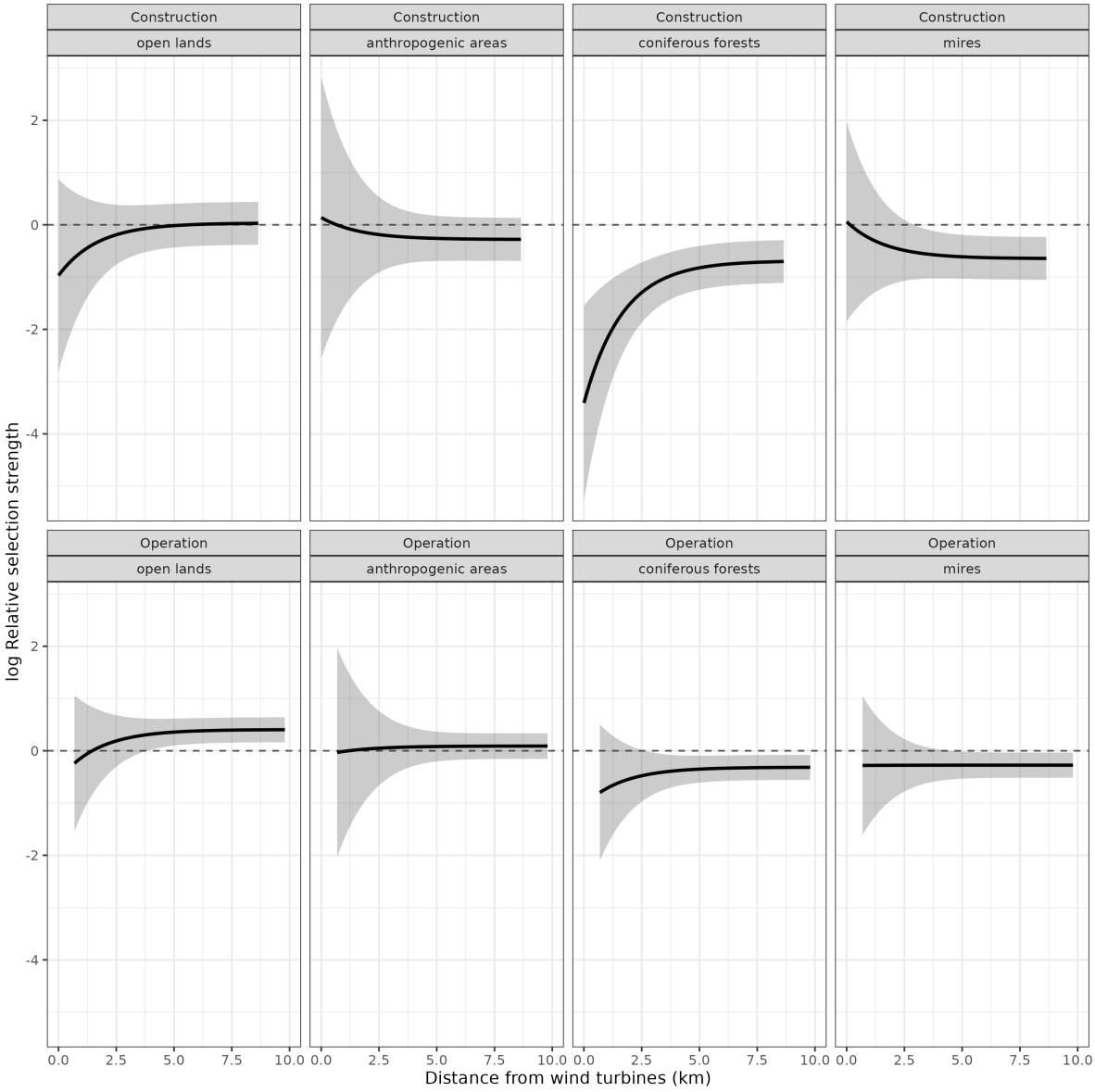

Figure C1. Comparison of response curves for calving during construction and operation of the wind power plants. The curves show the log-Relative selection strength as a function of the distance to wind turbines, considering the impact of 10 wind turbines. The model uses deciduous forests as the reference category.

12 Figure C2: Impacts of mining on habitat selection in summer

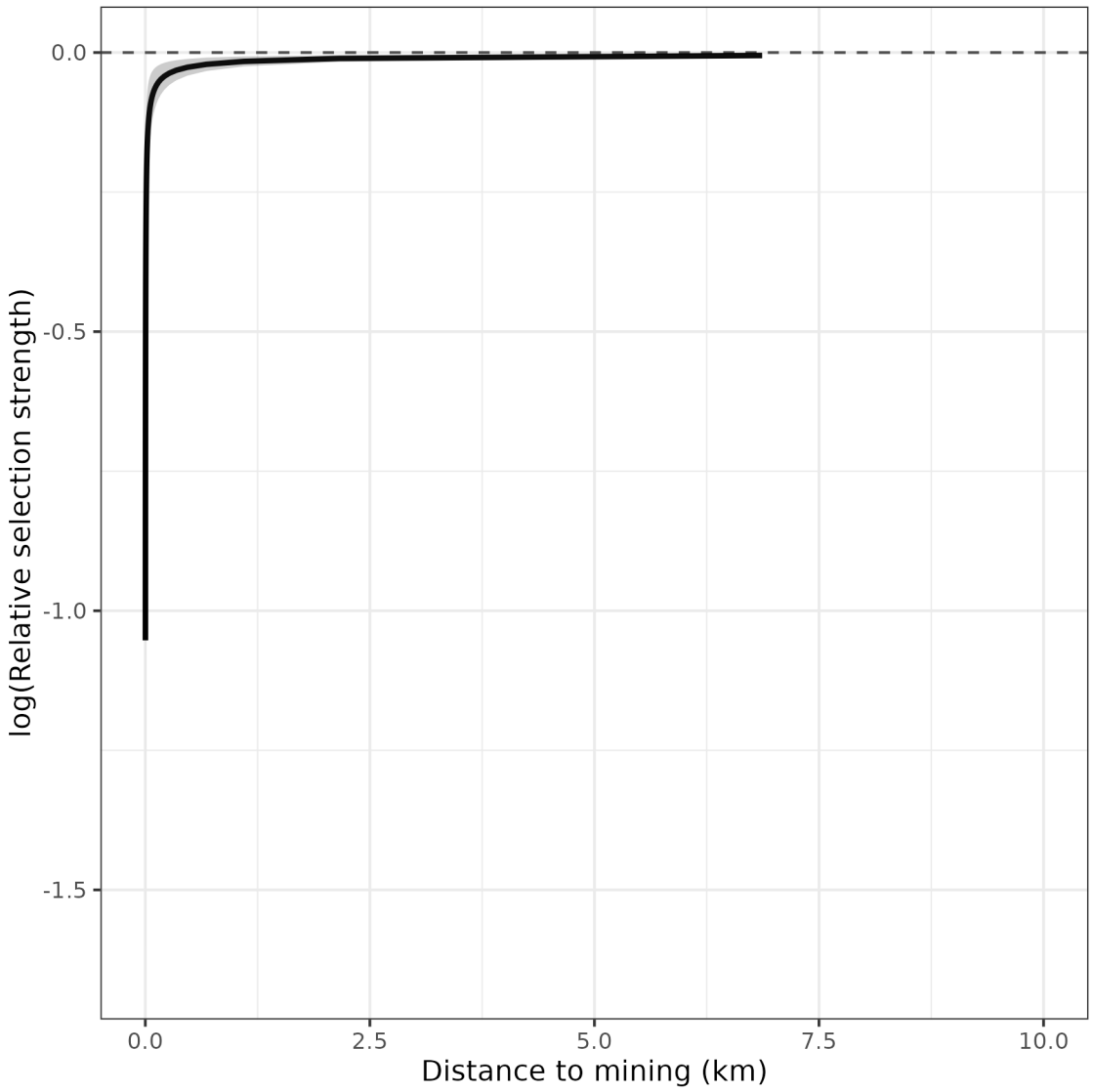

Figure C2. Log-Relative selection strength as a function of the distance to the mine in Kristineberget in summer.

13 Figure C3: Impacts of wind power on habitat selection in summer

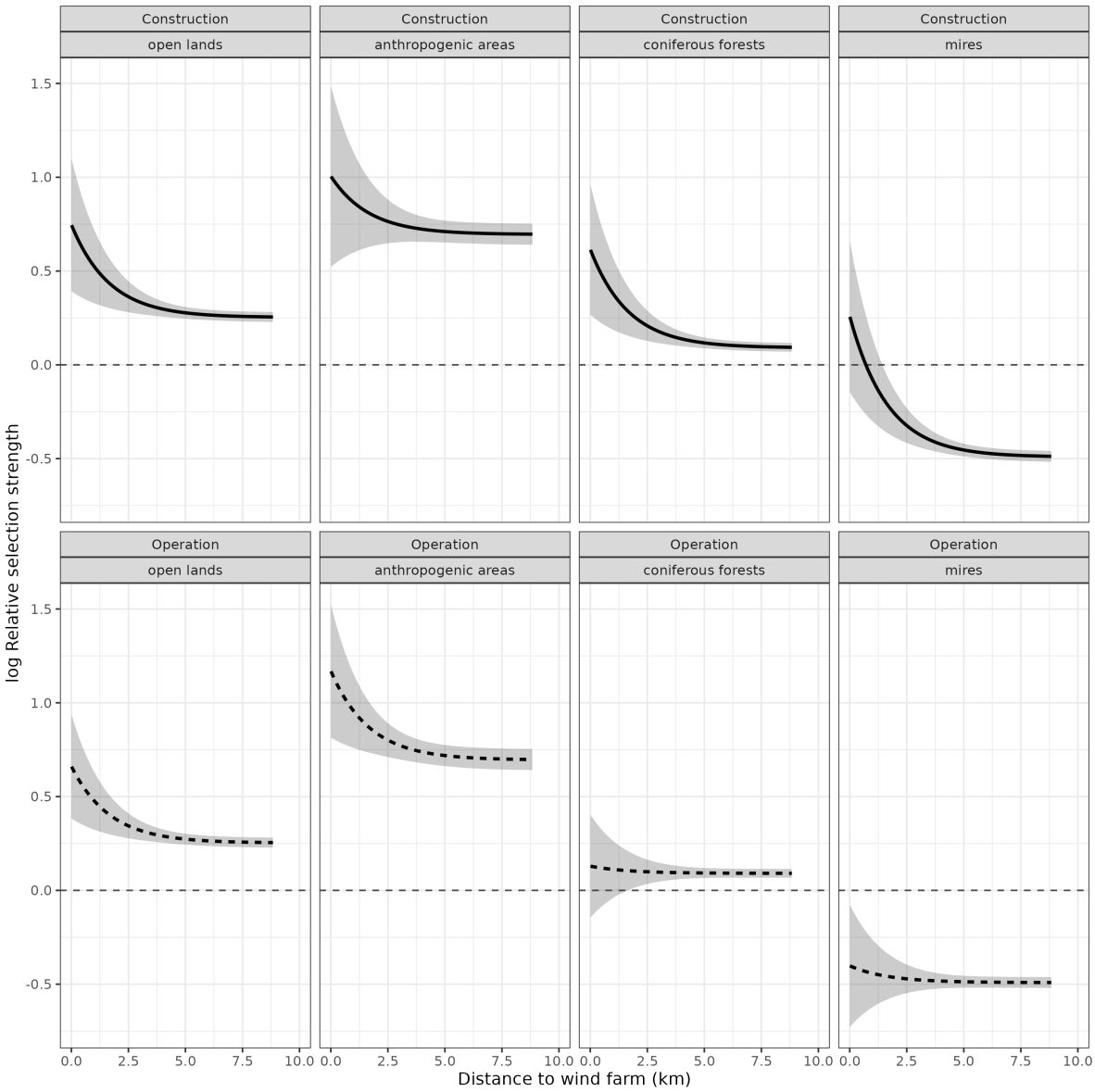

Figure C3. Comparison of response curves for summer during construction and operation of the wind power plants. The curves show the log-Relative selection strength as a function of the distance to the nearest wind turbine. The model uses deciduous forests as the reference category.

14 Figure C4: Impacts of wind power on habitat selection in autumn

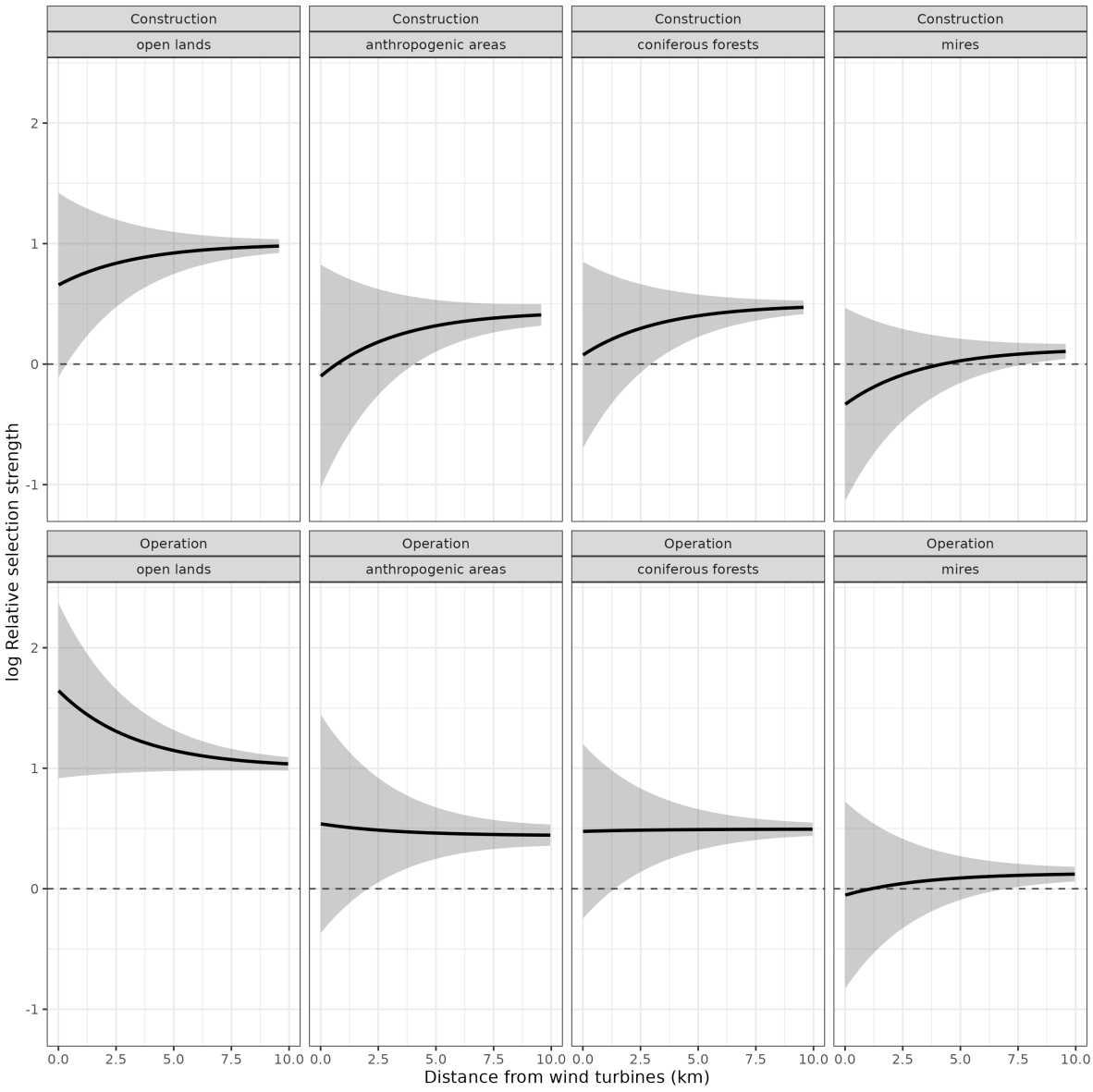

Figure C4. Comparison of response curves for autumn during construction and operation of the wind power plants. The curves show the log-Relative selection strength as a function of the distance to wind turbine, considering the impact of 10 turbines. The model uses deciduous forests as the reference category.

15 Figure C5: Impacts of wind turbines on movement patterns in calving

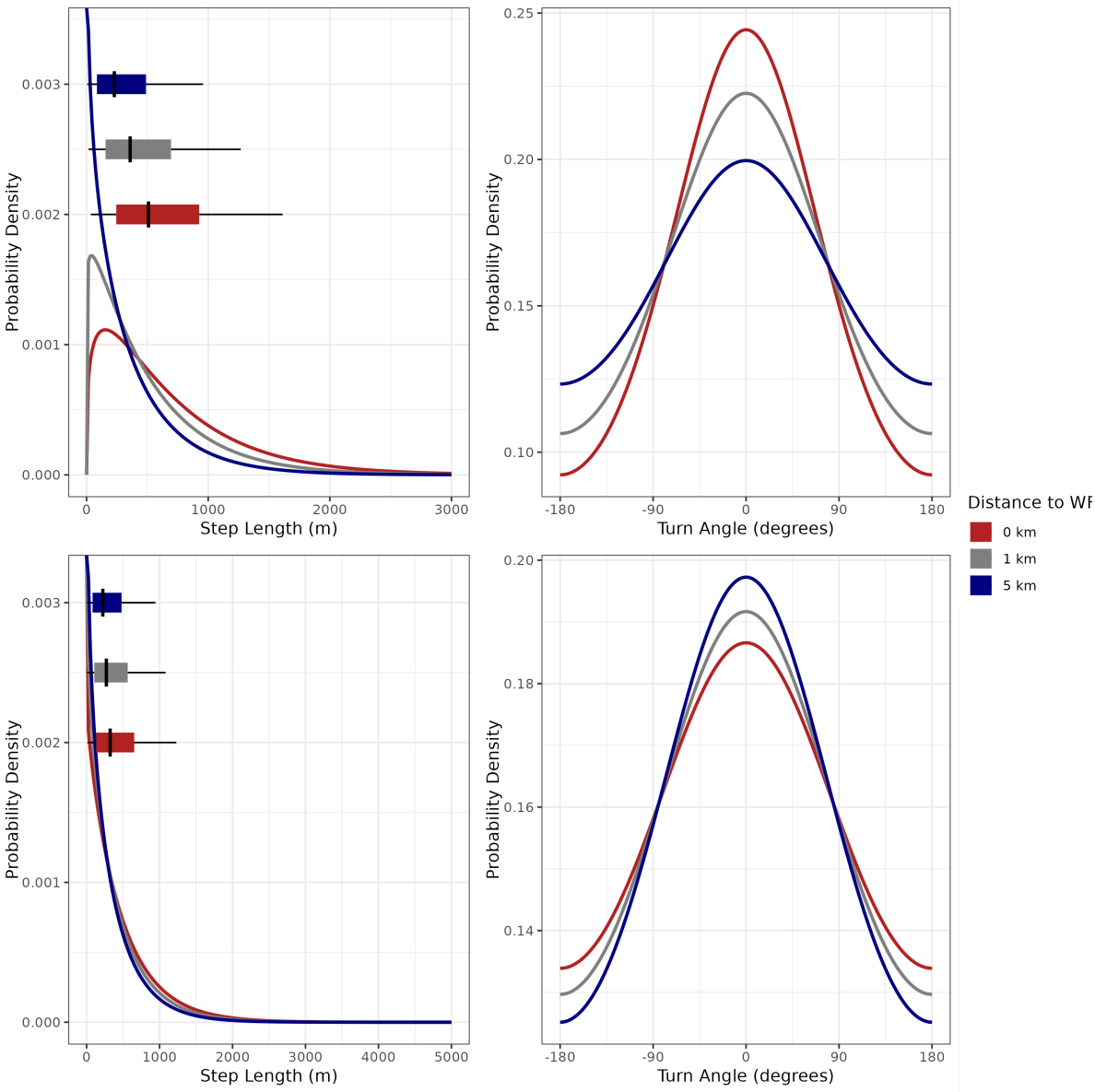

Figure C5. Predicted distribution of step length (left) and turning angles (right) at different distances from where the wind turbines were built, during the construction phase (upper row) and operation phase (bottom row). The plot in the left also shows boxplots of predicted movement rates. Reindeer moved faster and more directionaly when close to wind turbines during their construction, but the different was minimal during operation.

References

Avgar, Tal, Jonathan R. Potts, Mark A. Lewis, and Mark S. Boyce. 2016. "Integrated Step Selection Analysis: Bridging the Gap Between Resource Selection and Animal Movement." Edited by Luca Börger. *Methods in Ecology and Evolution* 7 (5): 619–30. https://doi.org/10.1111/2041-210X.12528.

Appendix D. Cumulative impacts of mining and wind power development on reindeer: calving-site selection data and analysis

Here we present a detailed description of the data, methods, and results related to the calving-site selection analysis for reindeer under the presence of the mine and the wind turbines in the Malå reindeer herding district in Sweden. The calving site is the location where the female gives birth and spends time with the calf outside the herd to create an attachment bond. We report: (i) the calving period and site identification; (ii) the statistical modeling of cumulative impact analysis; (iii) the model selection table; (iv) the analysis of calving site selection and forage quality.

Table of contents

1 Figure D1: Calving period and site identification

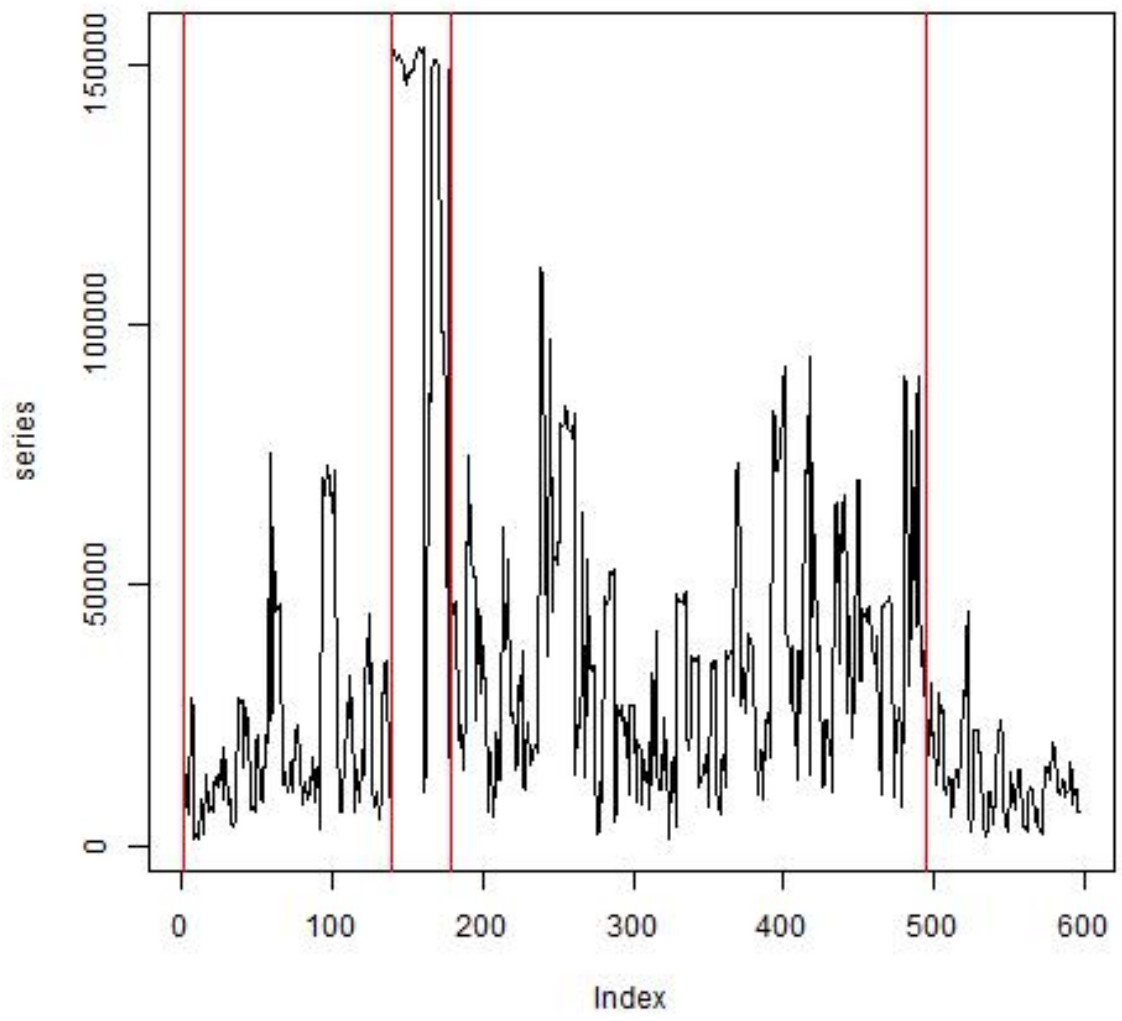

Figure D1. Example of residence time time series employed to find the calving period and calving sites using the function residenceTime() from the recurse package. The most probable calving period lies between the second and third red lines, corresponding to the group that includes the first-highest peak of the time series. The grouping was performed using the lavielle() and findpath() functions from the adehabitatLT package in R. The calving site was the mean location where calving occurred.

2 Text D1: Statistical modeling of cumulative impact analysis

As in the landscape-scale habitat selection analysis, we used a habitat selection function setup. However, considering only individuals within 2 km of the wind turbines during calving to assess the effect of wind power drastically reduced the number of observations, preventing the use of the habitat selection function for that purpose. The habitat selection function was used only to assess the mine's zone of influence.

Ten random available but unused sites were generated within the estimated calving area for each of the truly used calving sites (R package "amt", function "random points"). We determined the calving area by calculating the minimum convex polygon around all the used calving sites. To ensure consideration of the entire calving area, we extended the estimated area to half the mean net square displacement of individuals that calved at the border of the minimum convex polygon.

We adapted the formula described in Appendix B as follows:

```
base_formula <- case_ ~
  # habitat selection
  scale(dem) + I(scale(dem)^2) + scale(slope) + cos_aspect +
  log(power_lines_dist+1) + log(priv_road_dist+1) + log(public_road_dist+1) +
  log(trails_dist+1) +
  # mining habitat selection
  scale(mining_Krist_nearestXXX) +
  # wind habitat selection
  landcover + phase*log(wind_turbines_dist + 1) +
  # tpi habitat selection
  tpi_scale_TTT
```

where the terms are:

- `case_`: our response variable (0/1);
- `dem`: elevation, we include a linear and a quadratic term;
- `slope`: slope;
- `cos_aspect`: cosine of the aspect;
- `tpi_scale_TTT`: topographic position index (TPI) as a continuous variable and computed at a certain scale;
- `phase`: wind power plants development phase, with 3 categories: before construction, during construction, operation;
- `wf_name`: name of the wind power plant closest to each point, with four categories, added as a fixed effect to control for differential effects close to the Åmliden wind park, which lies along a large fenced area;

- `landcover`: land cover, with 5 categories: deciduous forest, coniferous forest, open areas, mires, and anthropogenic areas;
- `log(public_road_dist+1)`, `log(priv_road_dist+1)`, `log(trails_dist+1)`, `log(power_lines_dist+1) + 1)`: logarithm of the distance to the nearest infrastructure for public roads, private roads, trails, houses, power lines and wind turbines;
- `mining_Krist_nearestXXX`: ZOI (exponential decay distance) of the mine, computed considering a certain ZOI radius;

The terms `XXX`, and `TTT` in the model structure above represent scales or variables that varied across models fitted. To evaluate the most likely ZOI for the mine and the wind turbines, whether there was a cumulative impact of multiple wind power plants, and at which scale the TPI most affected reindeer habitat selection, we replaced these variables in the model structure above using each possible combination of ZOI radii and type (cumulative vs. nearest; Fig. B1) for wind power and the different ZOI radii for the mine, together with different scales for the TPI. Models were compared through Akaike information criterion (AIC), as described in the main text. The scales included were:

- Mining (`XXX`): 100 m, 250 m, 500 m, 1 km, 2.5 km, 5 km, 10 km.
- TPI (`TTT`): 150 m, 250 m, 510 m.

3 Table D1: Model selection table in calving sites

Mining ZOI radius	TPI	AIC	dAIC	formula
10000	tpi_s250r	1146.60	0.00	case_~scale(dem) + I(scale(dem)^2) + scale(slope) + cos_aspect + scale(sos) + log(power_lines_dist + 1) + log(priv_road_dist + 1) + log(public_road_dist + 1) + log(trails_dist + 1) + log(house_dist + 1) + landcover_cc + phase + log(wind_turbines_dist_comb + 1) + tpi_s250m + scale(mining_Krist_nearest10000) + phase:log(wind_turbines_dist_comb + 1)
10000	tpi_s510m	1147.30	0.69	case_~scale(dem) + I(scale(dem)^2) + scale(slope) + cos_aspect + scale(sos) + log(power_lines_dist + 1) + log(priv_road_dist + 1) + log(public_road_dist + 1) + log(trails_dist + 1) + log(house_dist + 1) + landcover_cc + phase + log(wind_turbines_dist_comb + 1) + tpi_s510m + scale(mining_Krist_nearest10000) + phase:log(wind_turbines_dist_comb + 1)
10000	tpi_s150r	1148.55	1.95	case_~scale(dem) + I(scale(dem)^2) + scale(slope) + cos_aspect + scale(sos) + log(power_lines_dist + 1) + log(priv_road_dist + 1) + log(public_road_dist + 1) + log(trails_dist + 1) + log(house_dist + 1) + landcover_cc + phase + log(wind_turbines_dist_comb + 1) + tpi_s150m + scale(mining_Krist_nearest10000) + phase:log(wind_turbines_dist_comb + 1)

(continued)

Mining ZOI radius	TPI	AIC	dAIC	formula
5000	tpi_s250m	1163.31	16.71	case_~scale(dem) + I(scale(dem)^2) + scale(slope) + cos_aspect + scale(sos) + log(power_lines_dist + 1) + log(priv_road_dist + 1) + log(public_road_dist + 1) + log(trails_dist + 1) + log(house_dist + 1) + landcover_cc + phase + log(wind_turbines_dist_comb + 1) + tpi_s250m + scale(mining_Krist_nearest5000) + phase:log(wind_turbines_dist_comb + 1)
5000	tpi_s510ı	1164.19	17.58	case_~scale(dem) + I(scale(dem)^2) + scale(slope) + cos_aspect + scale(sos) + log(power_lines_dist + 1) + log(priv_road_dist + 1) + log(public_road_dist + 1) + log(trails_dist + 1) + log(house_dist + 1) + landcover_cc + phase + log(wind_turbines_dist_comb + 1) + tpi_s510m + scale(mining_Krist_nearest5000) + phase:log(wind_turbines_dist_comb + 1)
5000	tpi_s150m	1165.26	18.66	case_~scale(dem) + I(scale(dem)^2) + scale(slope) + cos_aspect + scale(sos) + log(power_lines_dist + 1) + log(priv_road_dist + 1) + log(public_road_dist + 1) + log(trails_dist + 1) + log(house_dist + 1) + landcover_cc + phase + log(wind_turbines_dist_comb + 1) + tpi_s150m + scale(mining_Krist_nearest5000) + phase:log(wind_turbines_dist_comb + 1)
2500	tpi_s250ı	1170.09	23.49	case_~scale(dem) + I(scale(dem)^2) + scale(slope) + cos_aspect + scale(sos) + log(power_lines_dist + 1) + log(priv_road_dist + 1) + log(public_road_dist + 1) + log(trails_dist + 1) + log(house_dist + 1) + landcover_cc + phase + log(wind_turbines_dist_comb + 1) + tpi_s250m + scale(mining_Krist_nearest2500) + phase:log(wind_turbines_dist_comb + 1)
2500	tpi_s510m	1171.02	24.42	case_~scale(dem) + I(scale(dem)^2) + scale(slope) + cos_aspect + scale(sos) + log(power_lines_dist + 1) + log(priv_road_dist + 1) + log(public_road_dist + 1) + log(trails_dist + 1) + log(house_dist + 1) + landcover_cc + phase + log(wind_turbines_dist_comb + 1) + tpi_s510m + scale(mining_Krist_nearest2500) + phase:log(wind_turbines_dist_comb + 1)
500	tpi_s250ı	1171.49	24.89	case_~scale(dem) + I(scale(dem)^2) + scale(slope) + cos_aspect + scale(sos) + log(power_lines_dist + 1) + log(priv_road_dist + 1) + log(public_road_dist + 1) + log(trails_dist + 1) + log(house_dist + 1) + landcover_cc + phase + log(wind_turbines_dist_comb + 1) + tpi_s250m + scale(mining_Krist_nearest500) + phase:log(wind_turbines_dist_comb + 1)
1000	tpi_s250m	1171.68	25.07	case_~scale(dem) + I(scale(dem)^2) + scale(slope) + cos_aspect + scale(sos) + log(power_lines_dist + 1) + log(priv_road_dist + 1) + log(public_road_dist + 1) + log(trails_dist + 1) + log(house_dist + 1) + landcover_cc + phase + log(wind_turbines_dist_comb + 1) + tpi_s250m + scale(mining_Krist_nearest1000) + phase:log(wind_turbines_dist_comb + 1)

(continued)

Mining ZOI radius	TPI	AIC	dAIC	formula
2500	tpi_s150r	1172.16	25.56	case_~scale(dem) + I(scale(dem)^2) + scale(slope) + cos_aspect + scale(sos) + log(power_lines_dist + 1) + log(priv_road_dist + 1) + log(public_road_dist + 1) + log(trails_dist + 1) + log(house_dist + 1) + landcover_cc + phase + log(wind_turbines_dist_comb + 1) + tpi_s150m + scale(mining_Krist_nearest2500) + phase:log(wind_turbines_dist_comb + 1)
500	tpi_s510m	1172.47	25.87	case_~scale(dem) + I(scale(dem)^2) + scale(slope) + cos_aspect + scale(sos) + log(power_lines_dist + 1) + log(priv_road_dist + 1) + log(public_road_dist + 1) + log(trails_dist + 1) + log(house_dist + 1) + landcover_cc + phase + log(wind_turbines_dist_comb + 1) + tpi_s510m + scale(mining_Krist_nearest500) + phase:log(wind_turbines_dist_comb + 1)
1000	tpi_s510r	1172.63	26.03	case_~scale(dem) + I(scale(dem)^2) + scale(slope) + cos_aspect + scale(sos) + log(power_lines_dist + 1) + log(priv_road_dist + 1) + log(public_road_dist + 1) + log(trails_dist + 1) + log(house_dist + 1) + landcover_cc + phase + log(wind_turbines_dist_comb + 1) + tpi_s510m + scale(mining_Krist_nearest1000) + phase:log(wind_turbines_dist_comb + 1)
500	tpi_s150m	1173.66	27.06	case_~scale(dem) + I(scale(dem)^2) + scale(slope) + cos_aspect + scale(sos) + log(power_lines_dist + 1) + log(priv_road_dist + 1) + log(public_road_dist + 1) + log(trails_dist + 1) + log(house_dist + 1) + landcover_cc + phase + log(wind_turbines_dist_comb + 1) + tpi_s150m + scale(mining_Krist_nearest500) + phase:log(wind_turbines_dist_comb + 1)
1000	tpi_s150r	1173.82	27.22	case_~scale(dem) + I(scale(dem)^2) + scale(slope) + cos_aspect + scale(sos) + log(power_lines_dist + 1) + log(priv_road_dist + 1) + log(public_road_dist + 1) + log(trails_dist + 1) + log(house_dist + 1) + landcover_cc + phase + log(wind_turbines_dist_comb + 1) + tpi_s150m + scale(mining_Krist_nearest1000) + phase:log(wind_turbines_dist_comb + 1)
250	tpi_s250m	1173.99	27.38	case_~scale(dem) + I(scale(dem)^2) + scale(slope) + cos_aspect + scale(sos) + log(power_lines_dist + 1) + log(priv_road_dist + 1) + log(public_road_dist + 1) + log(trails_dist + 1) + log(house_dist + 1) + landcover_cc + phase + log(wind_turbines_dist_comb + 1) + tpi_s250m + scale(mining_Krist_nearest250) + phase:log(wind_turbines_dist_comb + 1)
250	tpi_s510r	1175.04	28.44	case_~scale(dem) + I(scale(dem)^2) + scale(slope) + cos_aspect + scale(sos) + log(power_lines_dist + 1) + log(priv_road_dist + 1) + log(public_road_dist + 1) + log(trails_dist + 1) + log(house_dist + 1) + landcover_cc + phase + log(wind_turbines_dist_comb + 1) + tpi_s510m + scale(mining_Krist_nearest250) + phase:log(wind_turbines_dist_comb + 1)

(continued)

Mining ZOI radius	TPI	AIC	dAIC	formula
250	tpi_s150m	1176.04	29.44	case_~scale(dem) + I(scale(dem)^2) + scale(slope) + cos_aspect + scale(sos) + log(power_lines_dist + 1) + log(priv_road_dist + 1) + log(public_road_dist + 1) + log(trails_dist + 1) + log(house_dist + 1) + landcover_cc + phase + log(wind_turbines_dist_comb + 1) + tpi_s150m + scale(mining_Krist_nearest250) + phase:log(wind_turbines_dist_comb + 1)
100	tpi_s250r	1176.59	29.98	case_~scale(dem) + I(scale(dem)^2) + scale(slope) + cos_aspect + scale(sos) + log(power_lines_dist + 1) + log(priv_road_dist + 1) + log(public_road_dist + 1) + log(trails_dist + 1) + log(house_dist + 1) + landcover_cc + phase + log(wind_turbines_dist_comb + 1) + tpi_s250m + scale(mining_Krist_nearest100) + phase:log(wind_turbines_dist_comb + 1)
100	tpi_s510m	1177.61	31.01	case_~scale(dem) + I(scale(dem)^2) + scale(slope) + cos_aspect + scale(sos) + log(power_lines_dist + 1) + log(priv_road_dist + 1) + log(public_road_dist + 1) + log(trails_dist + 1) + log(house_dist + 1) + landcover_cc + phase + log(wind_turbines_dist_comb + 1) + tpi_s510m + scale(mining_Krist_nearest100) + phase:log(wind_turbines_dist_comb + 1)
100	tpi_s150r	1178.63	32.03	case_~scale(dem) + I(scale(dem)^2) + scale(slope) + cos_aspect + scale(sos) + log(power_lines_dist + 1) + log(priv_road_dist + 1) + log(public_road_dist + 1) + log(trails_dist + 1) + log(house_dist + 1) + landcover_cc + phase + log(wind_turbines_dist_comb + 1) + tpi_s150m + scale(mining_Krist_nearest100) + phase:log(wind_turbines_dist_comb + 1)

Table D1. Table of model selection for the calving site selection model. Columns are zone of influence (ZOI) radius for mining and wind turbines, scale for the topographic position index (TPI), AIC of the model, dAIC of each model in relation to the most parsimonious model, and the formula with each model's structure. The model to select is the model with ZOI = 10km and TPI = 250m.

4 Table D2: Final model results

term	estimate	std.error	p	select
(Intercept)	-4.786	1.739	0.006	avoidance/negative
scale(dem)	-0.460	0.111	<0.001	avoidance/negative
I(scale(dem)^2)	-0.300	0.093	0.001	avoidance/negative
scale(slope)	-0.150	0.102	0.144	no effect
cos_aspect	0.183	0.114	0.108	no effect
log(priv_road_dist + 1)	0.325	0.089	<0.001	avoidance/negative
log(public_road_dist + 1)	0.303	0.088	0.001	avoidance/negative
tpi_s250m	0.085	0.030	0.005	selection/positive
scale(mining_Krist_nearest10000)	-1.380	0.411	0.001	avoidance/negative

(continued)

term	estimate	std.error	p	select
landcover_ccconiferous forests	0.132	1.076	0.903	no effect
landcover_ccdeciduous forests	-0.503	1.141	0.659	no effect
landcover_ccmires	-0.433	1.093	0.692	no effect
landcover_ccopen area	0.803	1.073	0.454	no effect
phaseConstruction	-0.898	1.882	0.634	no effect
phaseOperation	-1.827	1.732	0.291	no effect
log(wind_turbines_dist_comb + 1)	-0.201	0.132	0.129	no effect
phaseConstruction:log(wind_turbines_dist_comb + 1)	0.088	0.199	0.659	no effect
phaseOperation:log(wind_turbines_dist_comb + 1)	0.191	0.181	0.292	no effect

Table D2. Coefficient estimates of the most parsimonious generalized linear model testing the effect of infrastructures on reindeer calving site selection from the Malå reindeer herding community between 2008 and 2018. The table includes the estimates, the standard error (std.error) and the p-values (p).

5 Figure D2: Difference across years and phase in calving dates and between females that had been close to the wind turbines and those that had not

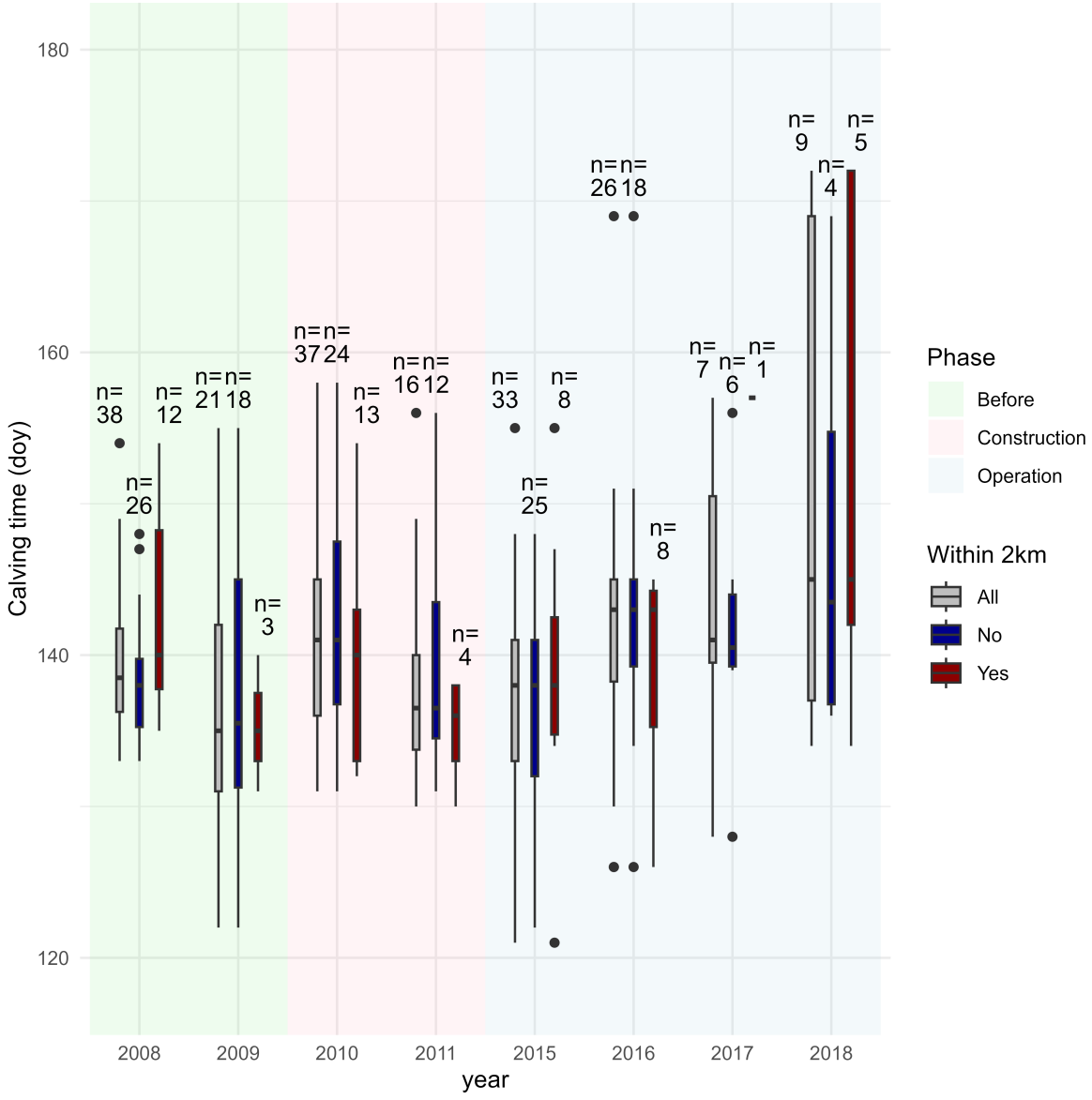

Figure D2. Distribution of the day of the year when calving occured in the Malå reindeer herding community from 2008 to 2018 according to year. The colors in the background represent the phase of construction of wind power plants (Before construction, during construction, during operation). Colors in the plots represent the distribution of all individuals, only those within 2km of the wind turbines during the calving period, and only those that were always more than 2km away. The results of the Kruskal-Wallis test showed no significant difference according to proximity or among phases for individuals who have been roaming close to the wind turbines during calving.

6 Figure D3: Synchrony between calving date and forage quality

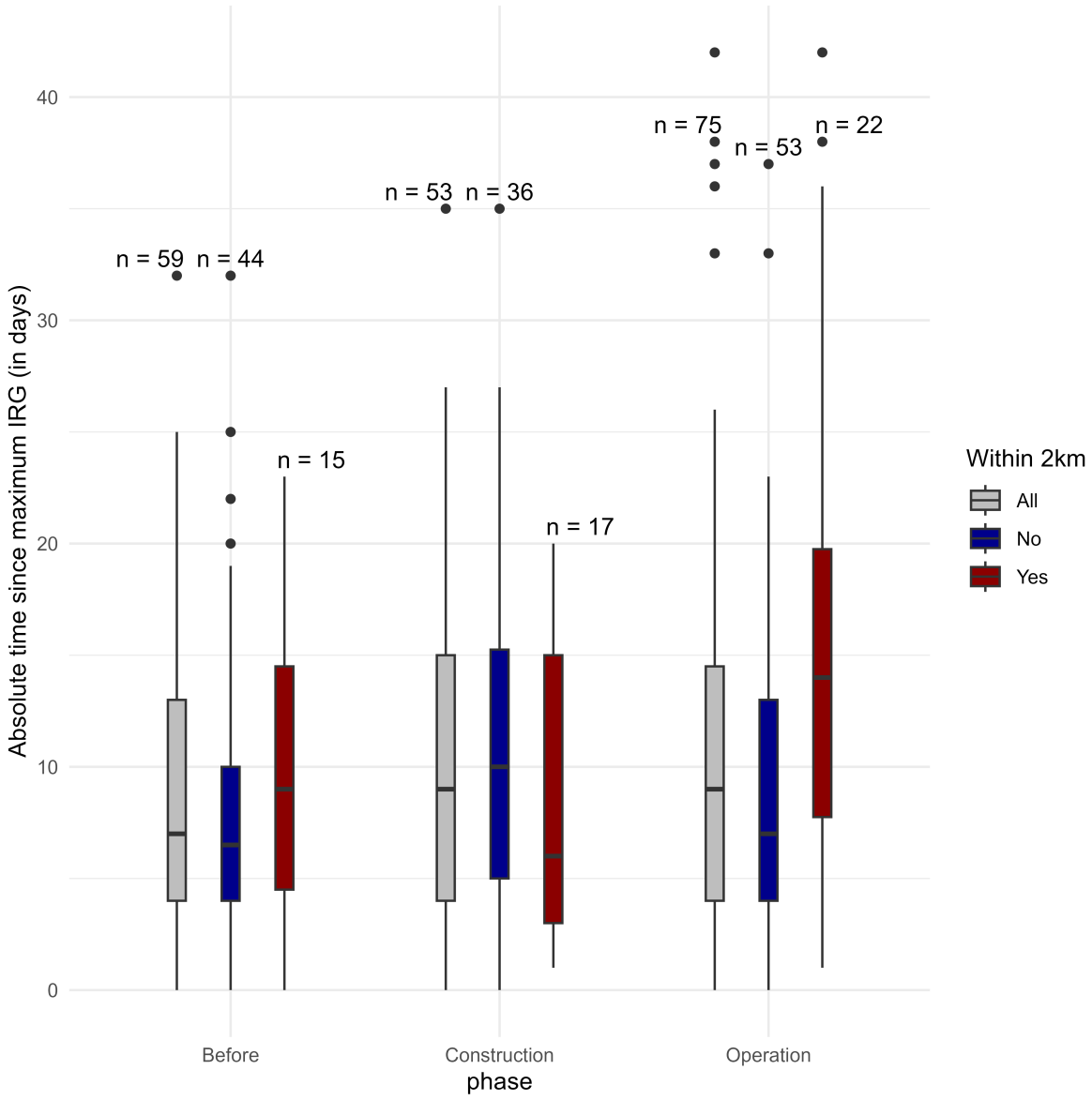

Figure D3. Distribution of the absolute difference in days between the maximum instantaneous rate of green up and the dates of calving at calving sites for the females that have been within 2km from the wind turbines during calving in Malå reindeer herding community for each year from 2008 to 2018. The colors represent the phase of construction of the wind turbines.